DNA methylation GrimAge version 2

Research Paper

DNA methylation GrimAge version 2

Ake T. Lu[1,2], Alexandra M. Binder[3,4], Joshua Zhang[1], Qi Yan[2], Alex P. Reiner [5], Simon R. Cox[6], Janie Corley[6], Sarah E. Harris[6], Pei-Lun Kuo[7], Ann Z. Moore[7], Stefania Bandinelli[8], James D. Stewart[9], Cuicui Wang[10], Elissa J. Hamlat[11], Elissa S. Epel[11], Joel D. Schwartz[10,12], Eric A. Whitsel[9,13], Adolfo Correa[14], Luigi Ferrucci[7], Riccardo E. Marioni[15], Steve Horvath[1,2,16]

[1]Dept. of Human Genetics, David Geffen School of Medicine, University of California Los Angeles, Los Angeles, CA 90095, USA
[2]San Diego Institute of Science, Altos Labs, San Diego, CA 92121, USA
[3]Population Sciences in the Pacific Program (Cancer Epidemiology), University of Hawaii Cancer Center, University of Hawaii at Manoa, Honolulu, HI 96813, USA
[4]Department of Epidemiology, UCLA Fielding School of Public Health, Los Angeles, CA 90095, USA
[5]Public Health Sciences Division, Fred Hutchinson Cancer Research Center, Seattle, WA 98109, USA
[6]Lothian Birth Cohorts, Department of Psychology, University of Edinburgh, Edinburgh, EH8 9JZ, Scotland, UK
[7]Longitudinal Studies Section, Translational Gerontology Branch, National Institute on Aging, National Institutes of Health, Baltimore, MD 21224, USA
[8]Geriatric Unit, Local Health Unit Tuscany Centre, Firenze, Tuscany 40125, Italy
[9]Dept. of Epidemiology, Gillings School of Global Public Health, University of North Carolina, Chapel Hill, NC 27516-8050, USA
[10]Department of Environmental Health, Harvard T.H. Chan School of Public Health, Boston, MA 02115, USA
[11]Department of Psychiatry and Behavioral Sciences, University of California, San Francisco, CA 94143-0848, USA
[12]Department of Epidemiology, Harvard T.H. Chan School of Public Health, Boston, MA 02115, USA
[13]Dept. of Medicine, School of Medicine, University of North Carolina, Chapel Hill, NC 27599, USA
[14]Departments of Medicine and Population Health Science, Jackson Heart Study, University of Mississippi Medical Center, Jackson, MS 39216, USA
[15]Centre for Genomic and Experimental Medicine, Institute of Genetics and Cancer, University of Edinburgh, Edinburgh, EH4 2XU, Scotland, UK
[16]Dept. of Biostatistics, Fielding School of Public Health, University of California Los Angeles, Los Angeles, CA 90095, USA

Correspondence to: Steve Horvath; **email:** shorvath@mednet.ucla.edu
Keywords: DNA methylation, epigenetic clock, mortality, healthspan
Received: September 22, 2022 **Accepted:** November 21, 2022 **Published:** December 14, 2022

ABSTRACT

We previously described a DNA methylation (DNAm) based biomarker of human mortality risk *DNAm GrimAge*. Here we describe version 2 of GrimAge (trained on individuals aged between 40 and 92) which leverages two new DNAm based estimators of (log transformed) plasma proteins: high sensitivity C-reactive protein (logCRP) and hemoglobin A1C (logA1C). We evaluate GrimAge2 in 13,399 blood samples across nine study cohorts. After adjustment for age and sex, GrimAge2 outperforms GrimAge in predicting mortality across multiple racial/ethnic groups (meta $P=3.6x10^{-167}$ versus $P=2.6x10^{-144}$) and in terms of associations with age related conditions such as coronary heart disease, lung function measurement FEV1 (correlation= -0.31, $P=1.1x10^{-136}$), computed tomography based measurements of fatty liver disease. We present evidence that GrimAge version 2 also applies to younger individuals and to saliva samples where it tracks markers of metabolic syndrome.

DNAm logCRP is positively correlated with morbidity count ($P=1.3x10^{-54}$). DNAm logA1C is highly associated with type 2 diabetes ($P=5.8x10^{-155}$). DNAm PAI-1 outperforms the other age-adjusted DNAm biomarkers including GrimAge2 in correlating with triglyceride (cor=0.34, $P=9.6x10^{-267}$) and visceral fat (cor=0.41, $P=4.7x10^{-41}$).
Overall, we demonstrate that GrimAge version 2 is an attractive epigenetic biomarker of human mortality and morbidity risk.

INTRODUCTION

We previously established DNA methylation based (DNAm) GrimAge for predicting mortality risk and showed it outperformed several widely-used DNAm biomarkers of aging [1]. While first generation clocks such as the pan tissue clock (Horvath, 2013) [2] and Hannum et al.'s blood based clock [3] estimate chronological age, second generation clocks estimate mortality risk e.g. the mortality risk score (Zhang et al., 2017 [4]), DNAm PhenoAge (Levine et al. [5], 2018), DNAm GrimAge [1] (2019), and longitudinal data based clocks such as DunedinPoAm [6] and Pace of Aging [7].

Comparative studies in epidemiological cohorts show that DNAm GrimAge often outperforms the afore-mentioned clocks in terms of a) predicting mortality risk and b) associations with age-related conditions research groups ([8–17]). GrimAge has been used to study many conditions including COVID [13], autism [15], major depression disorder [18], post-traumatic stress disorder (PTSD).

Here we describe a second version of GrimAge, GrimAge2, and demonstrate that it outperforms the original GrimAge with respect to its strength of association with a host of age-related conditions including mortality risk, computed tomography data, cognitive assessments, lifestyle factors, and applicability to saliva. We validate version 2 of GrimAge in almost 13,400 blood samples across nine human cohorts with participants of Hispanic-, European-, and African ancestries.

Review of version 1 of GrimAge

The first version of GrimAge was defined as a composite biomarker (weighted linear combination) of seven DNAm surrogates of plasma proteins, a DNAm-based estimator of smoking pack-years, age, and sex. GrimAge relied on the fact that some (but not all) plasma protein levels can be estimated based on cytosine methylation levels.

In the following, we denote a DNAm-based surrogate marker by adding the prefix "DNAm" to the respective variable name. To adjust for confounding by chronological age, we define age adjusted measures of DNAm-based variables as the residuals resulting from regressing the DNAm variable on chronological age. For example, we defined the age adjusted version of GrimAge, referred to as age acceleration AgeAccelGrim (in units of year), based on DNAm GrimAge [1]. Thus, a positive (or negative) value of AgeAccelGrim indicates that the DNAm GrimAge is higher (or lower) than expected based on chronological age. We use the same terminology to define AgeAccelGrim2 based on DNAm GrimAge2.

DNAm GrimAge was established based on a two-stage approach [1]. We trained and tested the GrimAge using individuals from the Framingham heart study (FHS) Offspring Cohort [19]. In the first stage, we established DNAm surrogates of plasma proteins as well as smoking pack-years (DNAm PACKYRS). In the second stage, we developed a predictor of mortality by regressing time-to-death due to all-cause mortality (dependent variable) on the following covariates: DNAm surrogates selected from the first stage, chronological age (Age) and sex (Female: 1 indicates females, 0 males), and batch effect as needed.

RESULTS

GrimAge version 2

The first version of DNAm GrimAge was defined as a linear combination of chronological age (Age), an indicator of female sex (Female), and eight DNAm biomarkers including DNAm PACKYRS and seven DNAm proteins that are implicated in kidney function, mitochondria dysfunction, inflammation, etc. (Supplementary Note 1). The 1030 unique CpGs underlying version 1 of GrimAge are proximal to genes which play a role in MHC class II, cytokine-mediated signaling pathway and other gene sets from GO, KEGG and PANTHER [1].

We used the same set of 1030 CpGs to construct version 2 of GrimAge. We randomly split the Framingham Heart Study data into training (n=1833) and test (n=711) data (Methods). The mean age of individuals in the training set and test set was 66 and 67 years, respectively. These participants in the training and test datasets have similar demographic profiles and number of years for follow-up (Table 1).

Table 1. Overview of the cohorts for validating DNAmGrimAge2.

Study	Race[2]	N		Female	Death	Age	Follow-up
		Samples	Subjects				
Training data							
FHS training	White	1833	1833	54%	13%	66.1±9.06 [59,73]	7.9±1.67 [7.4,9.89]
Validation data							
FHS test	White	711	711	54%	14%	66.8±8.62 [61,73]	7.7±1.77 [7.2,8.78]
	White	998	998	100%	67%	68.3±6.26 [65,72.77]	19.1±6.22 [15,23.92]
WHI BA23	AfricanA	676	676	100%	52%	63±6.61 [57.9,67.7]	19.5±6.81 [15.7,24.58]
	Hispanic	433	433	100%	43%	62.2±6.87 [56.5,67.5]	20.7±5.78 [18.2,24.48]
	White	1096	1096	100%	48%	64.3±7.1 [58.9,69.79]	21±5.95 [18.2,24.96]
WHI EMPC	AfricanA	558	558	100%	45%	62.5±6.98 [57.7,67.46]	21±5.67 [18.8,24.77]
	Hispanic	318	318	100%	30%	61.2±6.21 [56.5,65.96]	22±4.82 [21.9,24.59]
JHS	AfricanA	1746	1746	63%	16%	56.2±12.32 [46.5,65.35]	11.7±2.55 [11.2,13.11]
InCHIANTI	White	1430	728	56%	37%	67.4±16.17 [61,78]	10±4.87 [5.4,14.58]
BLSA	White	572	556	46%	32%	70.9±14.08 [62,82]	6.1±4.18 [2.1,9.32]
LBC21	White	692	469	60%	94%	82.3±4.31 [79,86.56]	8.8±5.2 [4.6,12.57]
LBC36	White	2796	1044	50%	30%	73.6±3.67 [70.3,76.63]	9.7±4.09 [6,13.05]
NAS	White	1373	732	0%	38%	74.5±6.99 [69,79]	10.5±4.71 [6,15]
Summary[1]	White, African A, Hispanic	13,399	10,065	71%	39%	67.9±11.33 [61.8,76]	13±6.9 [7.8,16.91]

[1]Summary statistics are based on the nine validation datasets.

[2]AfricanA denotes African American.

The table summarizes the characteristics of 1833 and 13,399 blood samples used in our training and validation process. The training dataset was based on the 1833 individuals from Framingham Heart Study Offspring Cohort (FHS). The validation datasets consist of 10,065 individuals came from nine independent cohorts: FHS test dataset, Women's Health Initiatives (WHI) BA23, WHI EMPC, Jackson Heart Study (JHS), InCHIANTI (baseline and the third follow-up), Baltimore Longitudinal Study of Aging (BLSA), Lothian Birth Cohort 1921 (LBC21) and LBC 1936 (LBC36), and Normative Aging Study (NAS). The studies cohorts were used in our validation analysis stratified by racial group within each cohort. Age and follow-up time (from methylation profile to last visit/death in units of years) are presented in the format of mean ±SD [25th, 75th]. Proportion of females are based on individual level.

We started out by developing two new DNAm based estimators of high sensitivity C-reactive protein (CRP) and hemoglobin A1C, respectively. CRP is a widely used biomarker of inflammation while hemoglobin A1C levels are used to assess the short term history of blood glucose levels.

To arrive at DNA methylation based surrogates of these plasma proteins, we used two elastic net regression models to predict log-transformed (base e) versions of high-sensitivity C-reactive protein (log CRP) and hemoglobin A1C (log A1C), respectively. Both elastic net regression models used the following candidate covariates: 1030 CpGs, Age and Female. The two elastic net regression models selected 132 CpGs (for log CRP) and 86 CpGs (for log A1C), respectively (Supplementary Table 1). The predicted values resulting from these regression models will be denoted by DNAm logCRP and DNAm logA1C, respectively. The Pearson correlation coefficients between the DNAm variables and their target proteins are biased in the training dataset (Supplementary Figure 1A, 1B) due to overfitting. Our unbiased analysis in the test dataset leads to the following: Pearson correlations r=0.48 for DNAm logCRP and r=0.34 for DNAm logA1C (Supplementary Figure 1C, 1D).

To define GrimAge2 we used a Cox regression model to regress time-to-death (due to all-cause mortality) on the following candidate covariates: eleven DNAm-based surrogates of plasma proteins, DNAm PACKYRS, Age, Female (Methods, Supplementary Table 1). We remind the readers that the first version of GrimAge was based on Age, Female, DNAm PACKYRS, and seven DNAm-based proteins: adrenomedullin (ADM), beta-2-microglobulim (B2M), cystatin C (Cystatin C), GDF-15, leptin (Leptin), PAI-1, and tissue inhibitor metalloproteinases 1 (TIMP-1, Supplementary Note 1). Interestingly, the Cox regression model with a elastic net penalty picked up the exactly same seven DNAm proteins, DNAm PACKYRS, as well as the two new biomarkers (DNAm logCRP and DNAm logA1C). Thus, GrimAge2 is based on 12 covariates: 10 DNAm based biomarkers and 2 demographic characteristics: Age, Female (Figure 1). The linear combination of covariates resulting from the elastic net Cox regression model can

be interpreted as an estimate of the logarithm of the hazard ratio of mortality. We calibrated this parameter into an age estimate by performing a linear transformation whose slope and intercept terms were chosen by forcing the mean and variance of DNAm GrimAge2 to match that of chronological age in the training data (Figure 1).

Pairwise correlations between DNAmGrimAge2 and its components

DNAm GrimAge2 correlates positively with its underlying components DNAm GDF15, DNAm TIMP1, DNAm CystatinC, DNAm B2M and chronological age (Pearson correlation r between 0.79 and 0.89, Supplementary Figure 2B). The new DNAm surrogate markers for logCRP and logA1C are positively correlated with DNAm GrimAge2 (r=0.58 and r=0.47) but only weakly with chronological age (r ~0.26). The fact that leptin levels are higher in females [20, 21] explains the strong correlation between DNAm Leptin and Female (r=0.88, Supplementary Figure 2B). Leptin suppresses hunger and is expected to exhibit a negative correlation with mortality/morbidity risk. Indeed, DNAm Leptin exhibits negative correlations with DNAm GrimAge2. The fact that GrimAge2 is defined as a mortality risk predictor explains its high correlation (r=0.42, Supplementary Figure 2B) with the deviance residuals from the Cox proportional hazards model (Methods).

Independent validation data

We compared the old and new versions of GrimAge in independent validation in datasets consisting of n=13,399 blood samples from 10,065 individuals from nine epidemiological cohorts including the FHS *test* data (Table 1 and Supplementary Note 2). The validation datasets consist of three racial/ethnic groups: 63% European ancestry (72% of all blood samples considered due to repeated measurements), 30% African Americans (22% blood samples) and 7% Hispanic ancestry (6% blood samples). The mean age at blood draw was

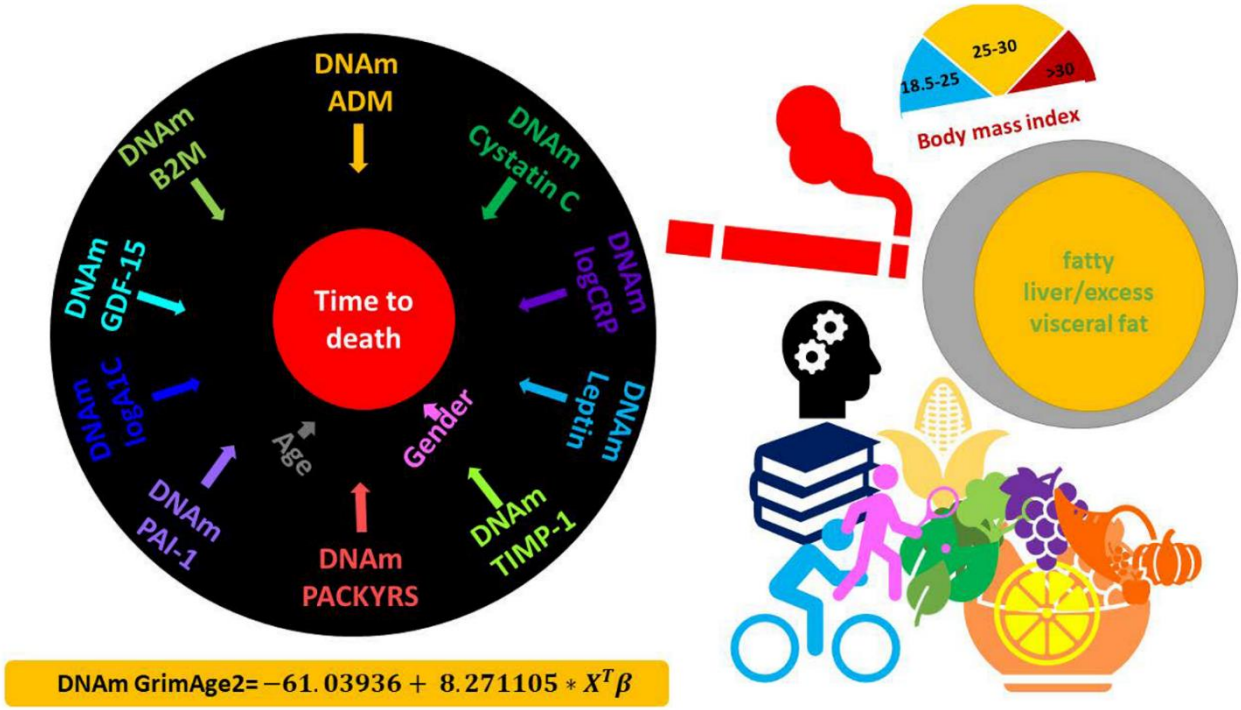

Figure 1. DNAm GrimAge2. The left panel displays the components of GrimAge2 trained by Cox regression with an elastic net penalty. The elastic net regression model automatically selected the following covariates: chronological age (Age), gender (Female), and ten DNAm based surrogates for smoking pack-years (DNAm PACKYRS), adrenomedullin levels (DNAm ADM), beta-2 microglobulin (DNAm B2M), cystatin C (DNAm Cystatin C), growth differentiation factor 15 (DNAm GDF-15), leptin (DNAm Leptin), log-scale high sensitivity C-reactive protein (DNAm logCRP), log-scale hemoglobin A1C (DNAm logA1C), plasminogen activation inhibitor 1 (DNAm PAI-1), tissue inhibitor metalloproteinase 1 (DNAm TIMP-1). The linear combination of the covariate values $X^T\beta$ was linearly transformed to be in units of years, as described in the bottom. Technically speaking, DNAm GrimAge2 is an epigenetic clock for mortality risk. Metaphorically speaking, it estimates biological age in units of years. The right panel displays selective factors including diet, lifestyle and clinical biomarkers that were significantly associated with age acceleration measure of GrimAge2 or age-adjusted DNAm biomarkers underlying GrimAge2 in our downstream analysis.

67.9 years with a standard deviation of SD=11.33. The mean follow-up time was 13.0 (SD=6.90) years with a mortality rate of 39%. More females (71%) than males were present in our validation data.

To demonstrate that DNAm GrimAge2 is more strongly associated with mortality risk than DNAm GrimAge, we applied both biomarkers to nine different study cohort studies: 1) the test data from the FHS, 2) BA23 and 3)EMPC study from the Women's Health Initiative (WHI) with three racial groups, 4) African Americans from the Jackson Heart Study (JHS), 5) the InCHIANTI cohort study, 6) individuals of European ancestry from Baltimore Longitudinal Study of Aging (BLSA), 7) Lothian Birth Cohort 1921 (LBC1921) and 8) Lothian Birth Cohort 1936 (LBC1936), and 9) individuals of European ancestry from Normative Aging Study (NAS, only recruiting male participants).

We also applied new and old GrimAge clocks to saliva samples.

Relation to age

Chronological age is highly correlated with DNAmGrimAge (***r*** ~0.78 to 0.95) and DNAmGrimAge2 (***r*** ~0.72 to 0.94, Supplementary Figure 3) at each cohort except LBC1921 and LBC1936, in which the low correlation estimates reflect that all subjects of the Lothian *Birth* cohorts were born in the same years - either 1921 or 1936 i.e. there is minimal variation in ages in these cohorts. The age correlation is lower with DNAm GrimAge2 compared with DNAm GrimAge, which may reflect the addition of two new variables (DNAm logCRP and DNAm logA1C). Unless indicated otherwise, we used the age-adjusted versions of GrimAge, i.e. the age acceleration measures AgeAccelGrim2 and AgeAccelGrim. The two GrimAge acceleration measures are highly correlated (***r***~0.92 to 0.97, Supplementary Figure 4).

We also defined age-adjusted versions of our DNA-based surrogate markers (for smoking pack-years and the nine plasma protein levels). To interpret the effect size of DNAm protein, we scaled the DNAm based estimators of plasma proteins based on the distributions in the FHS training data (Supplementary Table 1.2), e.g. the scaled version of DNAm logCRP is denoted as s.DNAmlogCRP and one unit of s.DNAmlogCRP denotes one standard deviation of DNAm logCRP.

Mortality risk analysis

We find that AgeAccelGrim2 is significantly associated with race in both WHI BA23 (Supplementary Figure 5A, Kruskal-Wallis $P=4.9x10^{-13}$) and WHI EMPC (Supplementary Figure 5C, $P=4.4x10^{-15}$). Both cohorts show the same trend: African-Americans have higher values of AgeAccelGrim2 than Hispanics and Caucasians. African-American and Hispanic women are on average 1.7 years ($P=1.5x10^{-13}$) and 0.5 years (P=4.2x10-3) older than Caucasian women according to AgeAccelGrim2 evaluated in the WHI BA23. A similar pattern can be observed for the original version of GrimAge (Supplementary Figure 5B, 5D). We briefly mention that different patterns can be observed for other epigenetic clocks and Caucasians [22].

We find that GrimAge2 outperforms GrimAge across a broad category of lifespan and healthspan related variables as summarized in Table 2.

All of our statistical analyses adjusted for obvious confounders such as racial/ethnic group, age, sex, or batch of data generation (e.g. in the LBC1936, Methods). We applied fixed effects meta analysis models (weighted by inverse variance) to combine the results for predicting all-cause mortality risk (time-to-death) from a total of 15 strata formed within the nine epidemiological cohorts.

Our meta-analysis shows that AgeAccelGrim2 (meta P-value=$3.6x10^{-167}$ for AgeAccelGrim2, Figure 2A) is a more significant predictor of time-to-death (due to all-cause mortality) than the original AgeAccelGrim (meta P-value=$2.6x10^{-144}$ for AgeAccelGrim, Figure 2B). The same applies when the analysis is restricted to former/current smokers (Figure 3C, 3D), never-smokers (Figure 3E, 3F), or specific racial groups. For instance, in postmenopausal African American women from the WHI BA23 study, a one-year increase in age acceleration is associated with a hazard ratio HR=1.08 (Cox regression $P=1.0x10^{-10}$) for AgeAccelGrim2, which is more significant than that for AgeAccelGrim (HR=1.07, $P=4.0x10^{-7}$, Figure 2A, 2B). The improvements of version 2 can be observed in all strata except for data set 2 from LBC1936. However, the two versions of GrimAge work almost equally well in this exception once the analysis is stratified by smoking status (Figure 3C–3F). In particular, a one-year increase in AgeAccelGrim2 ($P=4.0x10^{-7}$) and AgeAccelGrim ($P=3.0x10^{-6}$) are associated with the same hazard ratio (HR=1.10) for mortality risk in data set 2 of LBC1936 (Figure 3C, 3D).

Heart disease and time to cancer

We also compared the two versions of GrimAge with respect to predicting incident time-to-coronary heart disease (time-to-CHD), time to congestive heart failure (time-to-CHF). After adjustment for age, sex, race, batch, Cox regression models revealed that AgeAccelGrim2 has more significant associations with time-to-CHD (P-values: $4.5x10^{-28}$ vs $2.7x10^{-24}$, Figure 3A, 3B) and

time to congestive heart failure (P-values: $4.2x10^{-15}$ vs $6.9x10^{-10}$, Supplementary Figure 6). Both versions of GrimAge lead to similar Cox regression p-values in predicting time-to-any cancer (meta P-values: $1.1x10^{-10}$, vs $5.6x10^{-10}$, Supplementary Figure 7).

Comorbidity index and healthspan

AgeAccelGrim2 greatly outperforms AgeAccelGrim when it comes to associations with a comorbidity index (defined as the total number of age-related conditions, Methods): Stouffer meta analysis $P=3.0x10^{-37}$ for AgeAccelGrim2 versus $P=5.7x10^{-22}$ for AgeAccelGrim, Figure 4A, 4B). The superior performance of GrimAge2 can also be observed when focusing on individual age-related conditions: type 2 diabetes (meta P values: $1.1x10^{-30}$ versus $2.8x10^{-15}$, odds ratios [OR]: 1.07 vs 1.05, Supplementary Figure 8A, 8B), hypertension status (meta P values: $8.8x10^{-20}$ versus $P=2.2x10^{-13}$, OR: 1.05 vs 1.04, Supplementary Figure 9A, 9B), disease free status (meta $P=7.2x10^{-16}$ versus P-value=$1.1x10^{-10}$, Supplementary Figure 10A, 10B) and physical functioning level (meta $P=2.0x10^{-26}$ versus $P=1.3x10^{-17}$, Supplementary Figure 11A, 11B).

Age at menopause

We have previously shown that age at menopause in women is negatively associated with epigenetic age acceleration [23, 24]. Here we performed the regression analysis of epigenetic age acceleration measures (as dependent variables) on age at menopause (as an independent variable) and potential confounders. We found that both AgeAccelGrim2 and AgeAccelGrim were higher on average for those with an earlier age at menopause. One year earlier in age at menopause was associated with 0.08 additional years of AgeAccelGrim2 (meta P-value=$5.4x10^{-16}$) and 0.07 years of AgeAccelGrim (meta P-value=$8.5x10^{-16}$, Supplementary Figure 12A, 12B).

DNAm estimates of CRP, A1C, and PAI-1

Our previous study revealed that DNAm PAI-1 (plasminogen activator inhibitor 1) is associated with a host of age-related conditions [1]. Here we show that the two new DNAm biomarkers DNAm logCRP and DNAm logA1C exhibit comparable patterns with many age-related conditions. These three DNAm based surrogates of plasma proteins are sometimes superior to AgeAccelGrim2 for their strength of association with age-related traits such as the comorbidity index: Stouffer P-value=$1.0x10^{-61}$ for DNAm logA1C, $P=1.3x10^{-54}$ for DNAm logCRP, $P=5.0x10^{-57}$ for DNAmPAI-1, and $P=3.0x10^{-37}$ for AgeAccelGrim2 (Figure 5). Compared to AgeAccelGrim2, these three biomarkers show stronger positive associations with type 2 diabetes (led by DNAm logA1C: meta P-value =$5.8x10^{-155}$, Supplementary Figure 8), hypertension (led by DNAm PAI-1: meta P-value=$5.8x10^{-43}$, Supplementary Figure 9), and disease free status (led by DNAm logCRP: meta P-value=$4.0x10^{-21}$ but not in DNAm logA1C, Supplementary Figure 10).

Lower values of DNAm logCRP (meta P-value= $6.5x10^{-33}$) and AccelGrim2 (meta P-value=$2.0x10^{-26}$, Supplementary Figure 10) are associated with higher levels of physical functioning. These three age-adjusted DNA based biomarkers of plasma proteins are also associated with time-to-CHD (Figure 4), time-to-CHF, time-to-any cancer, and early age at menopause (Supplementary Figures 7, 8, 11) but P values are higher (i.e. less statistically significant) than those observed for AgeAccelGrim2 with one exception: time to CHF where age-adjusted DNAm logCRP ($P=6.0x10^{-16}$) and AgeAccelGrim2 ($4.2x10^{-15}$, Supplementary Figure 6) show comparable associations.

GrimAge analysis of diet and clinical biomarkers

Here we revisit the cross sectional relationships between GrimAge and dietary variables, clinical biomarkers, educational attainment [1, 25].

Our previous cross sectional analysis was based on approximately n=4000 postmenopausal women from the WHI. Here we greatly increased the sample size to n=13,420 blood samples from nine validation datasets. In total, we investigated 61 variables including 27 self-reported diet, 9 dietary biomarkers based on blood samples, and 19 clinical biomarkers for vital signs, metabolic traits, and markers of inflammation, cognitive function, lung function, anthropometric traits (Methods and Supplementary Table 2.1).

We correlated our DNAm based biomarkers with clinical plasma based biomarkers for inflammation/infection including interleukin 6 in plasma [IL-6], tumor necrosis factor [TNFA]), lung function (forced expiratory volume in one second [FEV1]), and cognitive function based on Mini–Mental State Examination (MMSE).

We also investigated oral supplements (vitamins, selenium, etc.) and biomarkers of aging such as leukocyte telomere length (LTL) and hand grip strength.

We used a robust correlation test (biweight midcorrelation bicor) that is less sensitive to outlier data points [26]. Our analysis was stratified by sex and racial group within each cohort. The results of different strata were meta-analyzed using the inverse variance weighted fixed effects models (Methods, Figure 6

Table 2. Summary of lifespan and healthspan associations with GrimAges.

Measure	Effect size	AgeAccelGrim2	AgeAccelGrim	Location
Time-to-death				
All[1]	Hazard ratio	1.10 (P=3.6e-167)	1.10 (P=2.0e-144)	Figure 2
Smokers[1]	Hazard ratio	1.10 (P=4.2e-104)	1.10 (P=3.0e-91)	Figure 3
Non smokers[1]	Hazard ratio	1.09 (P=4.4e-43)	1.10 (P=8.1e-34)	Figure 3
Adjusted for blood cell composition[2]	Hazard ratio	1.09 (P=5.2e-123)	1.09 (P=1.1e-104)	Supplementary Figure 16
Time-to-CHD	Hazard ratio	1.08 (P=4.5e-28)	1.08 (P=2.7e-24)	Figure 4
Comorbidity	--	Stouffer's P=3.0e-27	Stouffer's P=5.7e-22	Figure 5
Type 2 diabetes	Odds ratio	1.07 (P=1.1e-30)	1.05 (P=2.8e-15)	Supplementary Figure 8
Disease free	--	Stouffer's P=7.2e-16	Stouffer's P=1.1e-10	Supplementary Figure 10
Mean carotenoids	bicor	-0.29 (P=8.4e-42)	-0.25 (P=4.5e-32)	Figure 6
log2(C-reactive protein)	bicor	0.32 (P=9.9e-276)	0.26 (P=6.2e-178)	Figure 6
FEV1	bicor	-0.31 (P=1.1e-136)	-0.29 (P=2.1e-119)	Figure 6
log2 (Waist/hip ratio)	bicor	0.23 (P=3.9e-69)	0.18 (P=3.6e-45)	Figure 6
Current smoker	bicor	0.35 (P=4.5e-299)	0.36 (P=1.1e-363)	Figure 6
Liver attenuation (Hounsfield unit)	bicor	-0.27 (P=1.18e-14)	-0.24 (P=2.79e-10)	Figure 7
Visceral adipose tissue (CM^3)	bicor	0.22 (P=7.15e-12)	0.20 (P=2.75e-12)	Figure 7
HOMA-IR[3]	bicor	0.16 (5.27e-04)	0.14 (9.74e-03)	Figure 8
Granulocyte	Pearson correlation	0.29 (P=1.2e-232)	0.22 (P=1.1e-126)	Supplementary Figure 15
CD4+T	Pearson correlation	0.26 (P=3.7e-192)	-0.22 (P=6.1e-126)	Supplementary Figure 15

[1]refers to all and stratified by smoking group.

[2]refers to Cox regression models additionally adjusted for blood cell composition/count variables.

[3]GrimAge models were applied to saliva methylation data.

The table briefly summarizes our investigations for the associations of GrimAge2 and GrimAge with (1) mortality analysis across all validation datasets, stratification of smoking status, and specific Cox regression models adjusted for blood cell composition/counts and (2) a broad category of healthspan outcomes. The columns list names of mortality or healthspan related outcomes, type of effect size in association analysis, summary statistics in the format of effect size (meta P value) or Stuffer's P value for AgeAccelGrim2 and AgeAccelGrim, and the location of corresponding figure. Abbreviation: bicor denotes a robust correlation coefficient (biweight midcorrelation [26]).

and Supplementary Tables 2.2–2.13). In general, AgeAccelGrim2 has more significant associations than AgeAccelGrim (Figure 6 and Supplementary Tables 2.2–2.13). Inflammation biomarkers such as CRP levels showed stronger positive correlations with AgeAccelGrim2 (meta bicor=0.32, P-value=$9.9x10^{-276}$) than with AgeAccelGrim (meta bicor=0.26 and P-value= $6.2x10^{-178}$, Figure 6). Body fat distribution measures such as waist to hip ratio showed stronger positive correlation with AgeAccelGrim2 (meta bicor=0.23 and P-value=$3.9x10^{-69}$) than with AgeAccelGrim (meta bicor=0.18 and P-value=$3.6x10^{-45}$, Figure 6). Similarly, measures of lipid, insulin or glucose metabolism (triglyceride, HDL, hemoglobin A1C, insulin and glucose), TFNA, IL-6, plasma creatinine and body mass index (BMI) had stronger associations with AgeAccelGrim2 than AgeAccelGrim. AgeAccelGrim2 correlates with lung functioning (FEV1: meta bicor= -0.31, P-value=$1.1x10^{-136}$), brain functioning (mini mental state exam [MMSE]: meta bicor=-0.10, P-value=$1.4x10^{-18}$), leukocyte telomere length (LTL: meta bicor= -0.13, P-value=$3.2x10^{-9}$) and hand grip strength (meta bicor= -0.09, P-value=$6.4x10^{-13}$, Figure 6). The original measure of AgeAccelGrim exhibits weaker correlations with these variables except for LTL (meta bicor= -0.13, P-value=$7.9x10^{-10}$ for AgeAccelGrim). FEV1 shows strong correlation with (age-adjusted) DNAm PACKYRS (meta bicor= -0.27 and P-value=$5.6x10^{-97}$); however, it has even stronger associations with AgeAccelGrim2 (meta bicor= -0.31 and P-value=$1.1x10^{-136}$) and AgeAccelGrim (meta bicor= -0.29 and P-value=$2.1x10^{-119}$, Figure 6).

The identified associations with dietary variables and lifestyle factors are in general more significant for AgeAccelGrim2 than for AgeAccelGrim. AgeAccelGrim2 correlates negatively with plasma based biomarkers measuring vegetable consumption including mean carotenoid levels (meta bicor=-0.29, P-value=$8.4x10^{-42}$, Figure 6). Far less significant associations could be observed for self-reported measures of fruit- and vegetable intake, which

highlights the limitations of self-reported measures of dietary intake. AgeAccelGrim2 was inversely related to (self-reported) proportion of carbohydrate, fruit/vegetable consumption, and various supplements including calcium, vitamin C, and folic acid. AgeAccelGrim2 was positively related to self-reported fat intake but with protein intake.

Lastly, higher levels of education and income are associated with lower AgeAccelGrim2.

DNAm plasma proteins versus diet and clinical biomarkers

All (age-adjusted) DNAm-based biomarkers correlated with a large number of variables across the diet and clinical biomarker outcome categories (Figure 6 and Supplementary Tables 2.3–2.12). Age-adjusted DNAm PAI-1, DNAm logCRP and DNAm logA1C and DNAm PACKYRS stand out. Insulin, glucose and triglyceride are more strongly associated with DNAm PAI-1 or

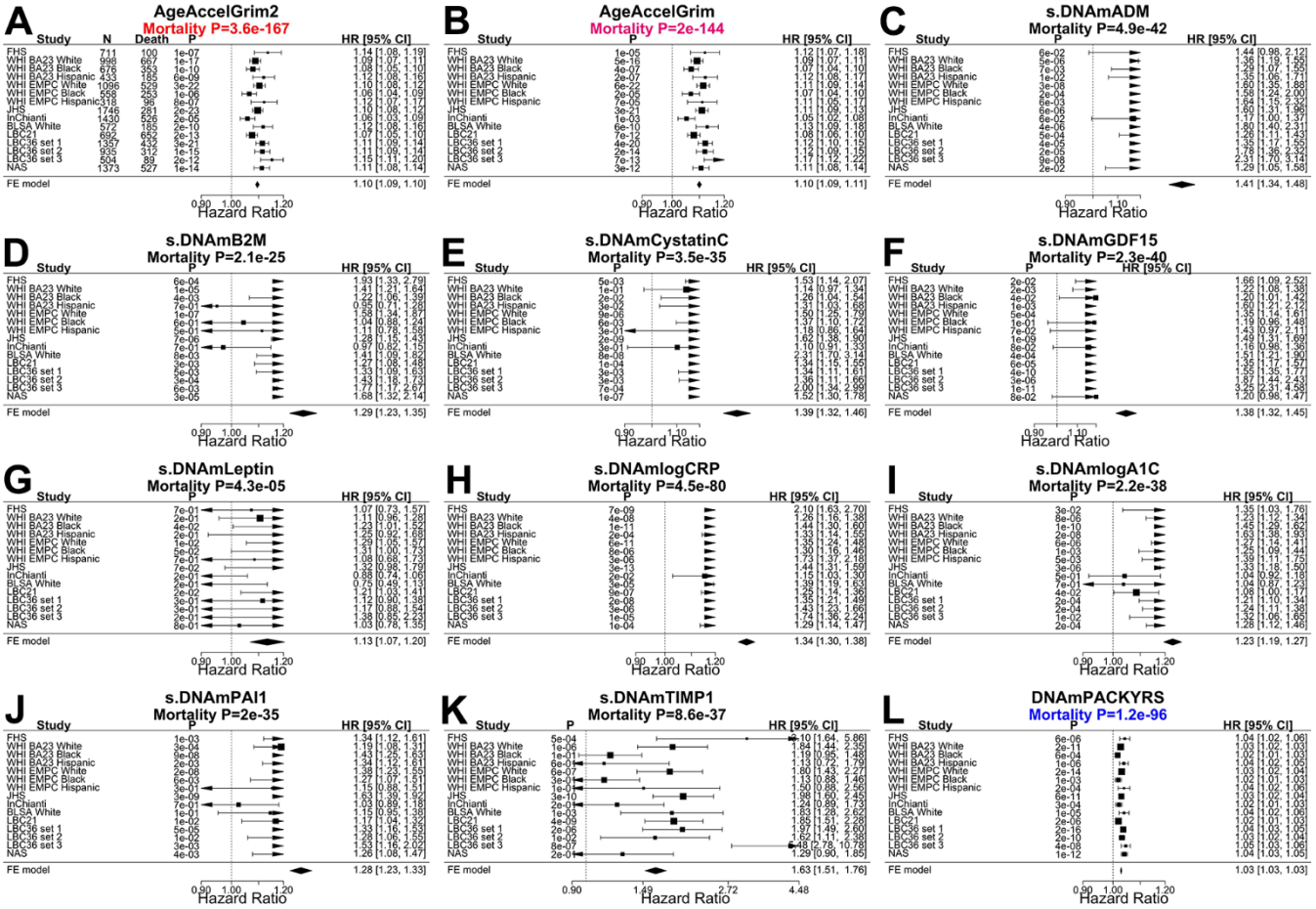

Figure 2. Meta analysis forest plots for predicting time-to-death due to all-cause mortality. Fixed effect meta analysis was performed to combine mortality analysis across 15 strata from 9 study cohorts: FHS test data, Women's Health Initiatives (WHI) BA23, WHI EMPC, Jackson Heart Study (JHS), InCHIANTI (baseline and the third follow-up), Baltimore Longitudinal Study of Aging (BLSA), Lothian Birth Cohort 1921 (LBC21) and LBC 1936 (LBC36), and Normative Aging Study (NAS). Each panel reports a meta analysis forest plot for combining hazard ratios predicting time-to-death based on a DNAm based biomarker (reported in the figure heading) across different strata formed by racial group within cohort and set within LBC36. (**A**, **B**) display the results for AgeAccelGrim2 and AgeAccelGrim. Each row reports a hazard ratio (for time-to-death) and a 95% confidence interval resulting from a Cox regression model in each of 15 strata. (**C**–**L**) display the results for (age-adjusted) DNAm based surrogate markers of (**C**) adrenomedullin (ADM), (**D**) beta-2 microglobulin (B2M), (**E**) cystatin C (Cystatin C), (**F**) growth differentiation factor 15 (GDF-15), (**G**) leptin, (**H**) log scale of C reactive protein (CRP), (**I**) log scale of hemoglobin A1C, (**J**) plasminogen activation inhibitor 1 (PAI-1), (**K**) tissue inhibitor metalloproteinase 1 (TIMP-1) and (**L**) smoking pack-years (PACKYRS). The sub-title of each panel reports the meta analysis P-value. (**A**, **B**) Each hazard ratio (HR) corresponds to a one-year increase in AgeAccel. (**C**–**K**) Each hazard ratio corresponds to an increase in one-standard deviation. (**L**) Hazard ratios correspond to a one-year increase in pack-years. The most significant meta analysis P-value is marked in red (AgeAccelGrim2), followed by hot pink (AgeAccelGrim) and blue (DNAm PACKYRS), respectively.

DNAm logA1C than with AgeAccelGrim2. For example, triglyceride levels have a positive correlation with DNAm PAI-1 (meta bicor=0.34 and P-value=$9.6x10^{-267}$) that is double the magnitude of its association with AgeAccelGrim2 (meta bicor=0.17 and P-value=$8.3x10^{-63}$). As expected, the highest correlation with CRP is DNAm logCRP (meta bicor=0.36 and P-value=$6.6x10^{-358}$) and the highest correlation with A1C is DNAm logA1C (meta bicor=0.25 and P=$8.6x10^{-12}$). As noted, the latter one was only based on 711 individuals from FHS test data. The analysis stratified by sex can be found in Supplementary Figure 13.

Computed tomography measures of fatty organs

Computed tomography imaging techniques provide "shadow images of fat" that can be used for the indirect quantification of organ quality (e.g. liver). Radiographic pixels measure the density of an organ (referred to as attenuation) in Hounsfield units (HU). Computed tomography scans are used for diagnosing fatty liver disease: a low density/attenuation value (low HU) is associated with *high* fat content in the liver. Previously, we analyzed CT scan data from liver, spleen, paraspinal muscle, visceral adipose tissue (VAT), and subcutaneous

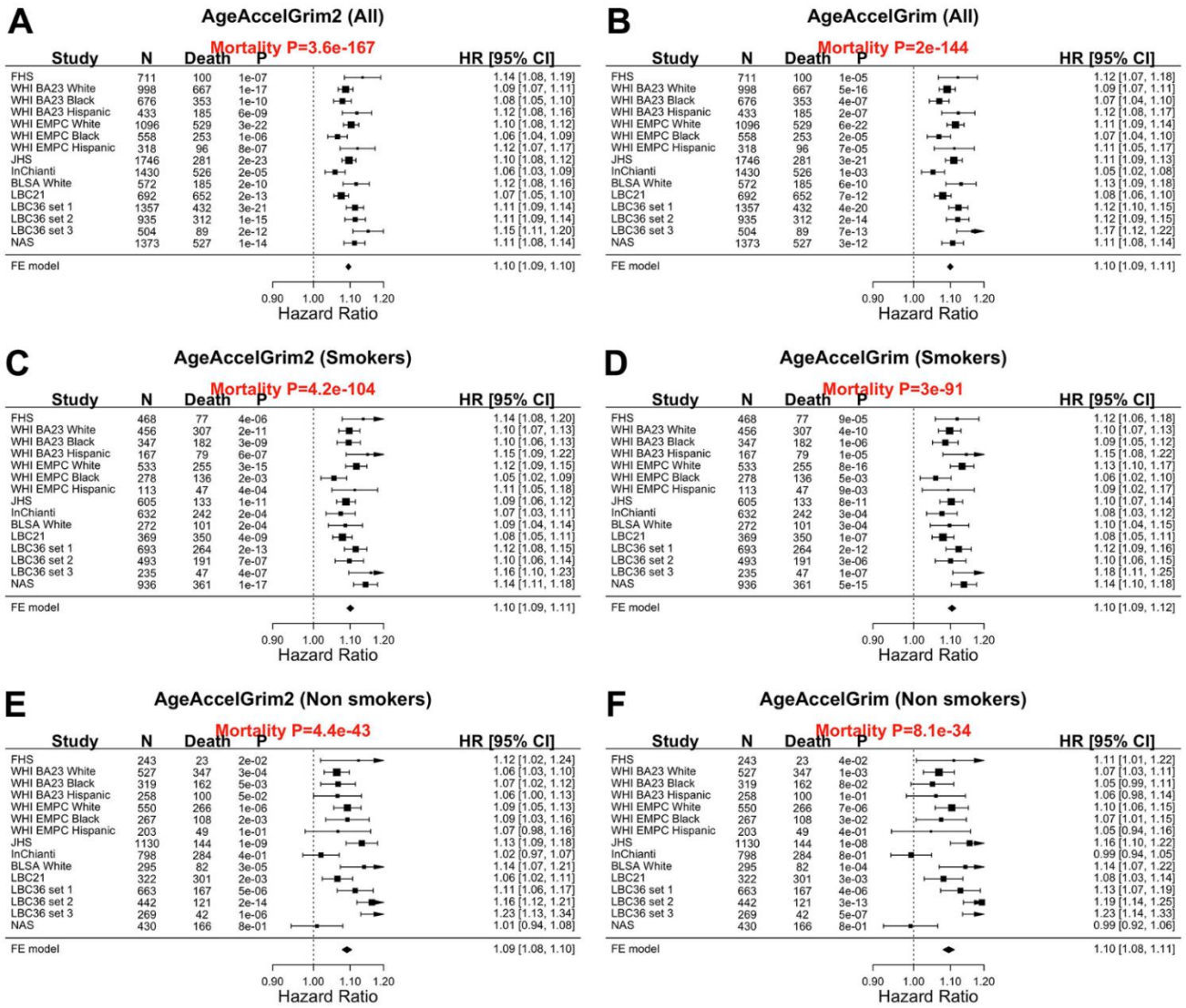

Figure 3. Meta analysis forest plots for predicting all-cause mortality in all, smokers and non-smokers. Fixed effect models meta analysis was performed to combine mortality analysis across 15 strata from 9 study cohorts. Analysis was performed across different strata formed by racial groups within cohort and set within LBC36, using (**A**, **B**) all individuals, (**C**, **D**) smokers (former and current), and (**E**, **F**) non-smokers, respectively. Each panel reports a meta-analysis forest plot for combining hazard ratios predicting time-to-death based on AgeAccelGrim2 (on the left panel) and AgeAccelGrim (on the right panel). The sub-title of each panel reports the meta analysis P-value. Each hazard ratio (HR) corresponds to a one-year increase in AgeAccel measure.

adipose tissue (SAT) from FHS [27, 28]. Volumetric measures of adipose tissue are also available for SAT and VAT volume measures (in units of CM^3). With the exception of muscle, CT values exhibit only weak correlations with chronological age (Supplementary Figure 14).

Previously, we showed that AgeAccelGrim and DNAm PAI-1 were strongly associated with CT-derived measures of adiposity [1]. Here we revisit this analysis using GrimAge2 (Figure 7)

We find that AgeAccelGrim2 outperforms AgeAccelGrim when it comes to associations with CT-derived measures of adiposity in both genders (Figure 7). For example, both AgeAccelGrim2 and AgeAccelGrim are negatively correlated with liver density (bicor= -0.27 [$P=1.18x10^{-14}$] and bicor=-0.24 [$P=2.79x10^{-10}$]) and positively correlated with VAT volume (bicor=0.26 [$P=1.34x10^{-15}$] and bicor=0.22 [$P=7.15x10^{-12}$], Figure 7).

The strong marginal correlations between AgeAccelGrim2 and CT measures are not confounded by BMI or sex as can be seen by several multivariate regression models that regressed AgeAccelGrim2 (dependent variable) on BMI, sex, and several CT derived measures of organ density and fat volume

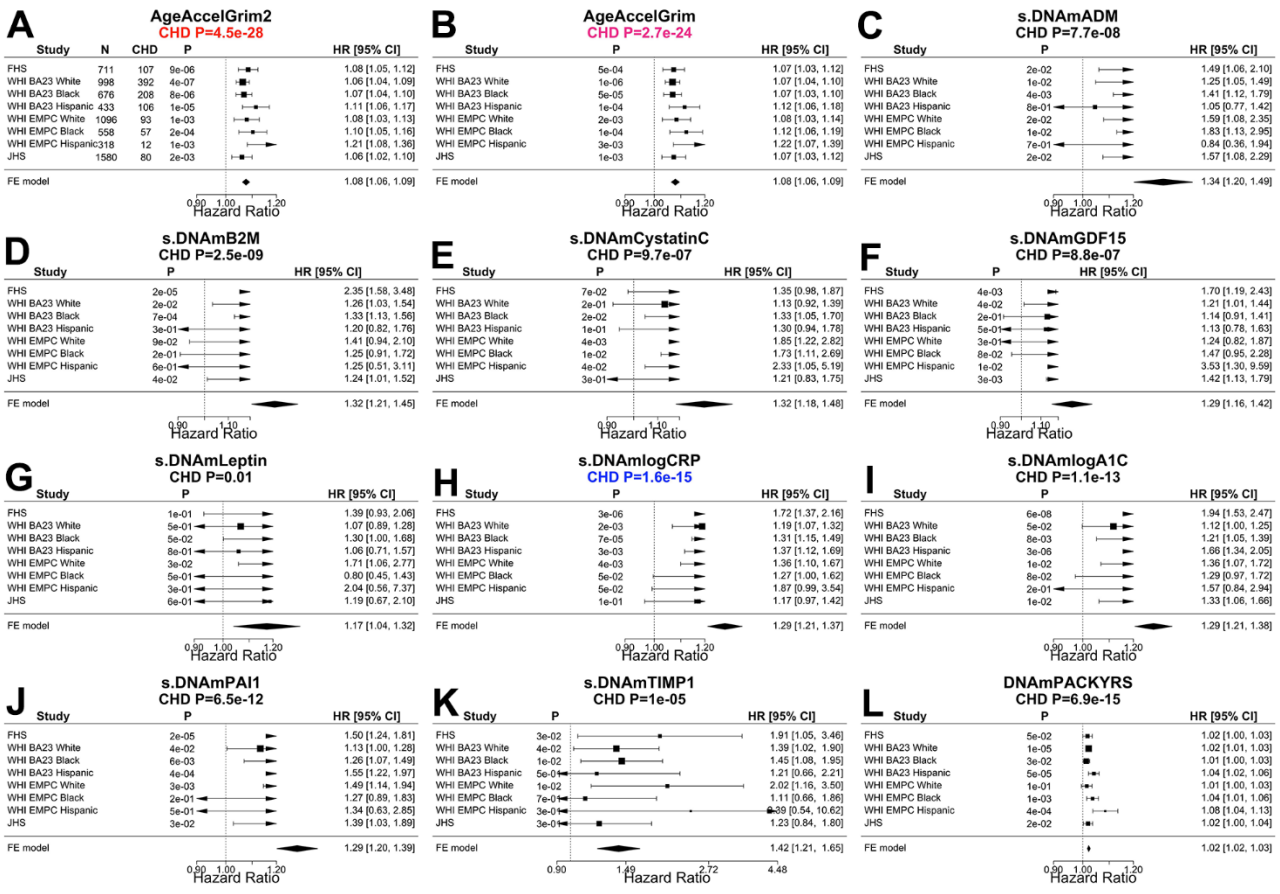

Figure 4. Meta analysis forest plots for predicting time-to-coronary heart disease. Fixed effect models meta analysis was performed to combine Cox regression analysis of coronary heart disease (CHD) across 8 strata from 4 study cohorts. Each panel reports a meta analysis forest plot for combining hazard ratios predicting time-to-CHD based on a DNAm based biomarker (reported in the figure heading) across different strata formed by racial groups within the cohort. (**A**, **B**) Results for AgeAccelGrim2 and AgeAccelGrim. Each row reports a hazard ratio (for time-to-CHD) and a 95% confidence interval resulting from a Cox regression model in each strata. (**C**–**L**) display the results for (age-adjusted) DNAm based surrogate markers of (**C**) adrenomedullin (ADM), (**D**) beta-2 microglobulin (B2M), (**E**) cystatin C (Cystatin C), (**F**) growth differentiation factor 15 (GDF-15), (**G**) leptin, (**H**) log scale of C reactive protein (CRP), (**I**) log scale of hemoglobin A1C, (**J**) plasminogen activation inhibitor 1 (PAI-1), (**K**) tissue inhibitor metalloproteinase 1 (TIMP-1) and (**L**) smoking pack-years (PACKYRS). The sub-title of each panel reports the meta analysis P-value. (**A**, **B**) Each hazard ratio (HR) corresponds to a one-year increase in AgeAccel. (**C**–**K**) Each hazard ratio corresponds to an increase in one-standard deviation. (**L**) Hazard ratios correspond to a one-year increase in pack-years. The most significant Meta analysis P-value is marked in red (AgeAccelGrim2), followed by hot pink (AgeAccelGrim) and blue (DNAm logCRP), respectively.

(Methods, Models I-IV in Supplementary Table 3.1). Even after adjusting for potential confounders, AgeAccelGrim2 exhibits a significant association with liver density ($P=5.3x10^{-6}$), spleen density (P=0.04) but not muscle density (P=0.17 in Model I in Supplementary Table 3.1). A multivariate model analysis, which adjusts for sex, age, and BMI reveals that AgeAccelGrim2 exhibits more significant associations for VAT volume ($P= 7.5x10^{-6}$) than SAT, which supports the widely held view that VAT is more dangerous than SAT. AgeAccelGrim2 is more sensitive to volumetric measures of VAT (in units of cm^3 and $P=2.1x10^{-3}$) compared to density based VAT (in units of HU, P>0.9, Supplementary Table 3.1). A comprehensive multivariate model (Model IV) that includes both organ density measures and volumetric measures of SAT/VAT reveals that liver density ($P=2.6x10^{-4}$) exhibits the most significant association with AgeAccelGrim2. All multivariate regression models show that BMI is no longer associated with AgeAccelGrim2 after adjusting for liver density, which suggests that liver density mediates the relationship between BMI and AgeAccelGrim2 (Supplementary Table 3.2)

Age-adjusted DNAm-based surrogate markers of PAI-1, exhibit the strongest associations with the CT measures, followed by the surrogates of our two new proteins, A1C and CRP (Figure 7). These three DNAm based proteins outperform AgeAccelGrim2 when it comes to

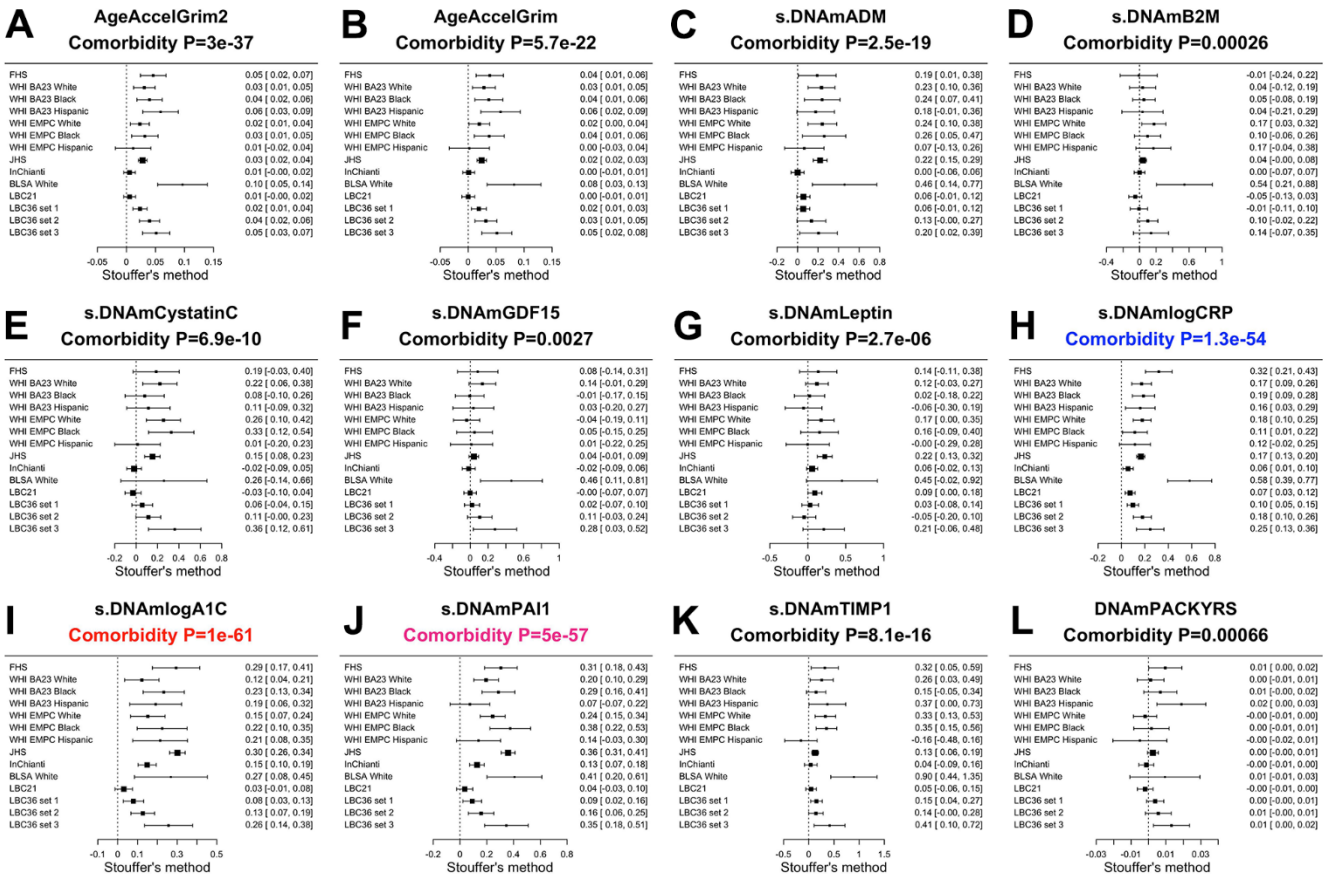

Figure 5. Meta analysis of associations with total number of age-related conditions. Each panel reports a meta analysis forest plot based on Stouffer's method for combining regression analysis Z statistics between the comorbidity index and the DNAm-based biomarker (reported in the figure heading) across different strata, which are formed by racial group within cohort and set within LBC36. (**A**, **B**) display the results for AgeAccelGrim2 and AgeAccelGrim. (**C**–**L**) display the results for scaled DNAm based surrogate markers of (**C**) adrenomedullin (ADM), (**D**) beta-2 microglobulin (B2M), (**E**) cystatin C (Cystatin C), (**F**) growth differentiation factor 15 (GDF-15), (**G**) leptin, (**H**) log scale of C reactive protein (CRP), (**I**) log scale of hemoglobin A1C, (**J**) plasminogen activation inhibitor 1 (PAI-1), (**K**) tissue inhibitor metalloproteinase 1 (TIMP-1) and (**L**) smoking pack-years (PACKYRS). The sub-title of each panel reports the meta analysis p-value. Each row reports a beta coefficient β and a 95% confidence interval resulting from a (linear-mixed) regression model in each strata (defined by cohort racial group). (**A**, **B**) Each β corresponds to a one-year increase in AgeAccel. (**C**–**K**) Each β corresponds to an increase in one-standard deviation. (**L**) β corresponds to a one-year increase in pack-years. The most significant meta-analysis P-value is marked in red (DNAm logA1C), followed by hot pink (DNAm PAI1) and blue (DNAm logCRP), respectively.

the association with CT-derived measures of adiposity (liver fat and measures of SAT and VAT in Figure 7 and Supplementary Tables 3.1, 3.3–3.5). For example, DNAm PAI1 is highly significantly associated all the CT measures including positive correlations with VAT volume (r=0.41, P=4.68x10^{-41}) and SAT volume (r=0.27, P=6.07x10^{-23}), and negative correlations with liver density (r=-0.41, P=6.61x10^{-39}), VAT density (r=-0.35, P=1.3x10^{-32}), and spleen density (r=-0.22, P=5.87x10^{-15}, Figure 7). A multivariate regression analysis of age-adjusted PAI-1 (dependent variable) reveals highly significant associations with liver density (P=6.3x10^{-16} in Model I) and VAT volume (P=1.0x10^{-13}, Model II in Supplementary Table 3.3) even after adjusting for BMI and other confounders. Including all CT variables as covariates in a multivariate model reveals significant associations with liver density (P=1.40x10^{-9}), VAT volume (P=9.3x10^{-8}), and SAT volume (P=0.02, Model IV in Supplementary Table 3.3). Model III shows that DNAm PAI1 is more

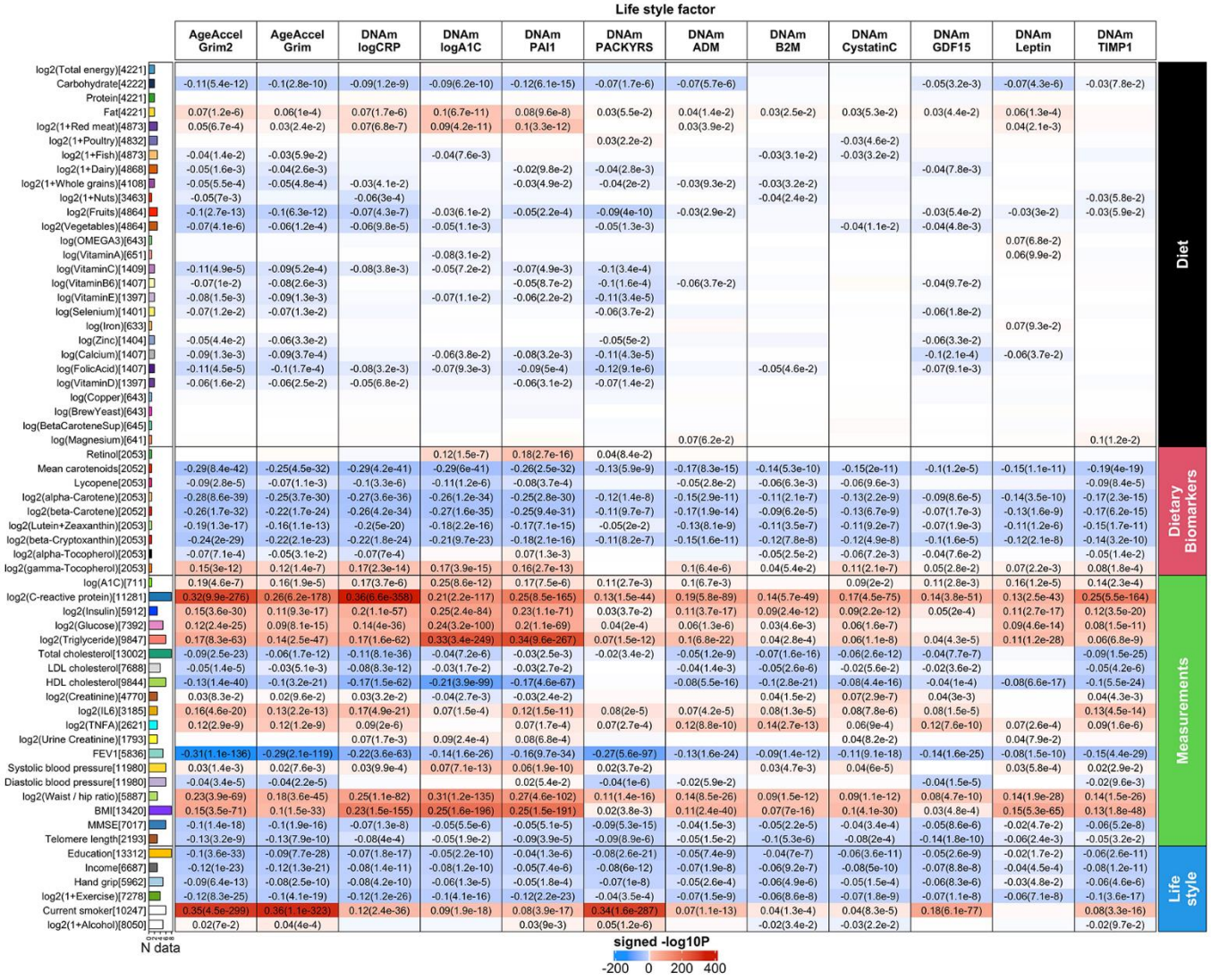

Figure 6. Meta cross-sectional correlations with diet, clinical biomarkers and lifestyle factors. Robust correlation coefficients (biweight midcorrelation [26]) between 1) AgeAccelGrim2, AgeAccelGrim, and ten age-adjusted underlying DNAm-based surrogate biomarkers underlying DNAmGrimAge2, and 2) 61 variables including 27 self-reported diet, 9 dietary biomarkers, 19 clinically relevant measurements related to vital signs, metabolic traits, inflammatory markers, cognitive function, lung function, central adiposity and leukocyte telomere length, and 6 lifestyle factors including hand grip strength. The y-axis lists variables in the format of name (sample size), followed by a bar plot denoting number of studies. Variables are arranged by category displayed on the right annotation. The x-axis lists AgeAccelGrim2, AgeAccelGrim, followed by DNAm estimates of log CRP, log A1C, PAI-1, smoking pack-years, etc. Each cell presents meta bicor estimates and P-value, provided P<0.1. The color gradient is based on -log10 P-values times sign of bicor. P-values are unadjusted. An analogous analysis stratified by gender can be found in Supplementary Figure 12.

associated with VAT and SAT in volume measures than with density measures (Supplementary Table 3.3). Similar results were observed for DNAm logCRP but not DNAm logA1C (Supplementary Tables 3.4, 3.5). Our analysis shows that DNAm logA1C is more significant related to SAT density ($P=3.0x10^{-5}$) than to SAT volume (P>0.4) and similar statements apply to VAT density ($P=8.0x10^{-5}$) and VAT volume ($P=8.0x10^{-3}$, Supplementary Table 3.5).

Finally, the surrogates of ADM, TIMP-1, leptin exhibit relatively weak correlations with the CT based measures (Figure 7).

Overall, our results suggest that fatty liver and excess VAT are the most significant CT-based correlates of (age-adjusted) DNAm PAI-1, DNAm logCRP, DNAm logA1C and AgeAccelGrim2.

Association with blood cell composition

DNAm data allow one to estimate several quantitative measures of blood cell types (both proportions and counts) as described in Methods [22, 29]. We previously showed that AgeAccelGrim and several age-adjusted DNAm biomarkers underlying GrimAge exhibited significant correlations with these imputed measures of blood cell composition. Not surprisingly, AgeAccelGrim2 and AgeAccelGrim exhibit similar patterns for their associations with blood cell composition (Supplementary Figures 15–17 and Supplementary Tables 4.1–4.3). The current results are based on a much larger sample size (n>11,600 across our validation datasets) than our previous study (n ~6000). AgeAccelGrim2 was positively correlated with a DNAm based estimates of granulocytes (r=0.29, $P=1.2x10^{-232}$, Supplementary Figure 15A, 15B and Supplementary Table 4.1), plasma

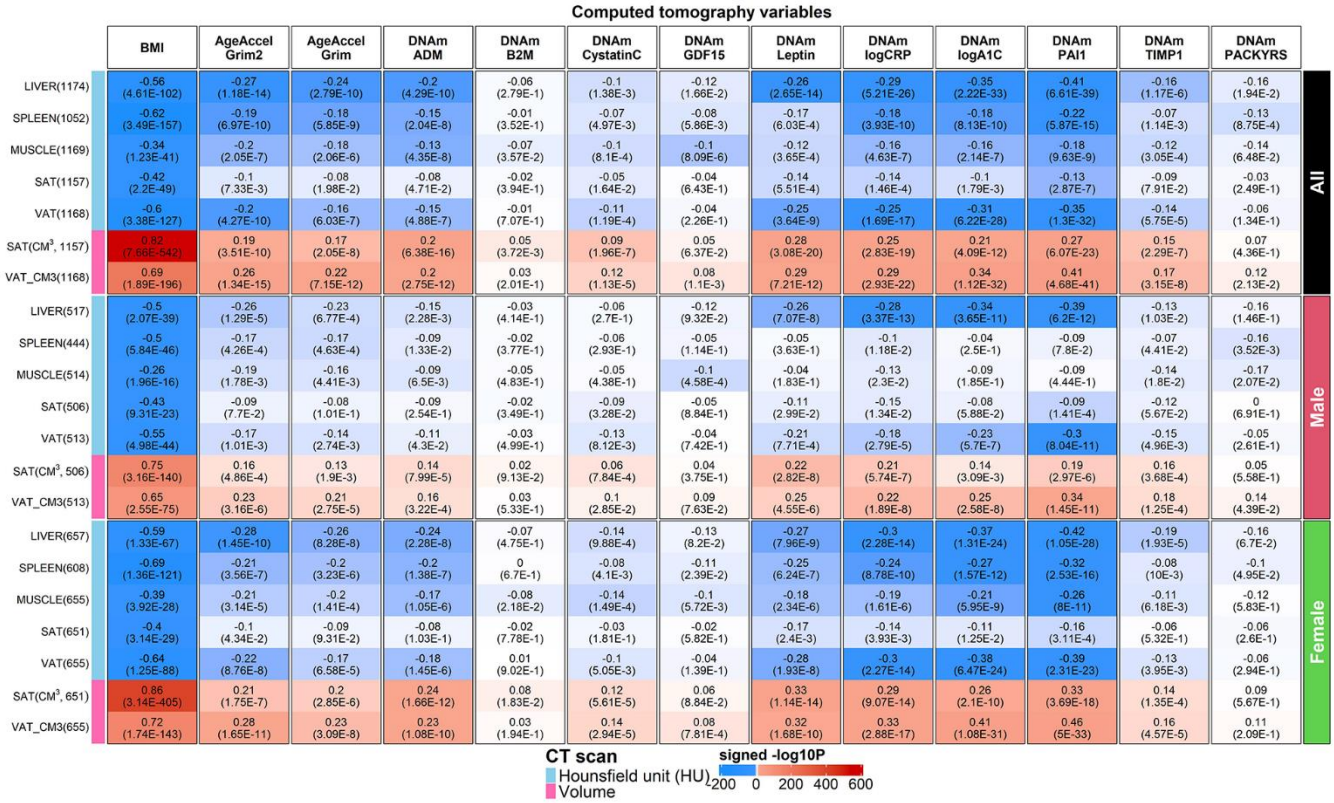

Figure 7. Computed tomography variables versus BMI and age-adjusted DNAm biomarkers in the FHS. Robust correlation coefficients (biweight midcorrelation [26]) between 1) AgeAccelGrim2, AgeAccelGrim, and ten age-adjusted DNAm-based surrogate biomarkers underlying DNAmGrimAge2, and 2) seven computed tomography-derived organ density measures (Hounsfield units) or volumetric measures for subcutaneous adipose tissue (SAT CM^3) or visceral adipose tissue (VAT CM^3). The y-axis lists computed tomography variables in the format of name (sample size in FHS), annotated by variable type. The x-axis lists body mass index (BMI), AgeAccelGrim2, AgeAccelGrim, followed by DNAm variables in alphabetical order. Each cell presents bicor (P-value). P-values are unadjusted and reported based on linear mixed analysis with pedigree as random effect to avoid confounding by pedigree structure. The color gradient is based on -log10 P-values times sign of bicor. We applied the correlation analysis to males and females, respectively, and then combined the results via fixed effect models weighted by inverse variance (listed in the top rows, denoted as "ALL"). The heatmap presents the results based on ALL and stratification results by gender, annotated on the right side.

blasts (r=0.26, P=3.7x10^{-181}) and negatively correlated with CD4+T cells (r = -0.26, P=3.7x10^{-192}) and CD8 naïve cells (r = -0.22, P=2.5x10^{-135}).

Similar to our previous findings, age-adjusted DNAm TIMP-1 exhibits the most significant correlations with the measures of blood cell composition (e.g. proportion of granulocytes r=0.40, P=2.1x10^{-495}, Supplementary Figure 15K). The TIMP-1 protein plays a role in promoting cell proliferation in a wide range of cell types and may also have an anti-apoptotic function [30]. Significant associations can also be observed for age-adjusted DNAm logCRP (proportion of granulocytes r=0.36, P=5.8x10^{-384}), and age-adjusted DNAm Cystatin C (proportion of CD4+ T cells counts r =-0.29, P=1.3x10^{-231}). By contrast, age-adjusted DNAm A1C is not associated with blood cell composition (Supplementary Figure 15I).

The improved performance of AgeAccelGrim2 compared to AgeAccelGrim1 does not reflect confounding by blood cell composition as can be seen from our multivariate Cox regression models that adjusted for seven imputed measures of blood cell counts or proportions (Supplementary Figure 16). AgeAccelGrim2 (P=5.2x10^{-123}) still outperforms AgeAccelGrim when it comes to the association with time-to-death (P=1.1x10^{-104}, Supplementary Figure 16A, 16B) after adjusting for blood cell composition. The same can be observed when predicting time-to-CHD where AgeAccelGrim2 (P=1.2x10^{-20}) outperforms AgeAccelGrim (P=9.2x10^{-18}, Supplementary Figure 17A, 17B). A one standard deviation increase in DNAm logA1C or in DNAm logCRP approximately increases the hazard ratio for CHD by 30% (Figure 4H, 4I). This increased HR is only lowered by 2% (from 1.29 to 1.28 for DNAm logCRP and from 1.29 to 1.27 for DNAm logA1C) after adjusting for blood cell counts (Supplementary Figure 17H, 17I).

Stratifying the analysis by sex indicates that our results are not sex-specific (Supplementary Figures 18, 19 and Supplementary Tables 4.2, 4.3).

Evaluation of younger individuals

Next, we examined the performance of GrimAge clocks on younger individuals (age < 40) using 173 individuals (minimum at 22 and mean age at 35.4 years) from JHS. As expected, AgeAccelGrim2 was still associated with age-related biomarkers including inflammation marker CRP (r=0.26 and P=5.5x10^{-4}), dyslipidemia marker triglyceride levels (r=0.23 and P=2.8x10^{-3}), and body mass index (r=0.25 and P=9.1x10^{-4}, Supplementary Figure 20B–20D). AgeAccelGrim2 is also associated with life style factors such as alcohol assumption (r=0.33 and P=1.3x10-5, Supplementary Figure 20E) and smoking (P=6.0x10^{-7}, Supplementary Figure 20E). The associations remain significant even after adjusting for age and gender in multivariate regression analysis (Supplementary Figure 20). However, DNAmGrimAge2 is not aligned with chronological age in younger individuals. Rather, it exhibits a systematic offset resulting in a median absolute error (MAE) of 11 years (Supplementary Figure 20A). The offset was lower for the original DNAmGrimAge (MAE=4.14 years, Supplementary Figure 20G). However, the original AgeAccelGrim showed less significant associations with all age-related conditions (Supplementary Figure 20H–20K) except for smoking.

GrimAge clocks can be applied to saliva samples

We applied both versions of GrimAge to saliva samples from n=432 mothers from the NHLBI Growth and Health Study (NGHS) cohort [31]. The cohort was a longitudinal study conducted from 1985 to 2000 that studied various factors related to the development of obesity in pre-adolescents (Methods, Supplementary Note 2). Our methylation samples were profiled in saliva from two racial groups: 50% White (n=218) and 50% Black (n=214). The ages of the mothers ranged from 36 to 43 years. The low age correlation estimates with DNAm GrimAge2 (r=0.13) and DNAm GrimAge (r=0.17) reflect the relatively narrow age range (Supplementary Figure 21).

The mean value of DNAmGrimAge2 was 61.6 years which indicates that there is a systematic offset between blood and saliva sample (Supplementary Figure 21A). Systematic offsets can be adjusted for by using multivariate regression models that include an intercept term. Our multivariate linear regression analysis revealed significant associations between saliva based AgeAccelGrim2 (independent variable) and clinically relevant measures (dependent variables): metabolic stress (Z score scale), high sensitivity C-reactive protein, insulin resistance and HOMA for insulin resistance (HOMA-IR) [32] (Methods and Figure 8). By contrast, the original version AgeAccelGrim exhibited less significant associations with these biomarkers (Figure 8).

We briefly mention that age-adjusted DNAm-based surrogate markers of *saliva* PAI-1, log-scale A1C, log-scale CRP, ADM and TIMP1 show significant associations with those clinical measures as well. Analogous to what we found in analyzing CT scan data, saliva based DNAm PAI-1 and A1C are more sensitive biomarkers than AgeAccelGrim2 when it comes to metabolic stress: positive associations with DNAmPAI-1 (P=1.11x10^{-14}), DNAmlogA1C (P=4.42x10^{-13}) or AgeAccelGrim2 (P=1.14x10^{-5}, Figure 8). Overall, this

analysis shows that DNAmGrimAge2 is superior to DNAmGrimAge when it comes to studying the relationship between saliva methylation data and clinical biomarkers of metabolic stress.

Polygenic risk score analysis

Recently, we performed a large-scale genome-wide association study (GWAS, n>40,000) on epigenetic biomarkers including AgeAccelGrim which described a polygenic risk score (PRS) for AgeAccelGrim in individuals of European ancestry [33]. Here, we repeated the PRS analysis in the WHI cohorts and showed that the PRS scores could explain 0.04% to 1.88% variation in AgeAccelGrim and 0.03% to 2.17% in AgeAccelGrim2 in postmenopausal women of European ancestry (Methods, Supplementary Figure 22). The PRS scores based on the SNPs with P<0.01 and P<0.05 tended to explain more variation in both versions of GrimAge acceleration measures.

Epigenome-wide association study of mortality related traits

We carried out epigenome-wide association study (EWAS) for 1) AgeAccelGrim2, 2) AgeAccelGrim, 3) time-to-death and 4) time-to-CHD using our validation data. For the censored time variables (time-to-death and time-to-CHD), we evaluated three Cox regression models: model I is a basic model that adjusted for age, gender and batch effects; model II additionally adjusted for smoking pack-years, and model III additionally adjusted for blood cell composition (Methods).

The individual EWAS results for each cohort were combined via inverse variance weighted fixed effect models (Methods). A considerable number of CpGs exhibit highly significant associations with both AgeAccelGrim2 and AgeAccelGrim (Supplementary Figure 23A, 23B). The cg05575921 on chromosome (Chr) 5, near *AHRR*, shows the strongest negative correlation for both GrimAge clocks (meta P=3.6x 10^{-1253} for AgeAccelGrim2 and P=1.5x10^{-2023} for AgeAccelGrim). The gene *AHRR* (Aryl Hydrocarbon Receptor Repressor) is implicated in regulation of cell growth and differentiation. The CpG cg23842572 on Chr17, near *MPRIP*, shows the strongest positive correlation with AgeAcceGrim2 (P=3.0x10^{-424}) and the CpG cg13525276 on Chr14, near *TSHR*, shows the strongest positive correlation with AgeAccelGrim (P=4.7x10^{-254}). *MPRIP* encodes a protein interacts with both myosin phosphatase and RhoA and *TSHR* encodes

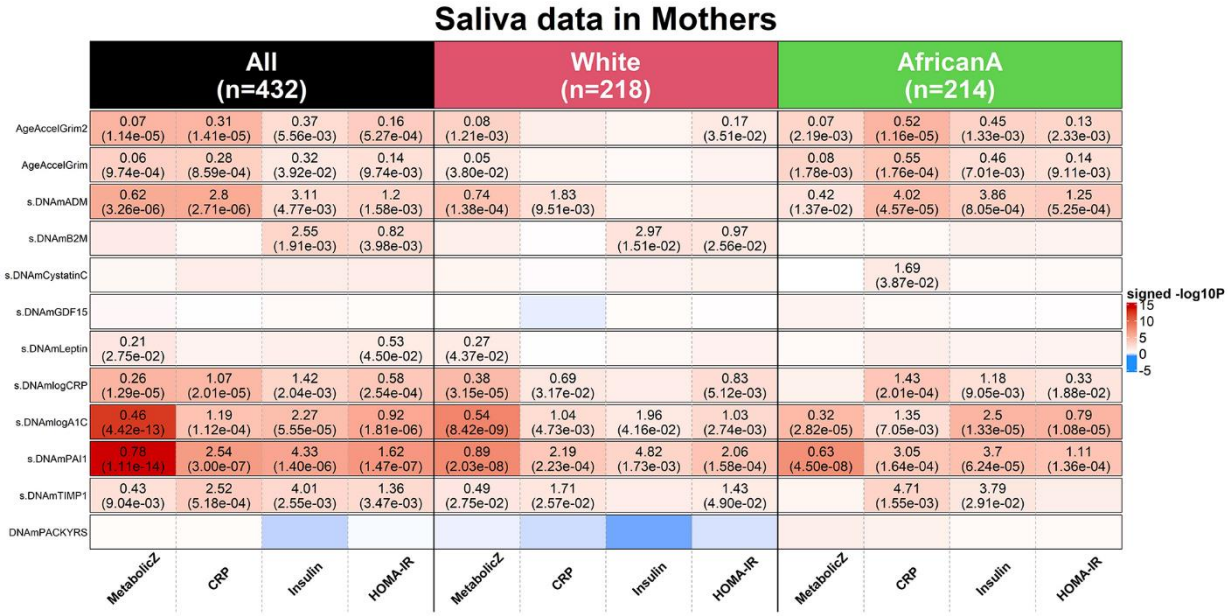

Figure 8. Applications of DNAm GrimAges on saliva methylation data in NGHS. DNAmGrimAge, DNAmGrimAge2 and its components were estimated in saliva methylation data from mothers. Linear regression analysis was performed to study the association between 1) dependent variables: clinically relevant measures: metabolic Z score, high sensitivity C-reactive protein (CRP), insulin resistant and HOMA for insulin resistance (HOMA-IR) [32] and 2) independent variables: AgeAccelGrim2, AgeAccelGrim, and nine scaled DNAm-based surrogates of proteins and DNAmPACKYRS. Regression models were performed in all mothers (n=432) and stratified by ethnic/racial groups: White (n=218) and African American (n=214). Analysis was adjusted for age and batch effect and adjusted for race as needed. The y-axis lists DNAm-based variables and the x-axis lists the clinically relevant measures. Each cell presents beta coefficient (P-value), provided P< 0.05 from the regression analysis. The color gradient is based on -log10 P-values times sign of beta coefficient. All P-values are unadjusted.

the receptor for the thyroid-stimulating hormone (TSH) or thyrotropin. These 3 genes were also identified in the EWAS of time-to-death (Supplementary Figure 23C–23E). Several studies previously showed hypomethylation of cg05575921 on *AHRR* was associated with smoking [34, 35]. Our analysis shows that cg05575921 is the best leading CpG hypo-methylated associated with mortality in Model I ($P=1.2x10^{-69}$). However, cg05575921 is still one of the top CpGs associated with mortality even after adjusting for smoking pack-years (top 10 on Model II, $P= 1.6x 10^{-26}$, Supplementary Figure 23D). Its association with mortality risk is not confounded by blood cell counts as it is the leading CpG associated with mortality in Model III ($P=7.8x10^{-53}$, Supplementary Figure 23E). We also broadly viewed the correlation between EWAS of age acceleration from our GrimAge clocks and EWAS of time-to-death. EWAS results for time-to-death are strongly correlated with those for AgeAccelGrim2 (r=0.616 in mortality Model I and r=0.54 in Model II, Supplementary Figure 24A, 24B). The pairwise EWAS correlation is attenuated (r=0.264, Supplementary Figure 24C) when using Model III which removes the effect of blood cell composition. The EWAS results for time to CHD (n=6143) exhibit a weaker correlation with EWAS of AgeAccelGrim2 (Supplementary Figures 25, 26).

DISCUSSION

Many studies have shown that the original version of GrimAge predicts mortality and morbidity risk (e.g. [8–17]). To arrive at version 2 of GrimAge, we developed two additional DNAm based surrogates for plasma proteins that are widely used in the clinic (DNAm logCRP and DNAm logA1C). Our comprehensive validation analysis show that GrimAge2 outperforms GrimAge with respect to its association with time-to-death, time-to-CHD, time-to-CHF, and assessing the associations with a host of age-related conditions: dysfunctions related to kidney, lung, metabolism, cognitive behavior, lipid, and vital signs, and CT-derived measures of adiposity. The reported associations remain highly significant even after adjusting for seven imputed measures of blood cell composition.

To evaluate the new version of GrimAge, our association analysis covered a broad category of age-related phenotypes including clinically relevant measures and lifestyle behaviors. These results confirm that AgeAccelGrim2 is more strongly associated with age related phenotypes than AgeAccelGrim. Further, our new estimators DNAm logCRP and DNAm logA1C, are associated with a host of age-related conditions. GrimAge2 was trained in 1833 individuals from the FHS cohort aged between 40 and 92 years old (median age at 65). Thus, it is expected to work well in older adults. We demonstrate that it can be applied to younger individuals, but it leads to a systematic offset compared to chronological age. This offset can be removed by using a suitable regression model.

For most protein markers (except for CRP and A1C), the protein measurement preceded the DNA methylation measurement by about 6.6 years. This suggests that the protein measurement (and the accompanying organ dysfunction) affected the methylation levels (as opposed to the other way around).

The first version of GrimAge (AgeAccelGrim) has been used in human clinical trials [36]. Our polygenic risk scores correlate only weakly with AgeAccelGrim2, similar to what has been observed for AgeAccelGrim [33]. Unlike genetic factors, lifestyle factors (as reflected in smoking, mean carotenoid levels, adiposity, educational level) exhibit strong correlations with AgeAccelGrim2. Lifestyle factors also relate to our DNAm based estimates of logCRP, logA1C, PAI-1, and smoking pack-years.

We also showed that GrimAge2 can be applied to saliva methylation data but leads to a noticeable offset.

GrimAge2 will not replace existing clinical biomarkers. Rather, GrimAge2 complements existing clinical biomarkers when evaluating an individual's aging rate.

MATERIALS AND METHODS

Framingham Heart Study cohort for training DNAmGrimAge2

The FHS offspring cohort [19] is a large-scale longitudinal study started in 1948, initially investigating risk factors for cardiovascular disease (CVD, Supplementary Note 2). Previously, we used 2,356 individuals from the FHS in training and testing DNAmGrimAge. In establishing DNAmGrimAge2, we used the same individuals plus about 200 more individuals from the same offspring cohort. Those individuals were excluded in establishing the first GrimAge clock due to lack of protein measures [1]. To build the new mortality clock, we applied more stringent quality controls to remove technical outliers. It yielded a total of 2,544 individuals from 939 pedigrees. We assigned 2/3 pedigrees (1833 individuals/622 pedigrees) to the training data and 1/3 pedigrees (711 individuals from 317 pedigrees) to the test data (Table 1).

The FHS cohort contains medical history and measurements, immunoassays at exam 7, and blood

DNA methylation profiling at exam 8. The technology of immunoassay was based on Luminex xMAP assay, an extension of the enzyme-linked immunosorbent assay (ELISA) performed with multiple analyte-specific capture antibodies bound to a set of fluorescent beads. The measurement of observed CRP, A1C and smoking pack aligned with the measurement of methylation array at exam 8 in FHS offspring cohort. But the measurement of the other seven plasma proteins (exam 7) preceded the measurement of blood DNAm data (exam 8) by 6.6 years, suggesting that the DNAm profiles may not represent a highly accurate snapshot of the status of these proteins at the time of blood collection.

The DNA methylation profiling was based on the Illumina Infinium HumanMethylation450K BeadChip.

Two-stage approach for establishing DNAmGrimAge2

Stage 1: develop DNAmlogCRP and DNAmlogA1C

The training dataset was used to build the two new DNAm based surrogate markers for the log scale of C-reactive protein (logCRP) and log scale of hemoglobin. Both plasma proteins were measured on exam 8. CRP levels were measured based on an immuno-turbidometric array. We scaled the CRP and A1C variables before log transformation and defined extreme values based on the raw values of the observations whose scale values were ≤6 and the closest to 6. The range of winsorized CRP is between 0.14 and 54.01 mg/L and the range of winsorized A1C level is between 4.7% and 10%. We applied log-transformation on the winsorized variables. Our previous DNAmGrimAge involves 1030 CpGs for establishing the surrogate of DNAm proteins or smoking pack-years. Each plasma protein (log CRP or log A1C) was regressed on the 1030 CpGs, chronological age (at exam 8) and sex (an indicator of female) using the elastic net regression model implemented in the R package *glmnet*. Ten-fold cross validation was performed in the FHS training data to specify the underlying tuning parameter λ.

Stage 2: define DNAmGrimAge2

In the second stage, we added chronological age, gender, DNAmlogCRP and DNAmlogA1C, the other 10 previously defined DNAm biomarkers to build a new GrimAge—*DNAmGrimAge2*. All the 12 DNAm biomarkers are moderately correlated with their targets (protein or smoking pack-years). The correlation estimates between DNAm biomarkers and their corresponding targets have a distribution of 0.64±0.12 [0.43, 0.86] (mean±SD [range]) in the training dataset and a distribution of 0.42±0.09 [0.34, 0.66] in the test dataset (Supplementary Table 1). The correlation estimates between DNAm biomarkers and chronological ages have a broad range in both training (0.48±0.31 [0.06, 0.92]) and test dataset (0.45±0.35 [0.05, 0.90], as listed in Supplementary Table 1. Of those, DNAmLeptin shows the lowest age correlation (r ~0.05) and DNAmTIMP1 shows the highest age correlation r~0.90). Regardless of whether the protein measures (based on immune assay) or self-report smoking pack-years were available or not, we estimated the 12 DNAm surrogates for all the FHS individuals (1833 in the training and 711 in the test data).

Definition of DNAm GrimAge

We used an elastic net Cox regression model [37] to regress time-to-death (due to all-cause mortality) since exam 7 on the 12 DNAm based surrogate markers (Supplementary Table 1.1), chronological age, and sex. The elastic net model selected all the available covariates except for DNAm CD56 and DNAm EFEMP1. As part of stage 2, we validated the accuracy of the DNAm based surrogate markers for their observed counterparts in the FHS test dataset. However, the mortality predictor (DNAmGrimAge2) was only fit in the FHS training dataset (N=1833). In the training dataset, we performed 10-fold cross validation to specify the value of the tuning parameter λ.

Calibration of DNAm GrimAge into units of years

The final elastic net Cox model is listed in Table 3 results in an uncalibrated DNAmGrimAge2 estimate, which can be interpreted as the linear combination of the covariates, $X^T\beta$, or alternatively as the logarithm of the hazard ratio, $h(t)/h_0(t) = X^T\beta$, where $h_0(t)$ is the baseline hazard at time t. The linear combination, $X^T\beta$, can be interpreted as an uncalibrated version of DNAm GrimAge. To facilitate an intuitive interpretation as a physiological age estimator, we linearly transformed it so that the resulting estimate would be in units of years. Toward this end, we imposed the following requirement: the mean and variance of the resulting value of DNA GrimAge2, should be the same as the mean and variance of the age variable in the FHS training data (average of exam 7 and exam8). This resulted in the following transformation

$$\text{DNAm GrimAge2} = -61.03936 + 8.271105 * X^T\beta.$$

A completely unbiased evaluation of DNAm GrimAge2 is achieved in eight large-scale cohorts independent from the FHS test, as described below.

Software

GrimAge2 approach is implemented in our online software, https://dnamage.clockfoundation.org/.

Table 3. Cox elastic net regression model.

Covariate (*X*)	Abbreviation	Coefficients (β)
DNAm adrenomedullin	DNAmADM	0.00609
DNAm beta-2-microglobulin	DNAmB2M	2.79E-07
DNAm cystatin-C	DNAmCystatin C	4.08E-06
DNAm growth differentiation factor 15	DNAmGDF-15	0.00035
DNAm leptin	DNAmLeptin	-2.03E-05
DNAm log C-reactive protein	DNAmlogCRP	1.90266
DNAm log hemoglobin A1C	DNAmlogA1C	0.40359
DNAm plasminogen activator inhibitor 1	DNAmPAI-1	0.02941
DNAm tissue inhibitor metalloproteinases 1	DNAmTIMP-1	3.67E-06
DNAm pack-years	DNAmPACKYRS	0.00014
Chronological age	Age	0.02676
Female	Female	-0.14212

The table lists the finalized covariates in the final Cox regression model with elastic net penalty and their coeffects. A linear combination of $X^T\beta$ yields an estimate of logarithm of proportional hazard, which is the raw value of DNAmGrimAge2 before calibration. The finalized DNAm GrimAge2 is based on transforming the raw variable into a distribution in units of year The columns report the name of the covariate (e.g. DNAm based biomarker), its abbreviation and coefficient under the final Cox regression model with tuning parameter λ determined by 10-fold cross validation.

Mortality risk: *mortality.res*

Formally, mortality.res is defined as the deviance residual from a Cox regression model for time-to-death due to all-cause mortality. The variable mortality.res can be interpreted as a measure of "excess" mortality risk compared to the baseline risk in a test data.

Validation data

We validated DNAmGrimAge2, DNAmGrimAge and their components in 13,399 blood samples from 10,065 individuals across 1) FHS test and the other eight cohorts: 2) BA23 and 3) EMPC study from the Women's Health Initiative (WHI) with three racial groups, 4) African Americans from the Jackson Heart Study (JHS), 5) the InCHIANTI cohort study, 6) individuals of European ancestry from Baltimore Longitudinal Study of Aging (BLSA), 7) Lothian Birth Cohort 1921 (LBC1921) and 8) LBC 1936 (LBC1936), and 9) individuals of European ancestry from Normative Aging Study (NAS, only recruiting male participants). Table 1 lists the characteristics of the samples. Descriptions of each study cohort including characteristics of participants, phenotype data and molecular array samples can be found in Supplementary Note 2. Methylation arrays were profiled in Illumina 450k for all cohorts except for the JHS which used the EPIC array. Methylation beta values were generated using the Bioconductor *minfi* package with Noob background correction [38] for all the validation data except WHI, INS and NAS, which were based on other algorithms such as BMIQ [39] or SeSAMe [40] (Supplementary Note 2).

Multivariate regression analysis for validation

We validated our new mortality clock DNAm GrimAge2 in two parts. In the first part, we focused on validating the new clock using multivariate regression analysis that adjusted for potential confounders including sex. Here we only analyzed the associations with age-related phenotypes such as mortality. In the second part, we validate the new clock in a broader category of variables including diet and other lifestyle factors that are not necessarily related to chronological age. Here, we addressed different effect sizes between males and females along with sex-stratified analyses. The details for the second part are described in the next section, In the first part, our validation analysis involved i) Cox regression for time to death, for time-to-CHD, for time to CHF, time-to-any cancer ii) linear regression for our DNAm based measures (independent variable) associated with and number of age-related conditions (dependent variable), respectively, iii) linear regression for age at menopause (independent variable) associated with our DNAm measure (dependent variable), with only one exception for the relationship with DNAm PACKYRS (as an independent variable), iv) logistic regression analysis for estimating the odds ratios of our DNAm based measure associated with hypertension,

type 2 diabetes, and disease free status. The variable of "number of age-related conditions" includes arthritis, cataract, cancer, CHD, CHF, emphysema, glaucoma, lipid condition, osteoporosis, type 2 diabetes, etc. (see Supplementary Note 1). In our validation analysis, we used AgeAccelGrim2, AgeAccelGrim, and used the scaled measures of seven DNAm surrogates for plasma proteins based on the mean and standard deviation (SD) of the FHS training dataset such that the effect size was approximately corresponding to one SD. All the models were adjusted for age, female, and adjusted for batch effect as needed. To avoid the bias due to familial correlations from pedigrees in the FHS cohort or the intra-subject correlations from the repeated measures in InCHIANTI, LBC1921, LBC1936 and NAS, we accounted for the correlations accordingly in all the analyses in the following. In Cox regression analysis, we used robust standard errors, the Huber sandwich estimator, implemented in R *coxph* function. We used linear mixed models with a random intercept term, implemented in *lme* R function. We used generalized estimation equation models (GEE), implemented in R *gee* function, for our logistic regression models. Analysis was performed across different strata formed by racial groups at each study cohort, with up to 15 strata for the meta analyses (Table 1). For the meta analyses, we used fixed effect models weighted by inverse variance to combine the results across validation study sets into a single estimate by using the *metafor* R function in most situations. We also used Stouffer's meta-analysis method (weighted by the square root of the sample size) in specific situations where the harmonization of covariates across cohorts was challenging, e.g. when evaluating the number of age-related conditions and disease free status.

Diet, clinical biomarkers and lifestyle factors

We performed a robust correlation analysis (biweight midcorrelation, bicor [26]) between our novel biomarkers (AgeAccelGrim2, AgeAccelGrim and its 10 age-adjusted components) and a total of 61 variables including 27 self-reported diet, 9 dietary biomarkers, 19 clinically relevant measurements, and 6 lifestyle factors including hand grip strength. The sample size for each variable is up to 13,420 across the nine validation datasets including the FHS test dataset. We combined the postmenopausal women from the WHI BA23 and WHI EMPC (roughly n= 4000 women). The 9 dietary biomarkers are only available in the WHI cohort. Blood biomarkers were measured from fasting plasma collected at baseline. Food groups and nutrients are inclusive, including all types and all preparation methods, e.g. folic acid includes synthetic and natural, dairy includes cheese and all types of milk. The individual variables of WHI are explained in [25].

The study variables are listed in Supplementary Table 2.1. We also included the individuals with African American (AfricanA) ancestry (n up to 216) from the BLSA cohort, who were excluded from mortality analysis due to the very low death rate (8%). For each study cohort, we stratified the samples based on ethnic_gender category. For instance, the BLSA samples were stratified to 4 strata: White_male, White_female, AfricanA_male, and AfricanA_female. The WHI samples were stratified by European-, African-, and Hispanic- ancestry groups. Ancestry information was verified using ancestry informative SNP markers. We conducted robust correlation (bicor) analysis stratified by study cohort/ethnicity/sex and meta-analyzed the results with fixed effect models weighted by inverse variance. The fixed effect models yield a meta estimate of bicor. As a caveat, the bicor analysis did not accommodate the intra-pedigree (e.g. FHS) or intra-subject correlation (e.g. LBC1921). We did not employ statistical analyses such as linear mixed models to accommodate these factors since some models failed to reach convergence due to the unbalanced design in the data structure or high intra-subject correlations. The patterns for the failures of convergence were heterogeneous in terms of study cohort or study variables (dependent or independent variables). Our robust correlation (bicor) results in individual strata were meta-analyzed across strata resulting in meta estimates of bicor and its P-value, which could be inflated by intra pedigree/subject correlations. The harmonization of educational level across cohorts was challenging since some cohorts report years of education while others simply report categorical variables for education status. Here correlation coefficients can be attractive since they are invariant with respect to linear transformations.

Polygenic risk score analysis

We performed polygenic risk score (PRS) analysis in women of European ancestry from the WHI BA23 and AS315, using the GWAS results of AgeAccelGrim from our previous study [33]. The PRS analysis was restricted to the women of European ancestry since the GWAS results were based on the European ancestry meta-analyses on 34,710 individuals. The PRS scores were generated using default settings of the PRSice software [41] (clump-window = 250 kb, clump-p = 1; clump-r2 = 0.25). P-value thresholds for SNP associations were set at $< 5 \times 10^{-8}$, < 0.01, < 0.05, < 0.1, < 0.5, and 1. The linkage disequilibrium (LD) estimation was calculated using the target data (WHI). The qualities of genotyped and imputed SNPs in the WHI cohort were controlled by empirical MAF >=0.005, Hardy-Weinberg equilibrium (HWE) P-value >=1.0e-06 and MaCH impute r2≥0.6 [42]. Genotyped and imputed SNP array information are described in the Supplementary Note 2. We performed

linear regression analyses of AgeAccelGrim2 (or AgeAccelGrim) on PRS to compute the proportions for the variation of the age acceleration measure explained by PRS at different thresholds. We report the proportion of R^2 in percentages (%).

Computed tomography data from the Framingham Heart Study

The computed tomography (CT) in liver, spleen, paraspinal muscle, subcutaneous adipose tissue (SAT), and visceral adipose tissue (VAT) were performed in n=2,803 individuals from the FHS Offspring, Third Generation and Omni 2 Cohort participants between September 2008 and December 2011 [27, 28]. Of those, 1,174 Offspring Cohort participants were included in our FHS study (869 in training and 305 in test data). The age at CT scan was in general slightly older than the age at blood draw for the DNA methylation profile (mean age difference= 3.7 years, ranging from 1.2 to 6.1 years).

Organ density measures, more precisely CT attenuation coefficients, reflect how easily a target can be penetrated by an X-ray. The Hounsfield unit (HU) scale is a linear transformation of the original linear attenuation coefficient measurement into one in which the radiodensity of distilled water is defined as zero Hounsfield units (HU). Radiation attenuation in liver, spleen, or muscle is inversely related to respective measures of fat content.

The CT measures from three areas of the liver, two areas of the spleen and two areas of the paraspinal muscle were averaged to determine the average Hounsfield units in liver, spleen and muscle, respectively. The CT-scan measures of visceral and subcutaneous adipose tissue are described in [28].

In our analysis, we first performed marginal robust correlation analysis (biweight midcorrelation, bicor coefficient) [26] to study the association between the CT-scan derived measures and DNAm based biomarkers. As sex affects adipose associated parameters, we performed the analysis in males and females, separately. Next we combined the results using fixed effects meta analysis. To adjust for potential confounders, we also performed four types of multivariate linear mixed effects models that included sex and BMI as fixed effects and pedigree structure as a random effect. In Model I, we regressed a DNAm based biomarker (e.g. AgeAccelGrim2) on CT derived covariates: liver density, spleen density, and paraspinal muscle density. In Model II, we regressed the DNAm based biomarker (dependent variable) on volumetric measures of adipose tissue (both SAT and VAT volume). In Model III, we regressed the DNAm based biomarker (dependent variable) on both volumetric (in units of cm3) and density (in units of HU) measures of adipose tissue (both SAT and VAT). This model allows us to assess which measure is more sensible for our DNAm biomarkers. In Model IV, we used all CT measures as covariates (i.e. liver, spleen and muscle density, SAT volume, and VAT volume). We did not include the density measures of SAT or VAT as Model III showed that they were not significant after adjusting for SAT/VAT volumes in most of our analysis. Also, it can protect the model fit in Model IV from the issue of multi-collinearity. We used the BMI measure assessed at exam 9 in the FHS, i.e. the closest exam following the CT-scan exam. We used all the FHS individuals from training and test dataset as our previous study showed the results were not biased by the training status [1].

Application in saliva samples in National Growth and Health Study (NGHS) cohort

We applied our mortality clocks in 432 mothers from the NHLBI Growth and Health Study (NGHS) cohort [31]. The NGHS cohort was a longitudinal study conducted from 1985 to 2000 that investigated the racial differences in factors relating to the development of obesity in Black and White pre-adolescent girls, who were recruited at age 9 or 10 years. A 30-year follow-up of the Contra Costa County cohort was conducted in 2016 [31] to assess midlife health and well-being. Methylation data from the Illumina 850k array were profiled in saliva samples from 688 individuals including mothers (n=442) and their most recent children (n=246). We only used mothers in our analysis. Of the 442 mothers, 10 women had either missing ethnic status, low confidence in the estimate of chronological age, or were technical outliers and removed from analysis, yielding 432 mothers for our study. The mothers in our study are balanced by ethnic/racial groups: White (n=218) and African American (n=214). More details of the NGHS cohort are described in Supplementary Note 2.

We performed multivariate linear regression analysis to study the association between 1) dependent variables: clinically relevant measures: metabolic Z score, high sensitivity C-reactive protein (CRP), insulin resistant and HOMA for insulin resistance (HOMA-IR) [32] and 2) independent variables: AgeAccelGrim2, AgeAccelGrim, and nine scaled DNAm-based surrogates of proteins and DNAm PACKYS. The HOMA-IR stands for homeostatic model assessment of insulin resistance defined by Matthews et al. [32, 43]. The equations for HOMA1-IR = (FPI × FPG)/22.5, where FPI is fasting plasma insulin concentration (mU/l) and FPG is fasting plasma glucose (mmol/l) [43]. Higher scores of HOMW-

IR represent greater levels of insulin resistance. We applied the analysis in all mothers and stratified analysis by ethnic/racial group, respectively. All the analysis was adjusted for chronological age, batch effect and for race as needed.

Meta analysis for EWAS of age acceleration of GrimAge clocks

We performed EWAS of AgeAccelGrim2 (and AgeAccelGrim) in each cohort stratified by gender and race. EWAS of epigenetic age acceleration was carried out with the R function *standardScreeningNumericTrait* from the R WGCNA package. AgeAccelGrim2 (AgeAccelGrim) was based on the residuals adjusted for pedigree correlation or intra-subject correlation via linear mixed analysis in the FHS, InChinanti, LBC21, LBC36 and NAS cohorts. EWAS results were combined via fixed effect models weighted by inverse variance with effect sizes based on correlation estimates, as implicated in R metafor.

Meta analysis for EWAS of time-to-death and time-to-CHD

We performed EWAS of time-to-death on each cohort based on three Cox regression models of models. Model I is a basicmodel that adjusted for chronological age and sex (Female: 1 indicates females, 0 males), and batch effect, pedigree correlation or intrasubject correlation as needed. Model II adjusted for the same variables as in Model I plus smoking history based on pack-years. Model III adjusted for the same variables as in Model I plus 7 imputed blood cell compositions/counts: CD8 naïve, CD8pCD28nCD45Ran (exhausted cytotoxic T cells), plasma blasts, CD4+ T, nature killer cells, monocytes and granulocytes (Houseman estimates, Horvath estimates). Robust standard errors (the Huber sandwich estimator) was used if the Cox regression analysis involved pedigree correlation or intrasubject correlation. As information on smoking pack-years was missing in JHS, BLSA and LBC21, we used smoking status (never, past and current) in the Model II. EWAS results were combined via fixed effect models weighted by inverse variance with effect sizes based on beta values (log hazard ratios), from the Cox regression models, as implicated in R metafor.

For all the individual EWAS, we restricted the analysis to CpGs present on 450k array. For each CpG, individuals with extreme methylation levels (six standard deviations away from the mean) were set to missing. EWAS of AgeAccelGrim2/AgeAccelGrim using the FHS cohort was only performed on the 711 individuals from the test set. The meta analysis for AgeAccelGrim2/AgeAccelGrim was performed on n=12,430. The meta analysis was performed on n=13,260 for time-to-death and n=6,143 for time-to-CHD based on FHS, WHI BA23 and JHS cohorts.

AUTHOR CONTRIBUTIONS

ATL and SH developed the DNAm based biomarkers (including DNAm GrimAge2) and conceived of the study. ATL carried out most of the statistical analyses. ATL, AB and QY carried out the analysis in evaluating DNAm GrimAge2. ATL and JC carried out the diet analysis in the LBC36 cohorts. ATL, JZ, ESE and SH carried out the analysis involving the NGHS cohort. The remaining authors contributed data, helped with the write up, and participated in the interpretation of the results.

ACKNOWLEDGEMENTS AND FUNDING

This study was mainly supported by 1U01AG060908 – 01 (Horvath, Lu). R. Marioni was supported by an Alzheimer's Society project grant AS-PG-19b-010y. E. Whitsel was supported by NIH/NIEHS R01-ES020836. The views expressed in this manuscript are those of the authors and do not necessarily represent the views of funding bodies such as the National Heart, Lung, and Blood Institute; the National Institutes of Health; or the U.S. Department of Health and Human Services.

The Women's Health Initiative program is funded by the National Heart, Lung, and Blood Institute, National Institutes of Health, U.S. Department of Health and Human Services through contracts HHSN268201600018C, HHSN268201600001C, HHSN268201600002C, HHSN268201600003C, and HHSN268201600004C. The authors thank the WHI investigators and staff for their dedication, and the study participants for making the program possible. A full listing of WHI investigators can be found at: http://www.whi.org/researchers/Documents%20%20Write%20a%20Paper/WHI%20Investigator%20Long%20List.pdf

The Jackson Heart Study (JHS) is supported and conducted in collaboration with Jackson State University (HHSN268201800013I), Tougaloo College (HHSN268201800014I), the Mississippi State Department of Health (HHSN268201800015I/HHSN26800001) and the University of Mississippi Medical Center (HHSN268201800010I, HHSN268201800011I and HHSN268201800012I) contracts from the National Heart, Lung, and Blood Institute (NHLBI) and the National Institute for Minority Health and Health Disparities (NIMHD). The authors also wish to thank the staffs and participants of the JHS.

The Framingham Heart Study is funded by National Institutes of Health contract N01-HC-25195 and HHSN2682015000001I. The laboratory work for this investigation was funded by the Division of Intramural Research, National Heart, Lung, and Blood Institute, National Institutes of Health. The analytical component of this project was funded by the Division of Intramural Research, National Heart, Lung, and Blood Institute, and the Center for Information Technology, National Institutes of Health, Bethesda, MD.

The BLSA study is conducted by the Intramural Research Program of the National Institute on Aging (NIA), part of the National Institutes of Health at the U.S. Department of Health and Human Services. The authors also wish to thank the staffs and participants of the BLSA.

The InCHIANTI is supported by the Intramural Research Program of the National Institute on Aging (NIA), Italian Health Ministry, Istituto Nazionale di Riposo e Cura per Anziani in Italy, and Tuscany Regional Health Agency. The authors also wish to thank the staffs and participants of the InCHIANTI study.

The authors thank all LBC1921 and LBC1936 study participants and research team members who have contributed, and continue to contribute, to ongoing studies. LBC1921 was supported by the UK's Biotechnology and Biological Sciences Research Council (BBSRC), The Royal Society, and The Chief Scientist Office of the Scottish Government. LBC1936 is supported by the Biotechnology and Biological Sciences Research Council, and the Economic and Social Research Council [BB/W008793/1] (which supports SEH and JC), Age UK (Disconnected Mind project), the Medical Research Council (MR/M01311/1), and the University of Edinburgh. SRC is supported by a Sir Henry Dale Fellowship jointly funded by the Wellcome Trust and the Royal Society (221890/Z/20/Z). Methylation typing was supported by the Centre for Cognitive Ageing and Cognitive Epidemiology (Pilot Fund award), Age UK, The Wellcome Trust Institutional Strategic Support Fund, The University of Edinburgh, and The University of Queensland.

AMB was supported by the National Cancer Institute of the National Institutes of Health under Award Number K07CA225856.

CONFLICTS OF INTEREST

The Regents of the University of California is the sole owner of a patent application directed at this invention for which ATL and SH are named inventors. SH is a founder and paid consultant of the non profit Epigenetic Clock Development Foundation that licenses this patent. REM is a scientific advisor to the Epigenetic Clock Development Foundation and Optima Partners and has received speaker fees from Illumina. AMB is a scientific advisor to the Epigenetic Clock Development Foundation.

REFERENCES

1. Lu AT, Quach A, Wilson JG, Reiner AP, Aviv A, Raj K, Hou L, Baccarelli AA, Li Y, Stewart JD, Whitsel EA, Assimes TL, Ferrucci L, Horvath S. DNA methylation GrimAge strongly predicts lifespan and healthspan. Aging (Albany NY). 2019; 11:303–27. https://doi.org/10.18632/aging.101684 PMID:30669119

2. Horvath S. DNA methylation age of human tissues and cell types. Genome Biol. 2013; 14:R115. https://doi.org/10.1186/gb-2013-14-10-r115 PMID:24138928

3. Hannum G, Guinney J, Zhao L, Zhang L, Hughes G, Sadda S, Klotzle B, Bibikova M, Fan JB, Gao Y, Deconde R, Chen M, Rajapakse I, et al. Genome-wide methylation profiles reveal quantitative views of human aging rates. Mol Cell. 2013; 49:359–67. https://doi.org/10.1016/j.molcel.2012.10.016 PMID:23177740

4. Zhang Y, Wilson R, Heiss J, Breitling LP, Saum KU, Schöttker B, Holleczek B, Waldenberger M, Peters A, Brenner H. DNA methylation signatures in peripheral blood strongly predict all-cause mortality. Nat Commun. 2017; 8:14617. https://doi.org/10.1038/ncomms14617 PMID:28303888

5. Levine ME, Lu AT, Quach A, Chen BH, Assimes TL, Bandinelli S, Hou L, Baccarelli AA, Stewart JD, Li Y, Whitsel EA, Wilson JG, Reiner AP, et al. An epigenetic biomarker of aging for lifespan and healthspan. Aging (Albany NY). 2018; 10:573–91. https://doi.org/10.18632/aging.101414 PMID:29676998

6. Belsky DW, Caspi A, Arseneault L, Baccarelli A, Corcoran DL, Gao X, Hannon E, Harrington HL, Rasmussen LJ, Houts R, Huffman K, Kraus WE, Kwon D, et al. Quantification of the pace of biological aging in humans through a blood test, the DunedinPoAm DNA methylation algorithm. Elife. 2020; 9:e54870. https://doi.org/10.7554/eLife.54870 PMID:32367804

7. Belsky DW, Caspi A, Corcoran DL, Sugden K, Poulton R, Arseneault L, Baccarelli A, Chamarti K, Gao X, Hannon E, Harrington HL, Houts R, Kothari M, et al. DunedinPACE, a DNA methylation biomarker of the pace of aging. Elife. 2022; 11:e73420.

https://doi.org/10.7554/eLife.73420
PMID:35029144

8. Verschoor CP, Lin DT, Kobor MS, Mian O, Ma J, Pare G, Ybazeta G. Epigenetic age is associated with baseline and 3-year change in frailty in the Canadian Longitudinal Study on Aging. Clin Epigenetics. 2021; 13:163.
https://doi.org/10.1186/s13148-021-01150-1
PMID:34425884

9. Crimmins EM, Thyagarajan B, Levine ME, Weir DR, Faul J. Associations of Age, Sex, Race/Ethnicity, and Education With 13 Epigenetic Clocks in a Nationally Representative U.S. Sample: The Health and Retirement Study. J Gerontol A Biol Sci Med Sci. 2021; 76:1117–23.
https://doi.org/10.1093/gerona/glab016
PMID:33453106

10. Hillary RF, Stevenson AJ, Cox SR, McCartney DL, Harris SE, Seeboth A, Higham J, Sproul D, Taylor AM, Redmond P, Corley J, Pattie A, Hernández MD, et al. An epigenetic predictor of death captures multi-modal measures of brain health. Mol Psychiatry. 2021; 26:3806–16.
https://doi.org/10.1038/s41380-019-0616-9
PMID:31796892

11. Kuo PL, Moore AZ, Lin FR, Ferrucci L. Epigenetic Age Acceleration and Hearing: Observations From the Baltimore Longitudinal Study of Aging. Front Aging Neurosci. 2021; 13:790926.
https://doi.org/10.3389/fnagi.2021.790926
PMID:34975461

12. Föhr T, Waller K, Viljanen A, Sanchez R, Ollikainen M, Rantanen T, Kaprio J, Sillanpää E. Does the epigenetic clock GrimAge predict mortality independent of genetic influences: an 18 year follow-up study in older female twin pairs. Clin Epigenetics. 2021; 13:128.
https://doi.org/10.1186/s13148-021-01112-7
PMID:34120642

13. Cao X, Li W, Wang T, Ran D, Davalos V, Planas-Serra L, Pujol A, Esteller M, Wang X, Yu H. Accelerated biological aging in COVID-19 patients. Nat Commun. 2022; 13:2135.
https://doi.org/10.1038/s41467-022-29801-8
PMID:35440567

14. Zheng Y, Habes M, Gonzales M, Pomponio R, Nasrallah I, Khan S, Vaughan DE, Davatzikos C, Seshadri S, Launer L, Sorond F, Sedaghat S, Wainwright D, et al. Mid-life epigenetic age, neuroimaging brain age, and cognitive function: coronary artery risk development in young adults (CARDIA) study. Aging (Albany NY). 2022; 14:1691–712.
https://doi.org/10.18632/aging.203918
PMID:35220276

15. Okazaki S, Kimura R, Otsuka I, Funabiki Y, Murai T, Hishimoto A. Epigenetic clock analysis and increased plasminogen activator inhibitor-1 in high-functioning autism spectrum disorder. PLoS One. 2022; 17:e0263478.
https://doi.org/10.1371/journal.pone.0263478
PMID:35113965

16. Dugué PA, Bassett JK, Wong EM, Joo JE, Li S, Yu C, Schmidt DF, Makalic E, Doo NW, Buchanan DD, Hodge AM, English DR, Hopper JL, et al. Biological Aging Measures Based on Blood DNA Methylation and Risk of Cancer: A Prospective Study. JNCI Cancer Spectr. 2020; 5:pkaa109.
https://doi.org/10.1093/jncics/pkaa109
PMID:33442664

17. Rutledge J, Oh H, Wyss-Coray T. Measuring biological age using omics data. Nat Rev Genet. 2022; 23:715–27.
https://doi.org/10.1038/s41576-022-00511-7
PMID:35715611

18. Protsenko E, Yang R, Nier B, Reus V, Hammamieh R, Rampersaud R, Wu GW, Hough CM, Epel E, Prather AA, Jett M, Gautam A, Mellon SH, Wolkowitz OM. "GrimAge," an epigenetic predictor of mortality, is accelerated in major depressive disorder. Transl Psychiatry. 2021; 11:193.
https://doi.org/10.1038/s41398-021-01302-0
PMID:33820909

19. Dawber TR, Meadors GF, MOORE FE Jr. Epidemiological approaches to heart disease: the Framingham Study. Am J Public Health Nations Health. 1951; 41:279–81.
https://doi.org/10.2105/ajph.41.3.279 PMID:14819398

20. Considine RV, Sinha MK, Heiman ML, Kriauciunas A, Stephens TW, Nyce MR, Ohannesian JP, Marco CC, McKee LJ, Bauer TL. Serum immunoreactive-leptin concentrations in normal-weight and obese humans. N Engl J Med. 1996; 334:292–5.
https://doi.org/10.1056/NEJM199602013340503
PMID:8532024

21. Rosenbaum M, Nicolson M, Hirsch J, Heymsfield SB, Gallagher D, Chu F, Leibel RL. Effects of gender, body composition, and menopause on plasma concentrations of leptin. J Clin Endocrinol Metab. 1996; 81:3424–7.
https://doi.org/10.1210/jcem.81.9.8784109
PMID:8784109

22. Horvath S, Gurven M, Levine ME, Trumble BC, Kaplan H, Allayee H, Ritz BR, Chen B, Lu AT, Rickabaugh TM, Jamieson BD, Sun D, Li S, et al. An epigenetic clock analysis of race/ethnicity, sex, and coronary heart disease. Genome Biol. 2016; 17:171.
https://doi.org/10.1186/s13059-016-1030-0
PMID:27511193

23. Levine ME, Lu AT, Chen BH, Hernandez DG, Singleton AB, Ferrucci L, Bandinelli S, Salfati E, Manson JE, Quach A, Kusters CD, Kuh D, Wong A, et al. Menopause accelerates biological aging. Proc Natl Acad Sci USA. 2016; 113:9327–32. https://doi.org/10.1073/pnas.1604558113 PMID:27457926

24. Lu AT, Xue L, Salfati EL, Chen BH, Ferrucci L, Levy D, Joehanes R, Murabito JM, Kiel DP, Tsai PC, Yet I, Bell JT, Mangino M, et al. GWAS of epigenetic aging rates in blood reveals a critical role for TERT. Nat Commun. 2018; 9:387. https://doi.org/10.1038/s41467-017-02697-5 PMID:29374233

25. Quach A, Levine ME, Tanaka T, Lu AT, Chen BH, Ferrucci L, Ritz B, Bandinelli S, Neuhouser ML, Beasley JM, Snetselaar L, Wallace RB, Tsao PS, et al. Epigenetic clock analysis of diet, exercise, education, and lifestyle factors. Aging (Albany NY). 2017; 9:419–46. https://doi.org/10.18632/aging.101168 PMID:28198702

26. Langfelder P, Horvath S. WGCNA: an R package for weighted correlation network analysis. BMC Bioinformatics. 2008; 9:559. https://doi.org/10.1186/1471-2105-9-559 PMID:19114008

27. Long MT, Pedley A, Massaro JM, Hoffmann U, Fox CS. The Association between Non-Invasive Hepatic Fibrosis Markers and Cardiometabolic Risk Factors in the Framingham Heart Study. PLoS One. 2016; 11:e0157517. https://doi.org/10.1371/journal.pone.0157517 PMID:27341207

28. Lee JJ, Pedley A, Hoffmann U, Massaro JM, Keaney JF Jr, Vasan RS, Fox CS. Cross-Sectional Associations of Computed Tomography (CT)-Derived Adipose Tissue Density and Adipokines: The Framingham Heart Study. J Am Heart Assoc. 2016; 5:e002545. https://doi.org/10.1161/JAHA.115.002545 PMID:26927600

29. Houseman EA, Accomando WP, Koestler DC, Christensen BC, Marsit CJ, Nelson HH, Wiencke JK, Kelsey KT. DNA methylation arrays as surrogate measures of cell mixture distribution. BMC Bioinformatics. 2012; 13:86. https://doi.org/10.1186/1471-2105-13-86 PMID:22568884

30. As, Chao C, Borgmann K, Brew K, Ghorpade A. Tissue inhibitor of metalloproteinases-1 protects human neurons from staurosporine and HIV-1-induced apoptosis: mechanisms and relevance to HIV-1-associated dementia. Cell Death Dis. 2012; 3:e332. https://doi.org/10.1038/cddis.2012.54 PMID:22739984

31. Hamlat EJ, Adler NE, Laraia B, Surachman A, Lu AT, Zhang J, Horvath S, Epel ES. Association of subjective social status with epigenetic aging among Black and White women. Psychoneuroendocrinology. 2022; 141:105748. https://doi.org/10.1016/j.psyneuen.2022.105748 PMID:35397259

32. Matthews DR, Hosker JP, Rudenski AS, Naylor BA, Treacher DF, Turner RC. Homeostasis model assessment: insulin resistance and beta-cell function from fasting plasma glucose and insulin concentrations in man. Diabetologia. 1985; 28:412–9. https://doi.org/10.1007/BF00280883 PMID:3899825

33. McCartney DL, Min JL, Richmond RC, Lu AT, Sobczyk MK, Davies G, Broer L, Guo X, Jeong A, Jung J, Kasela S, Katrinli S, Kuo PL, et al, Genetics of DNA Methylation Consortium, and NHLBI Trans-Omics for Precision Medicine (TOPMed) Consortium. Genome-wide association studies identify 137 genetic loci for DNA methylation biomarkers of aging. Genome Biol. 2021; 22:194. https://doi.org/10.1186/s13059-021-02398-9 PMID:34187551

34. Bojesen SE, Timpson N, Relton C, Davey Smith G, Nordestgaard BG. *AHRR* (cg05575921) hypomethylation marks smoking behaviour, morbidity and mortality. Thorax. 2017; 72:646–53. https://doi.org/10.1136/thoraxjnl-2016-208789 PMID:28100713

35. Fasanelli F, Baglietto L, Ponzi E, Guida F, Campanella G, Johansson M, Grankvist K, Johansson M, Assumma MB, Naccarati A, Chadeau-Hyam M, Ala U, Faltus C, et al. Hypomethylation of smoking-related genes is associated with future lung cancer in four prospective cohorts. Nat Commun. 2015; 6:10192. https://doi.org/10.1038/ncomms10192 PMID:26667048

36. Fahy GM, Brooke RT, Watson JP, Good Z, Vasanawala SS, Maecker H, Leipold MD, Lin DT, Kobor MS, Horvath S. Reversal of epigenetic aging and immunosenescent trends in humans. Aging Cell. 2019; 18:e13028. https://doi.org/10.1111/acel.13028 PMID:31496122

37. Zou H, Hastie T. Regularization and variable selection via the elastic net. Journal of the Royal Statistical Society: Series B (Statistical Methodology). 2005; 67:301–20. https://doi.org/10.1111/j.1467-9868.2005.00503.x

38. Aryee MJ, Jaffe AE, Corrada-Bravo H, Ladd-Acosta C, Feinberg AP, Hansen KD, Irizarry RA. Minfi: a flexible

and comprehensive Bioconductor package for the analysis of Infinium DNA methylation microarrays. Bioinformatics. 2014; 30:1363–9. https://doi.org/10.1093/bioinformatics/btu049 PMID:24478339

39. Teschendorff AE, Marabita F, Lechner M, Bartlett T, Tegner J, Gomez-Cabrero D, Beck S. A beta-mixture quantile normalization method for correcting probe design bias in Illumina Infinium 450 k DNA methylation data. Bioinformatics. 2013; 29:189–96. https://doi.org/10.1093/bioinformatics/bts680 PMID:23175756

40. Zhou W, Triche TJ Jr, Laird PW, Shen H. SeSAMe: reducing artifactual detection of DNA methylation by Infinium BeadChips in genomic deletions. Nucleic Acids Res. 2018; 46:e123. https://doi.org/10.1093/nar/gky691 PMID:30085201

41. Euesden J, Lewis CM, O'Reilly PF. PRSice: Polygenic Risk Score software. Bioinformatics. 2015; 31:1466–8. https://doi.org/10.1093/bioinformatics/btu848 PMID:25550326

42. Li Y, Willer CJ, Ding J, Scheet P, Abecasis GR. MaCH: using sequence and genotype data to estimate haplotypes and unobserved genotypes. Genet Epidemiol. 2010; 34:816–34. https://doi.org/10.1002/gepi.20533 PMID:21058334

43. Wallace TM, Levy JC, Matthews DR. Use and abuse of HOMA modeling. Diabetes Care. 2004; 27:1487–95. https://doi.org/10.2337/diacare.27.6.1487 PMID:15161807

SUPPLEMENTARY MATERIALS

Supplementary Note 1: DNAm based surrogates for plasma proteins

The model of DNAm GrimAge2 is composed of nine DNAm based plasma proteins, DNAm based pack years, age and gender. Below we briefly describe these nine plasma proteins.

A1C (hemoglobin A1C, HbA1c; glycosylated hemoglobin; Glycated hemoglobin) is a blood test that shows average blood sugar (glucose) levels over the last 3 months. This biomarker is widely used in clinic to check for prediabetes or diabetes and help guide diabetes treatment over time (http://uclahealthib.staywellsolutionsonline.com/Bedside/167,a1c). Previous studies also indicated that higher levels of A1C were associated with cardiovascular heart disease and mortality [1, 2]. The log scale of A1C is a new component in DNAm GrimAge2.

ADM (adrenomedullin) is a vasodilator peptide hormone. Plasma ADM, initially isolated from adrenal gland, is increased in individuals with hypertension and heart failure [3]. A recent study showed that ADM was involved in age-related memory loss in mice and aging human brains [4].

B2M (Beta-2 microglobulin) is a component of major histocompatibility complex class 1 (MHC I) molecular. Plasma B2M is a clinical biomarker associated with cardiovascular disease, kidney function, inflammation severity [5]. B2M is a pro-aging factor associated with cognitive and regenerative function in aging process and suggests B2M may be targeted therapeutically in old age [6]. A previous study showed that systemic B2M accumulation in aging blood promoted age-related cognitive dysfunction and impairs mouse models [6].

Cystatin C or cystatin 3 (formerly gamma trace, post-gamma-globulin, or neuroendocrine basic polypeptide) is mainly used as a biomarker of kidney function. Plasma cystatin-C is a clinical relevant biomarker indicating kidney function [7]. Cystatin-C seems plays a role in cardiovascular disease [8] or amyloid deposition associated with Alzheimer's disease [9].

C-reactive protein (CRP) test is clinically used to find inflammation in your body that could be caused by different types of conditions such as an infection or autoimmune disorders like rheumatoid arthritis or inflammatory bowel disease, (https://uclahealthib.staywellsolutionsonline.com/Search/167,c_reactive_protein_serum). Several previous studies indicated that CPR protein concentration is associated with coronary heart disease, stroke, and non-vascular mortality (e.g. [10, 11]). The log scale of CRP is a new component in DNAm GrimAge2.

GDF-15 (growth differentiation factor 15) is one of transforming growth factor beta subfamily. GDF-15 has been implicated in aging and age- related disorders. It also plays a role in age-related mitochondria dysfunction [12].

Leptin is a hormone predominantly in adipose cells. Leptin plays a role in regulating energy balance by inhibiting hunger and is implicated in Alzheimer's disease [13].

Plasminogen activator inhibitor antigen type 1(PAI-1) is the major inhibitor of tissue-type plasminogen activator and unokinase plasminogen activator. PAI-1, released in response to inflammation process, plays a central role in a number of age-related subclinical (i.e., inflammation, atherosclerosis, insulin resistance) and clinical conditions (i.e., obesity, comorbidities) [14].

TIMP-1 or TIMP metallopeptidase inhibitor 1 is a tissue inhibitor of metalloproteinases. It is also involves chromatin structures, promoting cell proliferation in a wide range of cell types, and may also have an anti-apoptotic function [15].

Supplementary Note 2: Description of datasets

Our study participants with blood samples came from nine independent cohorts: Framingham Heart Study Offspring Cohort (FHS), Women's Health Initiatives (WHI) BA23, WHI EMPC, Jackson Heart Study (JHS), InCHIANTI (baseline and the third follow-up), Baltimore Longitudinal Study of Aging (BLSA), Lothian Birth Cohort 1921 (LBC21) and LBC 1936 (LBC36), and Normative Aging Study (NAS). We also studied saliva samples collected from an independent study: the NHLBI Growth and Health Study (NGHS) cohort. Below we describe each study cohort/datasets in more details.

Study 1: Framingham Heart Study cohort

The FHS cohort [16] is a large-scale longitudinal study started in 1948, initially investigating the common factors of characteristics that contribute to cardiovascular disease (CVD), https://www.framinghamheartstudy.org/index.php. The study initially enrolled participants living in the town of Framingham, Massachusetts, who were free of overt symptoms of CVD, heart attack or stroke at enrollment. In 1971, the study started the FHS

Offspring Cohort to enroll a second generation of the original participants 'adult children and their spouses (n= 5124) to conduct similar examinations [17]. Participants from the FHS Offspring Cohort were eligible for our study if they attended both the seventh and eighth examination cycles and consented to having their molecular data used for the study. We used the 2,544 participants from the group of Health/Medical/Biomedical (IRB, MDS) consent with available DNA methylation array data. The FHS data are available in dbGaP (accession number: phs000363.v16.p10 and phs000724.v2.p9).

We computed the total number of age-related conditions based on dyslipidemia, hypertension, cardiovascular disease (including coronary heart disease [CHD] or congestive heart failure [CHF]), type 2 diabetes, cancer and arthritis. Time to CHD or time to CHF was truncated at zero if it occurred before exam 8. Deaths among the FHS participants that occurred prior to January 1, 2013 were ascertained using multiple strategies, including routine contact with participants for health history updates, surveillance at the local hospital and in obituaries of the local newspaper, and queries to the National Death Index. Death certificates, hospital and nursing home records prior to death, and autopsy reports were requested. When cause of death was undeterminable, the next of kin were interviewed. The date and cause of death were reviewed by an endpoint panel of 3 investigators.

DNA methylation quantification

Peripheral blood samples were collected at the 8th examination. Genomic DNA was extracted from buffy coat using the Gentra Puregene DNA extraction kit (Qiagen) and bisulfite converted using the EZ DNA Methylation kit (Zymo Research Corporation). DNA methylation quantification was conducted in two laboratory batches using the Illumina Infinium HumanMethylation450 array (Illumina). Methylation beta values were generated using the Bioconductor *minfi* package with Noob background correction [18].

Studies 2 and 3 :Women's Health Initiative

The WHI is a national study that enrolled postmenopausal women aged 50-79 years into the clinical trials (CT) or observational study (OS) cohorts between 1993 and 1998 [19, 20]. We included 4,079 WHI participants with available phenotype and DNA methylation array data: 2,107 women from "*Broad Agency Award 23*" (WHI BA23) and 1,972 women from "*Epigenetic Mechanisms of PM-Mediated CVD Risk*" (WHI EMPC). WHI BA23 focuses on identifying miRNA and genomic biomarkers of coronary heart disease (CHD), integrating the biomarkers into diagnostic and prognostic predictors of CHD and other related phenotypes, and other objectives can be found in https://www.whi.org/researchers/data/WHIStudies/StudySites/BA23/Pages/home.aspx. WHI EMPC is a study of epigenetic mechanisms underlying associations between ambient particulate matter (PM) air pollution and cardiovascular disease [21]. WHI EMPC and BA23 span three WHI sub-cohorts including GARNET, WHIMS and SHARe. 936 EMPC participants were not in any of the WHI GWAS (either GARNET, WHIMS, SHARe, MOPMAP, HIPFX, or GECCO). The largest overlap was with SHARE and GARNET. There was almost no overlap with WHIMS and MOPMAP. The death status was based on the variable DEATHALL (All Discovered Death) as listed in the form "All Discovered Death Outcome Detail (Form 124/120)". This variable does not censor deaths that occur after the participants 'last consent period. The original WHI study began in the early 1990s and concluded in 2005. Since 2005, the WHI has continued as Extension Studies (Ext1), which are annual collections of health updates and outcomes in active participants. The second Extension Study (Ext2) enrolled 93,500 women in 2010 and follow-up of these women continues annually. Death was adjudicated for clinical trial (CT) and observational study (OS) participants through Ext1. In Ext2, death is only adjudicated for the Medical Record Cohort (MRC). Non MRC cause of death is determined by the initial cause of death form (form 120).

The total number of age-related conditions was based on Alzheimer's disease, amyotrophic lateral sclerosis, arthritis, cancer, cataract, CVD, glaucoma, emphysema, hypertension, and osteoporosis.

DNA methylation quantification for BA23

In brief, bisulfite conversion using the Zymo EZ DNA Methylation Kit (Zymo Research, Orange, CA, USA) as well as subsequent hybridization of the HumanMethylation450k Bead Chip (Illumina, San Diego, CA), and scanning (iScan, Illumina) were performed according to the manufacturers protocols by applying standard settings. DNA methylation levels (β values) were determined by calculating the ratio of intensities between methylated (signal A) and un-methylated (signal B) sites. Specifically, the β value was calculated from the intensity of the methylated (M corresponding to signal A) and un-methylated (U corresponding to signal B) sites, as the ratio of fluorescent signals $\beta = \text{Max}(M,0)/[\text{Max}(M,0)+\text{Max}(U,0)+100]$. Thus, β values range from 0 (completely un-methylated) to 1 (completely methylated).

DNA methylation quantification for WHI EMPC

Illumina Infinium HumanMethylation450 BeadChip data from the Northwestern University Genomics Core

Facility for WHI EMPC participants sampled in stages 1a, 1b, and 2 were quality controlled, normalized and batch adjusted. Beta-mixture quantile normalization was implemented using BMIQ [22] and empirical Bayes methods of batch adjustment for stage and plate were implemented in ComBat [23].

SNP array data

WHI SNP array data were generated under different sub-study groups: GARNET, SHARe and WHIM. The genotyped SNPs were profiled in different platforms. The information is presented in the format of platform (dbGAP access number): Illumina HumanOmni1-Quad v1-0 B (phs000200.v10.p3), Illumina HumanOmniExpressExome-8v1_B (phs000200.v10.p3), Affymetrix 6.0 (phs000200.v10.p3) and Affymetrix 6.0 (phs000200.v10.p3). More details can be found in our earlier GWAS study [24].

Lifestyle factors and dietary assessment in the Women's Health Initiative (WHI)

WHI participants completed self-administered questionnaires at baseline which provided personal information on a wide range of topics, including sociodemographic information (age, education, race, income), and current health behaviors (recreational physical activity, tobacco and alcohol exposure, and diet). Participants also visited clinics at baseline where certified Clinical Center staff collected blood specimens and measured anthropometrics (weight, height, hip and waist circumferences) and blood pressures (systolic, diastolic). Body mass index and waist to hip ratio were calculated from these measurements.

Dietary intake was assessed at baseline using the WHI Food Frequency Questionnaire [25]. Briefly, participants were asked to report on dietary habits in the past three months, including intake, frequency, and portion sizes of foods or food groups, along with questions concerning topics such as food preparation practices and types of added fats. Nutrient intake levels were then estimated from these responses. For current drinker, we use the threshold of more than one serving equivalent (14g) within the last 28 days.

Study 4: Jackson Heart Study

The JHS is a large, population-based observational study evaluating the etiology of cardiovascular, renal, and respiratory diseases among African Americans residing in the three counties (Hinds, Madison, and Rankin) that make up the Jackson, Mississippi metropolitan area [26] The age at enrollment for the unrelated cohort was 35-84 years; the family cohort included related individuals >21 years old. Participants provided extensive medical and social history, had an array of physical and biochemical measurements and diagnostic procedures, and provided genomic DNA during a baseline examination (2000-2004) and two follow-up examinations (2005-2008 and 2009-2012). Annual follow-up interviews and cohort surveillance are ongoing. In our analysis, we used the visits at baseline from 1747 individuals as part of project JHS ancillary study ASN0104, available with both phenotype and DNA methylation array data. Total numbers of age-related conditions were based on hypertension, type 2 diabetes, kidney dysfunction based on ever dialysis, and CVD.

DNA methylation quantification

Peripheral blood samples were collected at the baseline. Methylation beta values were generated using the Bioconductor *minfi* package with Noob background correction [18].

Study 5: Invecchiare in Chianti, aging in the Chianti area (InCHIANTI)

The InCHIANTI (Invecchiare in Chianti, aging in the Chianti area) cohort is a representative population-based study of older persons enrolling individuals aged 20 years and older from two areas in the Chianti region of Tuscany, Italy, http://inchiantistudy.net/wp/. One major goal of the study is to translate epidemiological research into geriatric clinical tools, ultimately advancing clinical applications in older persons. Of the cohort, 1430 observations from 728 individuals with both phenotype information and DNA methylation data were including in our studies. The observations were collected from baseline in 1998 and the third follow-up visit in 2007. All participants provided written informed consent to participate in this study. The study complied with the Declaration of Helsinki. The Italian National Institute of Research and Care on Aging Institutional Review Board approved the study protocol. We computed the total number of age-related conditions based on cancer, hypertension, myocardial infarction, Parkinson's disease, stroke and type 2 diabetes.

DNA methylation quantification

Genomic DNA was extracted from buffy coat samples using an AutoGen Flex and quantified on a Nanodrop1000 spectrophotometer prior to bisulfite conversion. Genomic DNA was bisulfite converted using Zymo EZ-96 DNA Methylation Kit (Zymo Research Corp., Irvine, CA) as per the manufacturer's protocol. CpG methylation status of 485,577 CpG sites was determined using the Illumina Infinium HumanMethylation450 BeadChip (Illumina Inc., San Diego, CA) as per the manufacturer's protocol and as previously described [27]. Initial data analysis was performed using GenomeStudio 2011.1 (Model M

Version 1.9.0, Illumina Inc.). Threshold call rate for inclusion of samples was 95%. Quality control of sample handling included comparison of clinically reported sex versus sex of the same samples determined by analysis of methylation levels of CpG sites on the X chromosome [27]. Methylation beta values were generated using SeSAMe [28].

Study 6: Baltimore Longitudinal Study of Aging (BLSA)

Established in 1958 The Baltimore Longitudinal Study of Aging (BLSA) is the longest-running scientific study of human aging in the United States [29], https://www.blsa.nih.gov/. The study population is a continuously enrolled cohort of community dwelling adults aged 20 or older who meet rigorous screening criteria. BLSA Participants return at age dependent intervals for study visits that include comprehensive clinical testing as well as evaluations of physical and cognitive function [30]. In the BLSA, blood samples were collected for DNA extraction. The mortality analysis was restricted to participants who self-identify as White (n=572). The downstream analysis including lifestyle factors was also performed among participants who self-identify as Black or African American (n=216). We computed the total number of age-related conditions based on the number of chronic diseases as defined in Fabbri et al. [31]. The BLSA data can be applied from https://www.blsa.nih.gov/.

DNA methylation quantification

DNA was quantified using Quant-iT Picogreen Reagent (Invitrogen, Grand Island, NY, USA) according to the manufacturer's instructions. 1 ug of DNA was bisulfite treated using the EZ-96 DNA methylation kit (Zymo Research, Irvine, CA, USA) according to the manufacturer's specifications for the 450k array. Converted genomic DNA was eluted in 22 µl of elution buffer. DNA methylation level was measured using Illumina Infinium HD Methylation Assay (Illumina) according to the manufacturer's instructions. Background subtraction was applied using the *preprocessIllumina* command in the *minfi* Bioconductor package [18].

There are a total 501 participants available for both DNA methylation and SNP array data remained in analysis.

Studies 7 and 8: Lothian Birth Cohorts (LBC) of 1921 and 1936

The Lothian Birth Cohorts (LBC) [32] of 1921 and 1936 are longitudinal studies of distribution and causes of cognitive functioning changes across most of the human life course, http://www.lothianbirthcohort.ed.ac.uk/. The participants of LBC1921 (born in 1921) took part in the Scottish Mental Survey (SMS) of 1932 while the participants of LBC1936 (born in 1936) took part in the SMS in 1947. Both surveys were associated with general intelligence tests for children at age 11 years and were carried out by the Scottish Council for Research in Education. The LBC1921 (n=550) began in 1999 and examined 5 waves at mean ages 79, 83, 87. 90 and 92 years while the LBC1936 (n=1091) began in 2004 and examined 5 waves at mean ages 70,73, 76, 79 and 82 years [32, 33].

We obtained DNA methylation data used in the earlier study for predicting all-cause mortality [34] in which SNP array data were also available for the study individuals. The LBC1921 is composed of 469 individuals across waves 1 and 3 individuals (n_{deaths}=451) and the LBC1936 is composed of 1044 individuals (n_{deaths}=378) across waves 1,2,3, and 4. All participants were of White Scottish ancestry. Following informed consent, venesected whole blood was collected for DNA extraction in both LBC1921 and LBC1936. Ethics permission for the LBC1921 was obtained from the Lothian Research Ethics Committee (Wave 1: LREC/1998/4/183). Ethics permission for the LBC1936 was obtained from the Multi-Centre Research Ethics Committee for Scotland (Wave 1: MREC/01/0/56), the Lothian Research Ethics Committee (Wave 1: LREC/2003/2/29). Written informed consent was obtained from all individuals. LBC methylation data have been submitted to the European Genome-phenome Archive under accession number EGAS00001000910.

DNA methylation quantification

As described in [34], DNA was extracted from 514 whole blood samples in LBC1921 and from 1,004 samples in LBC1936. Raw intensity data were backgroundcorrected and methylation beta-values generated using the R minfi package [18]. Quality control analysis was performed to remove probes with a low (<95%) detection rate at P <0.01. Manual inspection of the array control probe signals was used to identify and remove low quality samples. The Illumina-recommended threshold was used to eliminate samples with a low call rate (samples with <450,000 probes detected at P <0.01). As SNP genotyping was previously performed on LBC samples, genotypes derived from the 65 SNP control probes on the methylation array using the wateRmelon package [35] were compared to those obtained from the genotyping array to ensure sample integrity. Samples with a low match of genotypes with SNP control probes, which could indicate sample contamination or mix-up, were excluded (n = 9). Moreover, eight subjects whose predicted sex, based on XY probes, did not match reported sex were also excluded.

Study 9: Normative Aging Study

The Normative Aging Study (NAS) is a closed and ongoing cohort established in 1963 by the U.S. Veterans Administration in the Greater Boston Area [36]. The participants were aged 21–82 years and were free of any known chronic diseases at enrollment. They have undergone health examinations in a clinical center, including blood collection, every 3–5 years. We only analyzed participants who self-identify as White (98% of our samples). DNA methylation arrays were profiled in 1455 blood samples across 751 participants from first to 4th visit. Of the blood samples, 82 were entirely removed from our study based on our quality control for missingness in CpG sites (number of sites > 5000), yielding 732 participants (1373 blood samples) remained in our study. All study participants provided written informed consent before enrollment and sample collection. This study was approved by the Harvard T.H. Chan School of Public Health and the Institutional Review Boards of the Department of Veterans Affairs.

DNA methylation quantification

DNA samples were extracted using the IQAamp DNA Blood Kit (Qiagen, CA, U.S.) from the buffy coat of the whole blood collected between 1999 and 2013. We measured DNAm by the Illumina Infinium Human Methylation450K BeadChip (450 K; Illumina Inc., San Diego, CA, U.S.), which provides information on ~ 485,000 CpG sites. To minimize batch effects, we randomized the samples across 450 K BeadChip and 96-well plates based on a two-stage age-stratified algorithm so that age distributed similarly across plates [37]. Quality control analysis was quided by detection P values. More details for quality control can be found in the study from Wang et al. [38].

Saliva study: NHLBI Growth Health Study Cohort

The NHLBI Growth and Health Study (NGHS) cohort [39] was a longitudinal study conducted from 1985 to 2000 that investigated the racial differences in factors relating to the development of obesity in Black and White pre-adolescent girls. The study initially recruited girls 9 and 10 years of age from Richmond (CA, USA), Cincinnati (OH, USA), and Washington (D.C., USA). The NGHS Contra Costa County cohort (n = 887) was recruited in 1987-1988 from public and parochial schools in the Richmond Unified School District area. The area was chosen due to census data that showed approximately equal percentages of Black and White children with the smallest degree of income and occupational disparity between races. A 30-year follow-up of the Contra Costa County cohort was conducted in 2016 [39], enrolling eligible Black (n = 307) and White (n = 317) women from the original cohort approximately at 39 to 42 years of age to assess midlife health and well-being. Eligibility criteria included not being pregnant at the time of recruitment, not experiencing a pregnancy, miscarriage, or abortion in the three months prior to recruitment, and not living abroad, being incarcerated, or being otherwise institutionalized. Consenting participants participated in a baseline survey as well as biospecimen collection, which included saliva collection.

DNA methylation quantification

Methylation arrays were profiled in saliva samples from 688 individuals including mothers (n=442) and their most recent children (n=246). The saliva samples were analyzed at the Semel Institute UCLA Neurosciences Genomics Core (UNGC) using the Illumina 850k BeadChip. Genomic DNA was isolated using temperature denaturation and subjected to bisulfite conversion, PCR amplification, and DNA sequencing (EZ DNA Methylation-Gold Kit, Zymo Research). Of the 442 mothers, 10 women missing for ethnic status, with low confidence in the estimate of chronological age, or technical outliers were removed from our analysis, yielding 432 mothers (218 White and 214 Black) remained in our study.

Supplementary Methods: Estimation of blood cell counts based on DNAm levels

We estimated blood cell counts using two different software tools. First, Houseman's estimation method [40] was used to estimate the proportions of CD8+ T cells, CD4+ T, natural killer, B cells, and granulocytes (mainly neutrophils). Second, the Horvath blood cell estimation method, implemented in the advanced analysis option of the epigenetic clock software [41, 42], was used to estimate the percentage of exhausted CD8+ T cells (defined as CD28-CD45RA-), the number (count) of naïve CD8+ T cells (defined as CD45RA+CCR7+) and plasma blasts cells. We and others have shown that the estimated blood cell counts have moderately high correlations with corresponding flow cytometric measures [40, 43].

Supplementary Figures

In the figures, we use abbreviations for the names of our study cohorts as the following: FHS train and test datasets, Women's Health Initiatives (WHI) BA23, WHI EMPC, Jackson Heart Study (JHS), InCHIANTI (baseline and the third follow-up), Baltimore Longitudinal Study of Aging (BLSA), Lothian Birth Cohort 1921 (LBC21) and LBC 1936 (LBC36), and Normative Aging Study (NAS). The three racial/ethnic groups (notations) in our study cohorts are Caucasian

(White), African American (AfricanA) and Hispanic (Hispanic).

Supplementary References

1. Gerstein HC, Swedberg K, Carlsson J, McMurray JJ, Michelson EL, Olofsson B, Pfeffer MA, Yusuf S, and CHARM Program Investigators. The hemoglobin A1c level as a progressive risk factor for cardiovascular death, hospitalization for heart failure, or death in patients with chronic heart failure: an analysis of the Candesartan in Heart failure: Assessment of Reduction in Mortality and Morbidity (CHARM) program. Arch Intern Med. 2008; 168:1699–704. https://doi.org/10.1001/archinte.168.15.1699 PMID:18695086

2. Cavero-Redondo I, Peleteiro B, Álvarez-Bueno C, Rodriguez-Artalejo F, Martínez-Vizcaíno V. Glycated haemoglobin A1c as a risk factor of cardiovascular outcomes and all-cause mortality in diabetic and non-diabetic populations: a systematic review and meta-analysis. BMJ Open. 2017; 7:e015949. https://doi.org/10.1136/bmjopen-2017-015949 PMID:28760792

3. Wong HK, Cheung TT, Cheung BM. Adrenomedullin and cardiovascular diseases. JRSM Cardiovasc Dis. 2012; 1. https://doi.org/10.1258/cvd.2012.012003 PMID:24175071

4. Larrayoz IM, Ferrero H, Martisova E, Gil-Bea FJ, Ramírez MJ, Martínez A. Adrenomedullin Contributes to Age-Related Memory Loss in Mice and Is Elevated in Aging Human Brains. Front Mol Neurosci. 2017; 10:384. https://doi.org/10.3389/fnmol.2017.00384 PMID:29187812

5. Liabeuf S, Lenglet A, Desjardins L, Neirynck N, Glorieux G, Lemke HD, Vanholder R, Diouf M, Choukroun G, Massy ZA, and European Uremic Toxin Work Group (EUTox). Plasma beta-2 microglobulin is associated with cardiovascular disease in uremic patients. Kidney Int. 2012; 82:1297–303. https://doi.org/10.1038/ki.2012.301 PMID:22895515

6. Smith LK, He Y, Park JS, Bieri G, Snethlage CE, Lin K, Gontier G, Wabl R, Plambeck KE, Udeochu J, Wheatley EG, Bouchard J, Eggel A, et al. β2-microglobulin is a systemic pro-aging factor that impairs cognitive function and neurogenesis. Nat Med. 2015; 21:932–7. https://doi.org/10.1038/nm.3898 PMID:26147761

7. Ferguson TW, Komenda P, Tangri N. Cystatin C as a biomarker for estimating glomerular filtration rate. Curr Opin Nephrol Hypertens. 2015; 24:295–300. https://doi.org/10.1097/MNH.0000000000000115 PMID:26066476

8. van der Laan SW, Fall T, Soumaré A, Teumer A, Sedaghat S, Baumert J, Zabaneh D, van Setten J, Isgum I, Galesloot TE, Arpegård J, Amouyel P, Trompet S, et al. Cystatin C and Cardiovascular Disease: A Mendelian Randomization Study. J Am Coll Cardiol. 2016; 68:934–45. https://doi.org/10.1016/j.jacc.2016.05.092 PMID:27561768

9. Paterson RW, Bartlett JW, Blennow K, Fox NC, Shaw LM, Trojanowski JQ, Zetterberg H, Schott JM, and Alzheimer's Disease Neuroimaging Initiative. Cerebrospinal fluid markers including trefoil factor 3 are associated with neurodegeneration in amyloid-positive individuals. Transl Psychiatry. 2014; 4:e419. https://doi.org/10.1038/tp.2014.58 PMID:25072324

10. Kaptoge S, Di Angelantonio E, Lowe G, Pepys MB, Thompson SG, Collins R, Danesh J, and Emerging Risk Factors Collaboration. C-reactive protein concentration and risk of coronary heart disease, stroke, and mortality: an individual participant meta-analysis. Lancet. 2010; 375:132–40. https://doi.org/10.1016/S0140-6736(09)61717-7 PMID:20031199

11. Shrivastava AK, Singh HV, Raizada A, Singh SK. C-reactive protein, inflammation and coronary heart disease. The Egyptian Heart Journal. 2015; 67:89–97. https://doi.org/10.1016/j.ehj.2014.11.005

12. Fujita Y, Taniguchi Y, Shinkai S, Tanaka M, Ito M. Secreted growth differentiation factor 15 as a potential biomarker for mitochondrial dysfunctions in aging and age-related disorders. Geriatr Gerontol Int. 2016 (Suppl 1); 16:17–29. https://doi.org/10.1111/ggi.12724 PMID:27018280

13. Maioli S, Lodeiro M, Merino-Serrais P, Falahati F, Khan W, Puerta E, Codita A, Rimondini R, Ramirez MJ, Simmons A, Gil-Bea F, Westman E, Cedazo-Minguez A, and Alzheimer's Disease Neuroimaging Initiative. Alterations in brain leptin signalling in spite of unchanged CSF leptin levels in Alzheimer's disease. Aging Cell. 2015; 14:122–9. https://doi.org/10.1111/acel.12281 PMID:25453257

14. Cesari M, Pahor M, Incalzi RA. Plasminogen activator inhibitor-1 (PAI-1): a key factor linking fibrinolysis and age-related subclinical and clinical conditions. Cardiovasc Ther. 2010; 28:e72–91. https://doi.org/10.1111/j.1755-5922.2010.00171.x PMID:20626406

15. As, Chao C, Borgmann K, Brew K, Ghorpade A. Tissue inhibitor of metalloproteinases-1 protects human neurons from staurosporine and HIV-1-induced

apoptosis: mechanisms and relevance to HIV-1-associated dementia. Cell Death Dis. 2012; 3:e332. https://doi.org/10.1038/cddis.2012.54 PMID:22739984

16. Dawber TR, Meadors GF, MOORE FE Jr. Epidemiological approaches to heart disease: the Framingham Study. Am J Public Health Nations Health. 1951; 41:279–81. https://doi.org/10.2105/ajph.41.3.279 PMID:14819398

17. Kannel WB, Feinleib M, McNamara PM, Garrison RJ, Castelli WP. An investigation of coronary heart disease in families. The Framingham offspring study. Am J Epidemiol. 1979; 110:281–90. https://doi.org/10.1093/oxfordjournals.aje.a112813 PMID:474565

18. Aryee MJ, Jaffe AE, Corrada-Bravo H, Ladd-Acosta C, Feinberg AP, Hansen KD, Irizarry RA. Minfi: a flexible and comprehensive Bioconductor package for the analysis of Infinium DNA methylation microarrays. Bioinformatics. 2014; 30:1363–9. https://doi.org/10.1093/bioinformatics/btu049 PMID:24478339

19. Design of the Women's Health Initiative clinical trial and observational study. The Women's Health Initiative Study Group. Control Clin Trials. 1998; 19:61–109. https://doi.org/10.1016/s0197-2456(97)00078-0 PMID:9492970

20. Anderson GL, Manson J, Wallace R, Lund B, Hall D, Davis S, Shumaker S, Wang CY, Stein E, Prentice RL. Implementation of the Women's Health Initiative study design. Ann Epidemiol. 2003; 13:S5–17. https://doi.org/10.1016/s1047-2797(03)00043-7 PMID:14575938

21. Whitsel E. Epigenetic Mechanisms of PM-Mediated CVD Risk (WHI-EMPC; R01-ES020836). National Institutes of Health US Department of Health and Human Services Research Portfolio Online Reporting Tools. 2016.

22. Teschendorff AE, Marabita F, Lechner M, Bartlett T, Tegner J, Gomez-Cabrero D, Beck S. A beta-mixture quantile normalization method for correcting probe design bias in Illumina Infinium 450 k DNA methylation data. Bioinformatics. 2013; 29:189–96. https://doi.org/10.1093/bioinformatics/bts680 PMID:23175756

23. Johnson WE, Li C, Rabinovic A. Adjusting batch effects in microarray expression data using empirical Bayes methods. Biostatistics. 2007; 8:118–27. https://doi.org/10.1093/biostatistics/kxj037 PMID:16632515

24. Lu AT, Xue L, Salfati EL, Chen BH, Ferrucci L, Levy D, Joehanes R, Murabito JM, Kiel DP, Tsai PC, Yet I, Bell JT, Mangino M, et al. GWAS of epigenetic aging rates in blood reveals a critical role for TERT. Nat Commun. 2018; 9:387. https://doi.org/10.1038/s41467-017-02697-5 PMID:29374233

25. Patterson RE, Kristal AR, Tinker LF, Carter RA, Bolton MP, Agurs-Collins T. Measurement characteristics of the Women's Health Initiative food frequency questionnaire. Ann Epidemiol. 1999; 9:178–87. https://doi.org/10.1016/s1047-2797(98)00055-6 PMID:10192650

26. Taylor HA Jr, Wilson JG, Jones DW, Sarpong DF, Srinivasan A, Garrison RJ, Nelson C, Wyatt SB. Toward resolution of cardiovascular health disparities in African Americans: design and methods of the Jackson Heart Study. Ethn Dis. 2005; 15:S6–4. PMID:16320381

27. Moore AZ, Hernandez DG, Tanaka T, Pilling LC, Nalls MA, Bandinelli S, Singleton AB, Ferrucci L. Change in Epigenome-Wide DNA Methylation Over 9 Years and Subsequent Mortality: Results From the InCHIANTI Study. J Gerontol A Biol Sci Med Sci. 2016; 71:1029–35. https://doi.org/10.1093/gerona/glv118 PMID:26355017

28. Zhou W, Triche TJ Jr, Laird PW, Shen H. SeSAMe: reducing artifactual detection of DNA methylation by Infinium BeadChips in genomic deletions. Nucleic Acids Res. 2018; 46:e123. https://doi.org/10.1093/nar/gky691 PMID:30085201

29. Ferrucci L. The Baltimore Longitudinal Study of Aging (BLSA): a 50-year-long journey and plans for the future. J Gerontol A Biol Sci Med Sci. 2008; 63:1416–9. https://doi.org/10.1093/gerona/63.12.1416 PMID:19126858

30. Kuo PL, Schrack JA, Shardell MD, Levine M, Moore AZ, An Y, Elango P, Karikkineth A, Tanaka T, de Cabo R, Zukley LM, AlGhatrif M, Chia CW, et al. A roadmap to build a phenotypic metric of ageing: insights from the Baltimore Longitudinal Study of Aging. J Intern Med. 2020; 287:373–94. https://doi.org/10.1111/joim.13024 PMID:32107805

31. Fabbri E, An Y, Zoli M, Simonsick EM, Guralnik JM, Bandinelli S, Boyd CM, Ferrucci L. Aging and the burden of multimorbidity: associations with inflammatory and anabolic hormonal biomarkers. J Gerontol A Biol Sci Med Sci. 2015; 70:63–70. https://doi.org/10.1093/gerona/glu127 PMID:25104822

32. Deary IJ, Gow AJ, Pattie A, Starr JM. Cohort profile: the Lothian Birth Cohorts of 1921 and 1936. Int J Epidemiol. 2012; 41:1576–84.
https://doi.org/10.1093/ije/dyr197
PMID:22253310

33. Taylor AM, Pattie A, Deary IJ. Cohort Profile Update: The Lothian Birth Cohorts of 1921 and 1936. Int J Epidemiol. 2018; 47:1042–2r.
https://doi.org/10.1093/ije/dyy022
PMID:29546429

34. Marioni RE, Shah S, McRae AF, Chen BH, Colicino E, Harris SE, Gibson J, Henders AK, Redmond P, Cox SR, Pattie A, Corley J, Murphy L, et al. DNA methylation age of blood predicts all-cause mortality in later life. Genome Biol. 2015; 16:25.
https://doi.org/10.1186/s13059-015-0584-6
PMID:25633388

35. Pidsley R, Y Wong CC, Volta M, Lunnon K, Mill J, Schalkwyk LC. A data-driven approach to preprocessing Illumina 450K methylation array data. BMC Genomics. 2013; 14:293.
https://doi.org/10.1186/1471-2164-14-293
PMID:23631413

36. Bell B, Rose CL, Damon A. The Veterans Administration longitudinal study of healthy aging. Gerontologist. 1966; 6:179–84.
https://doi.org/10.1093/geront/6.4.179
PMID:5342911

37. Dai L, Mehta A, Mordukhovich I, Just AC, Shen J, Hou L, Koutrakis P, Sparrow D, Vokonas PS, Baccarelli AA, Schwartz JD. Differential DNA methylation and $PM_{2.5}$ species in a 450K epigenome-wide association study. Epigenetics. 2017; 12:139–48.
https://doi.org/10.1080/15592294.2016.1271853
PMID:27982729

38. Wang C, Cardenas A, Hutchinson JN, Just A, Heiss J, Hou L, Zheng Y, Coull BA, Kosheleva A, Koutrakis P, Baccarelli AA, Schwartz JD. Short- and intermediate-term exposure to ambient fine particulate elements and leukocyte epigenome-wide DNA methylation in older men: the Normative Aging Study. Environ Int. 2022; 158:106955.
https://doi.org/10.1016/j.envint.2021.106955
PMID:34717175

39. Hamlat EJ, Adler NE, Laraia B, Surachman A, Lu AT, Zhang J, Horvath S, Epel ES. Association of subjective social status with epigenetic aging among Black and White women. Psychoneuroendocrinology. 2022; 141:105748.
https://doi.org/10.1016/j.psyneuen.2022.105748
PMID:35397259

40. Houseman EA, Accomando WP, Koestler DC, Christensen BC, Marsit CJ, Nelson HH, Wiencke JK, Kelsey KT. DNA methylation arrays as surrogate measures of cell mixture distribution. BMC Bioinformatics. 2012; 13:86.
https://doi.org/10.1186/1471-2105-13-86
PMID:22568884

41. Horvath S. DNA methylation age of human tissues and cell types. Genome Biol. 2013; 14:R115.
https://doi.org/10.1186/gb-2013-14-10-r115
PMID:24138928

42. Horvath S, Levine AJ. HIV-1 Infection Accelerates Age According to the Epigenetic Clock. J Infect Dis. 2015; 212:1563–73.
https://doi.org/10.1093/infdis/jiv277
PMID:25969563

43. Horvath S, Gurven M, Levine ME, Trumble BC, Kaplan H, Allayee H, Ritz BR, Chen B, Lu AT, Rickabaugh TM, Jamieson BD, Sun D, Li S, et al. An epigenetic clock analysis of race/ethnicity, sex, and coronary heart disease. Genome Biol. 2016; 17:171.
https://doi.org/10.1186/s13059-016-1030-0
PMID:27511193

44. Langfelder P, Horvath S. WGCNA: an R package for weighted correlation network analysis. BMC Bioinformatics. 2008; 9:559.
https://doi.org/10.1186/1471-2105-9-559
PMID:19114008

Supplementary Figures

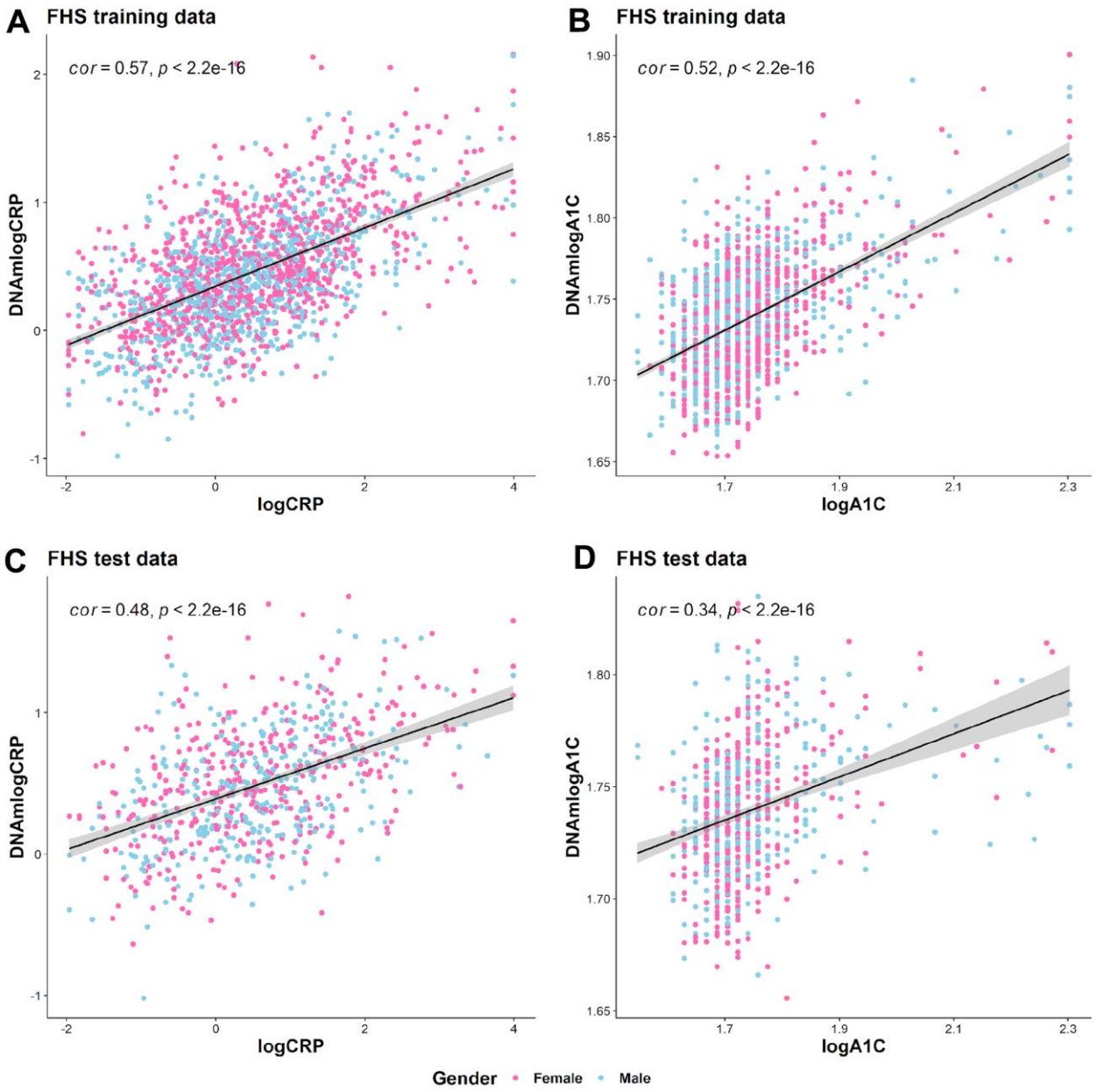

Supplementary Figure 1. New DNAm proteins. The top panels (**A**, **B**) and bottom panels (**C**, **D**) are based on FHS training and test dataset, respectively. (**A**, **C**) The panels depict scatter plots of log scale of C-reactive protein (CRP, x-axis) versus DNAmlogCRP (y-axis). (**B**, **D**) The panels depict scatter plots of log scale of hemoglobin A1C (x-axis) versus DNAmlogA1C (y-axis). The title of each panel reports the data set. The Pearson correlation coefficient (cor) and a corresponding correlation test p-value are report at each panel. The top panels are based on the training dataset (70% pedigrees) of Framingham Heart Study (FHS) pedigree data that were used to develop DNAm based biomarkers. The bottom panels are based on FHS test dataset with individuals from the remaining 30% pedigrees to test the predictive power of the DNAm biomarkers. The extreme values for the CRP and A1C variables were defined if their scaled values were ≥ 6 and were winsorized before the training process. The plots depict the log scale applying on the variables after winsorization.

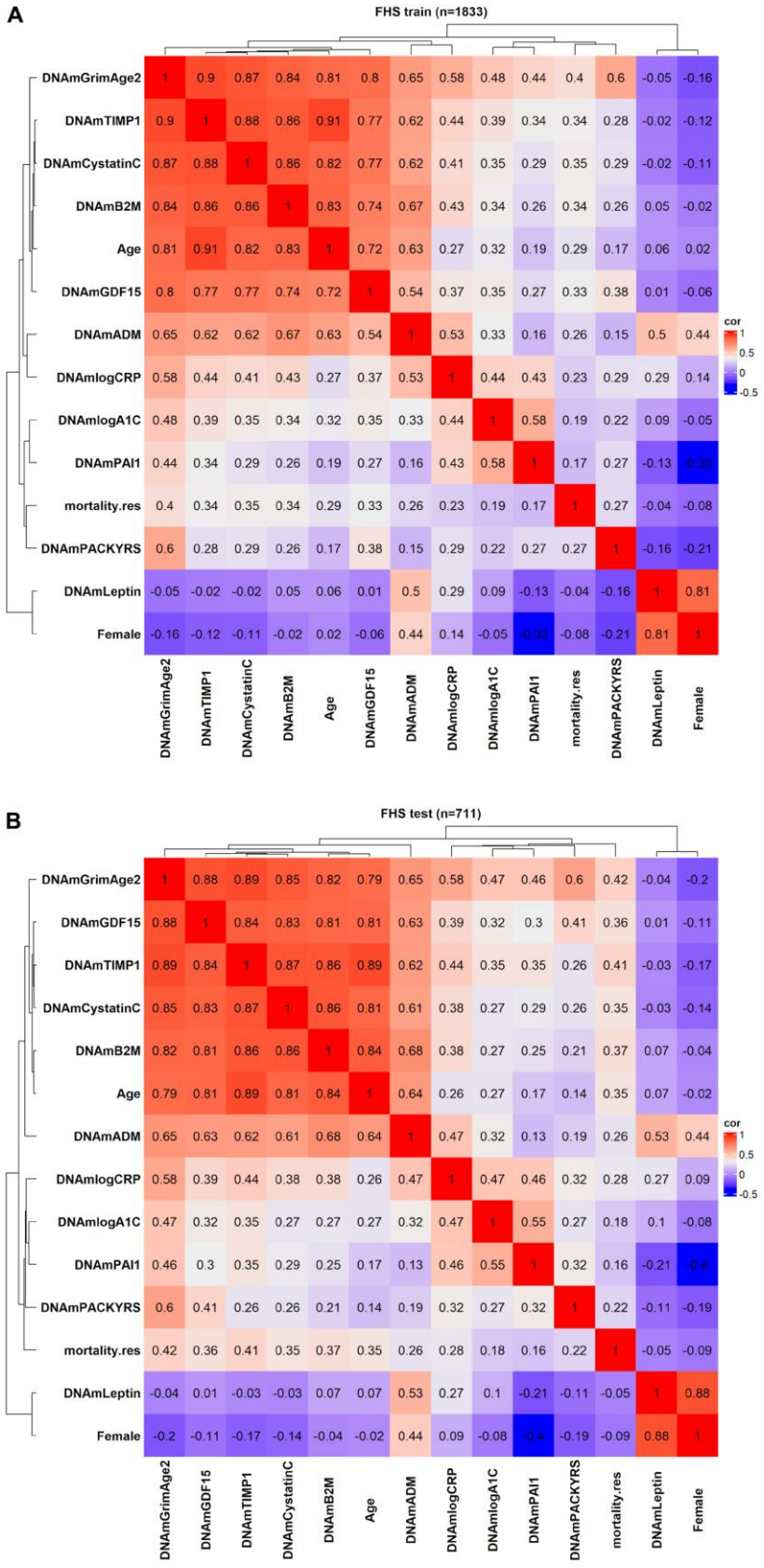

Supplementary Figure 2. Correlation heatmap among DNAmGrimAge2. The heatmap color-codes the pairwise Pearson correlations of DNAmGrimAge2 and its 10 components: (**A**) the heatmap based on the training dataset in FHS (n=1833), and (**B**) the heatmap based on the

test dataset in FHS (n=711). DNAm GrimAge2 is defined as a linear combination of chronological age (Age), sex (Female takes on the value 1 for females and 0 otherwise), and ten DNAm-based surrogate markers for smoking pack-years (DNAm PACKYRS), adrenomedullin levels (DNAm ADM), beta-2 microglobulin (DNAm B2M), cystatin C (DNAm Cystatin C), growth differentiation factor 15 (DNAm GDF-15), leptin (DNAm Leptin),) log scale of C reactive protein (CRP), log scale of hemoglobin A1C,plasminogen activation inhibitor 1 (DNAm PAI-1), and tissue inhibitor metalloproteinase 1 (DNAm TIMP-1). The figure also includes an estimator of mortality risk, *mortality.res*, which can be interpreted as a measure of "excess" mortality risk compared to the baseline risk in the study data. Formally, mortality.res is defined as the deviance residual from a Cox regression model for time-to-death due to all-cause mortality. The rows and columns of the figure are sorted according to a hierarchical clustering tree. The shades of color (blue, white, and red) visualize correlation values from -1 to 1. Each square reports a Pearson correlation coefficient.

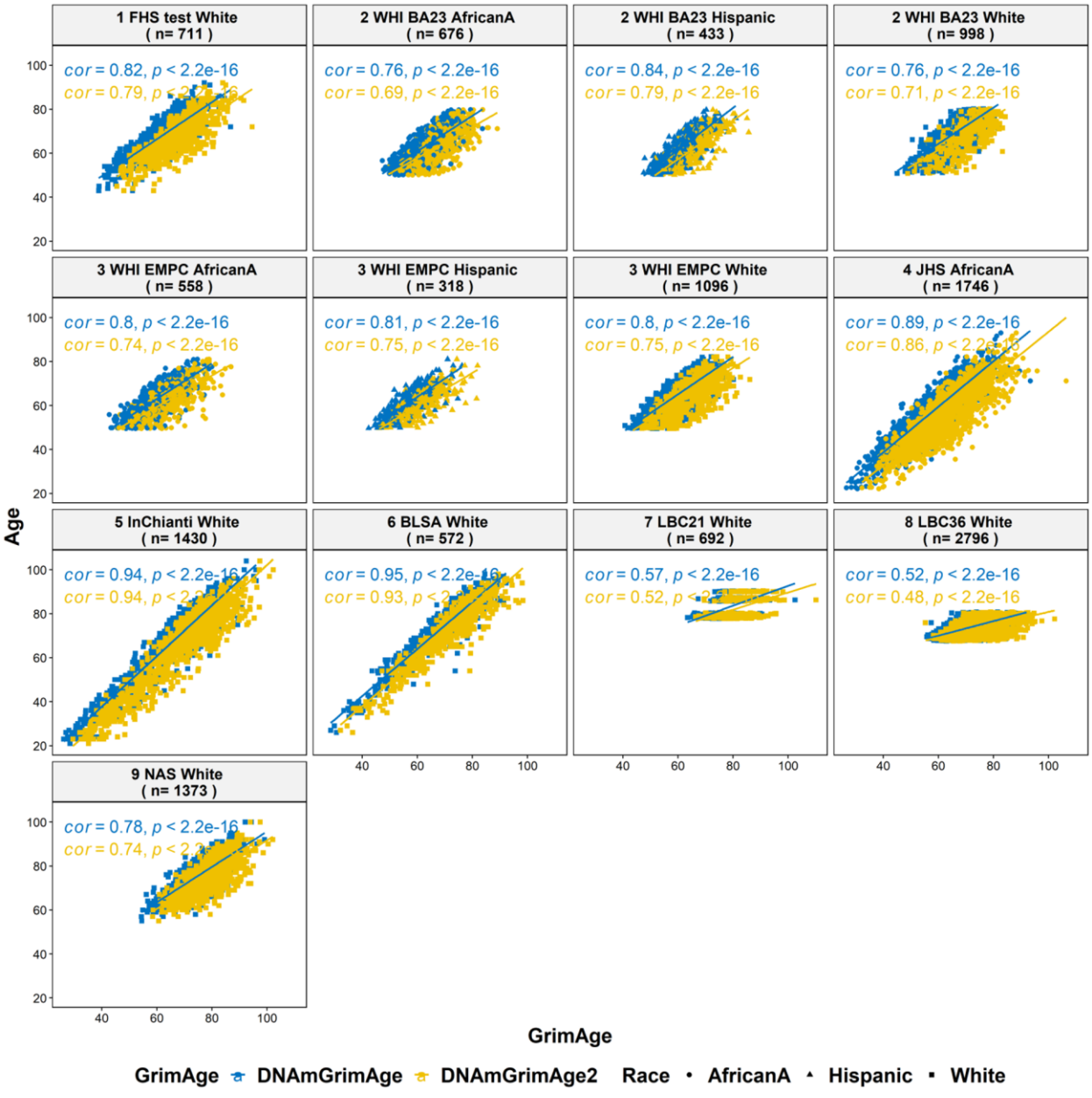

Supplementary Figure 3. DNAm GrimAge(2) versus chronological age in different study cohorts. Each panel depicts a scatter plot of GrimAge2/GrimAge (x-axis) versus chronological age at the time of the blood draw (x-axis). The title of each panel reports the data set and the sample size. The plots of the WHI cohorts are stratified by race/ethnic groups. The statistics Pearson correlation coefficient, and a corresponding correlation test p-value are reported at each panel stratified by DNAmGrimAge2 and DNAmGrimAge, respectively. Each point is marked by blue for DNAmGrimAge and yellow for DNAmGrimAge2, with a point shape based on race/ethnicity, as listed in legend. AfricanA denotes African American.

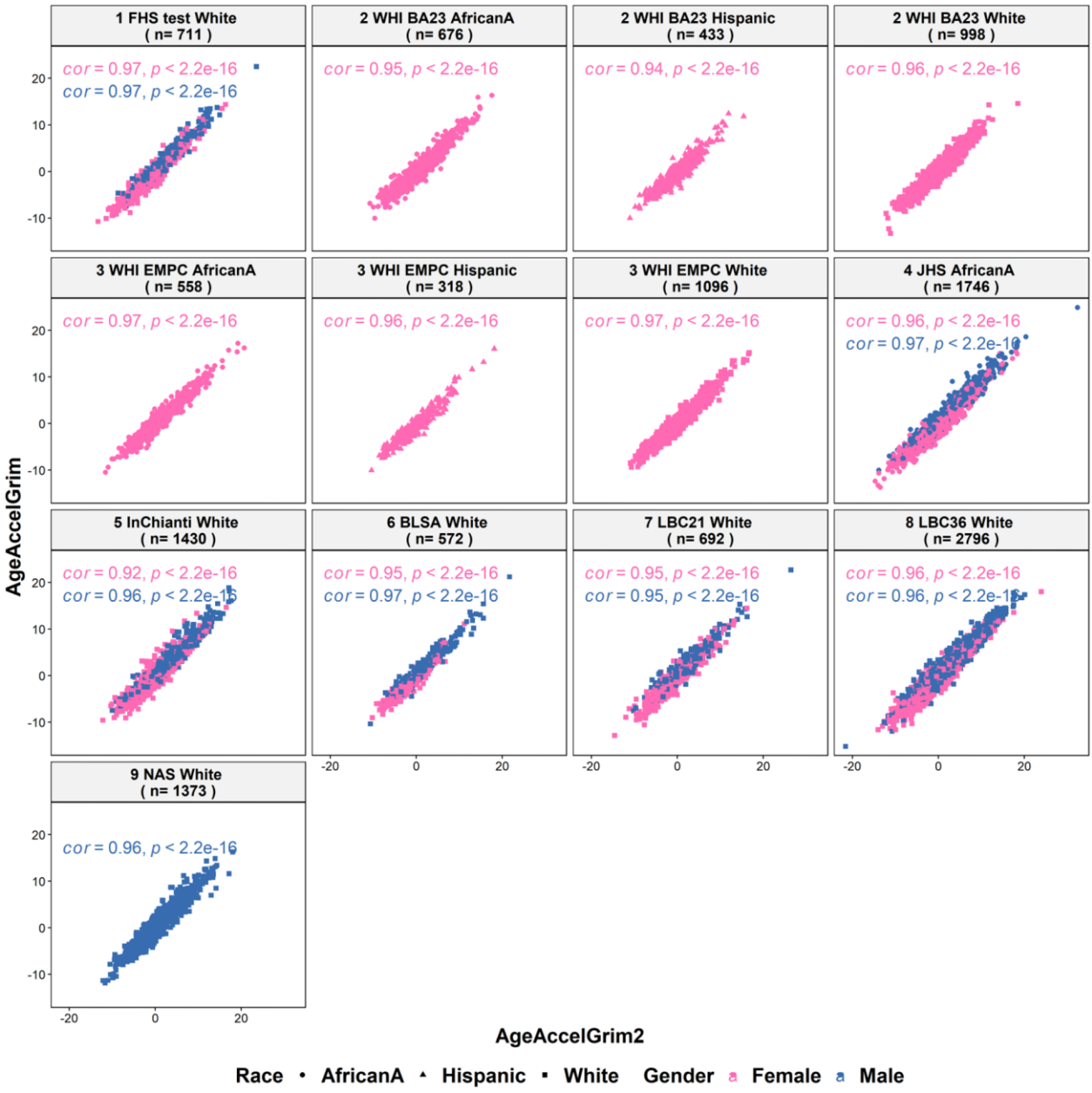

Supplementary Figure 4. AgeAccelGrim2 versus AgeAccelGrim in different study cohorts. Each panel depicts a scatter plot of AgeAccelGrim2(x-axis) versus AgeAccelGrim (y-axis) at the time of the blood draw. The title of each panel reports the data set and the sample size. The plots of the WHI cohorts are stratified by race/ethnic groups. The statistics Pearson correlation coefficient, and a corresponding correlation test p-value are reported at each panel stratified by gender. Each point is marked by blue for males and hot pink for females, with a point shape based on race/ethnicity, as listed in legend. AfricanA denotes African American.

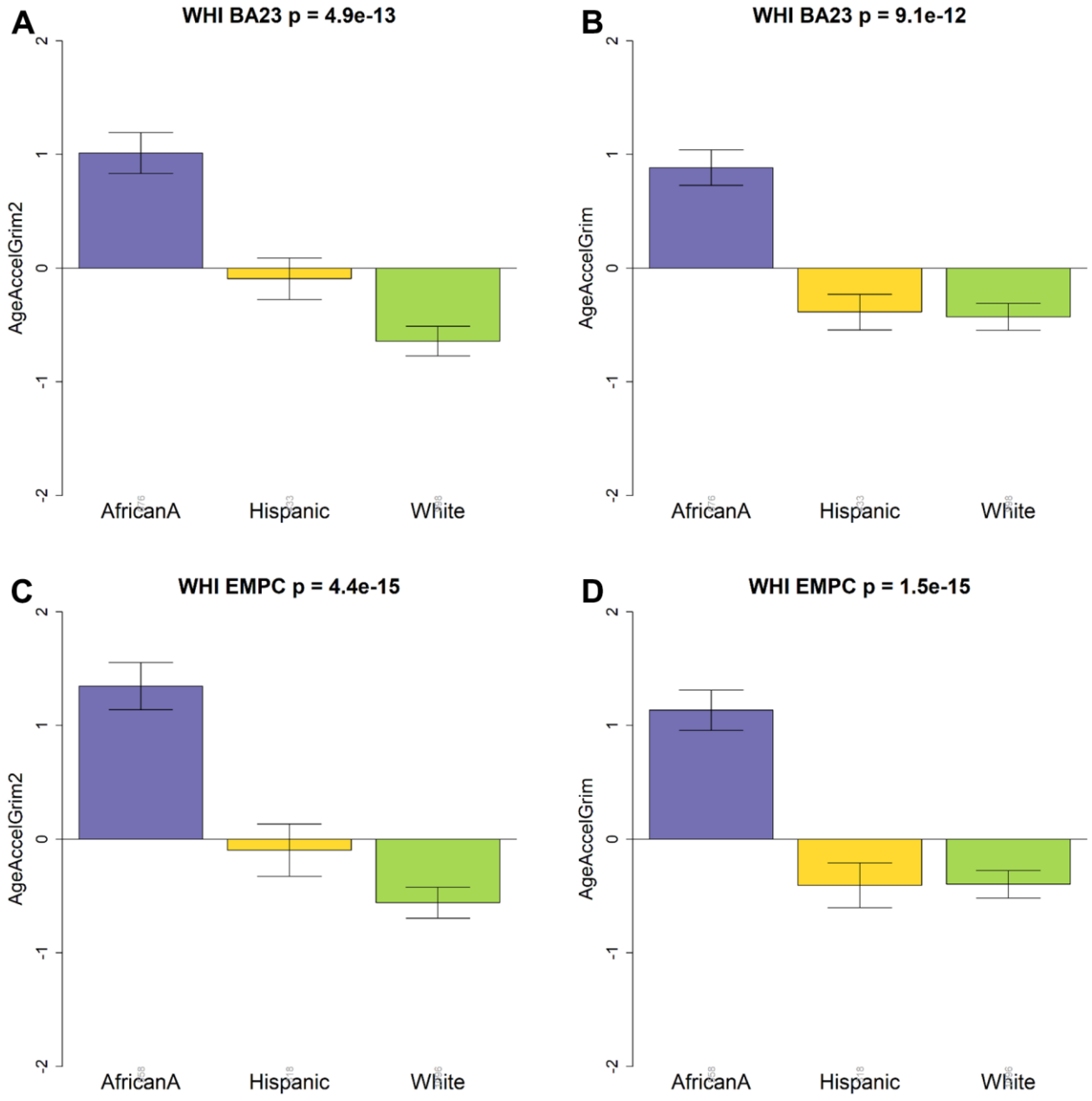

Supplementary Figure 5. Association between epigenetic age acceleration of GrimAges versus ethnicity. The figure presents bar plots for the associations between AgeAccelGrim2/AgeAccelGrim (y-axis) and three racial/ethnic group: African American (AfricanA), Hispanic and White. The upper (**A**, **B**)/lower (**C**, **D**) panels are based on WHI BA23/WHI EMPC datasets, respectively. The left/right panels display AgeAccelGrim2/AgeAccelGrim on y-axis, respectively. The bar plots report the p-value of a non-parametric group comparison test (Kruskal-Wallis). The y-axis of the bar plots depicts the mean and one standard error. The number under each bar presents number of individuals at each racial group.

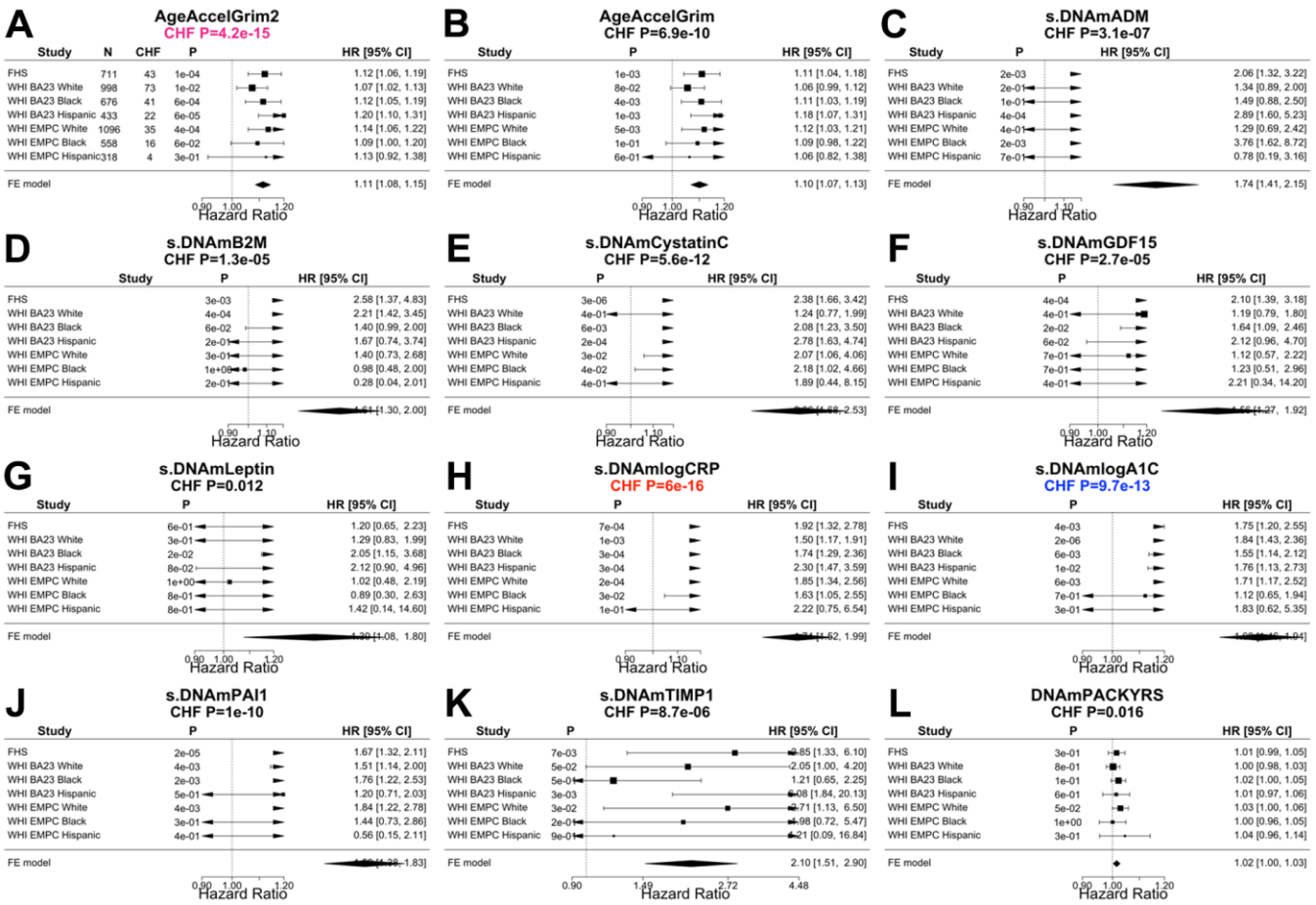

Supplementary Figure 6. Meta analysis forest plots for predicting time-to-congestive heart failure. Fixed effect models meta analysis was performed to combine Cox regression analysis of congestive heart failure (CHF) across 7 strata from 3 study cohorts. Each panel reports a meta analysis forest plot for combining hazard ratios predicting time-to-CHF based on a DNAm based biomarker (reported in the figure heading) across different strata formed by racial group within cohort. (**A**, **B**) display the results for AgeAccelGrim2 and AgeAccelGrim. Each row reports a hazard ratio (for time-to-CHF) and a 95% confidence interval resulting from a Cox regression model in each stratum. (**C**–**L**) display the results for (age-adjusted) DNAm based surrogate markers of (**C**) adrenomedullin (ADM), (**D**) beta-2 microglobulin (B2M), (**E**) cystatin C (Cystatin C), (**F**) growth differentiation factor 15 (GDF-15), (**G**) leptin, (**H**) log scale of C reactive protein (CRP), (**I**) log scale of hemoglobin A1C, (**J**) plasminogen activation inhibitor 1 (PAI-1), (**K**) tissue inhibitor metalloproteinase 1 (TIMP-1) and (**L**) smoking pack-years (PACKYRS). The sub-title of each panel reports the meta analysis P-value. (**A**, **B**) Each hazard ratio (HR) corresponds to a one-year increase in AgeAccel. (**C**–**K**) Each hazard ratio corresponds to an increase in one-standard deviation. (**L**) Hazard ratios correspond to a one-year increase in pack-years. The most significant meta analysis P-value is marked in red (DNAm logCRP), followed by hot pink (AgeAccelGrim2) and blue (DNAm logA1C), respectively.

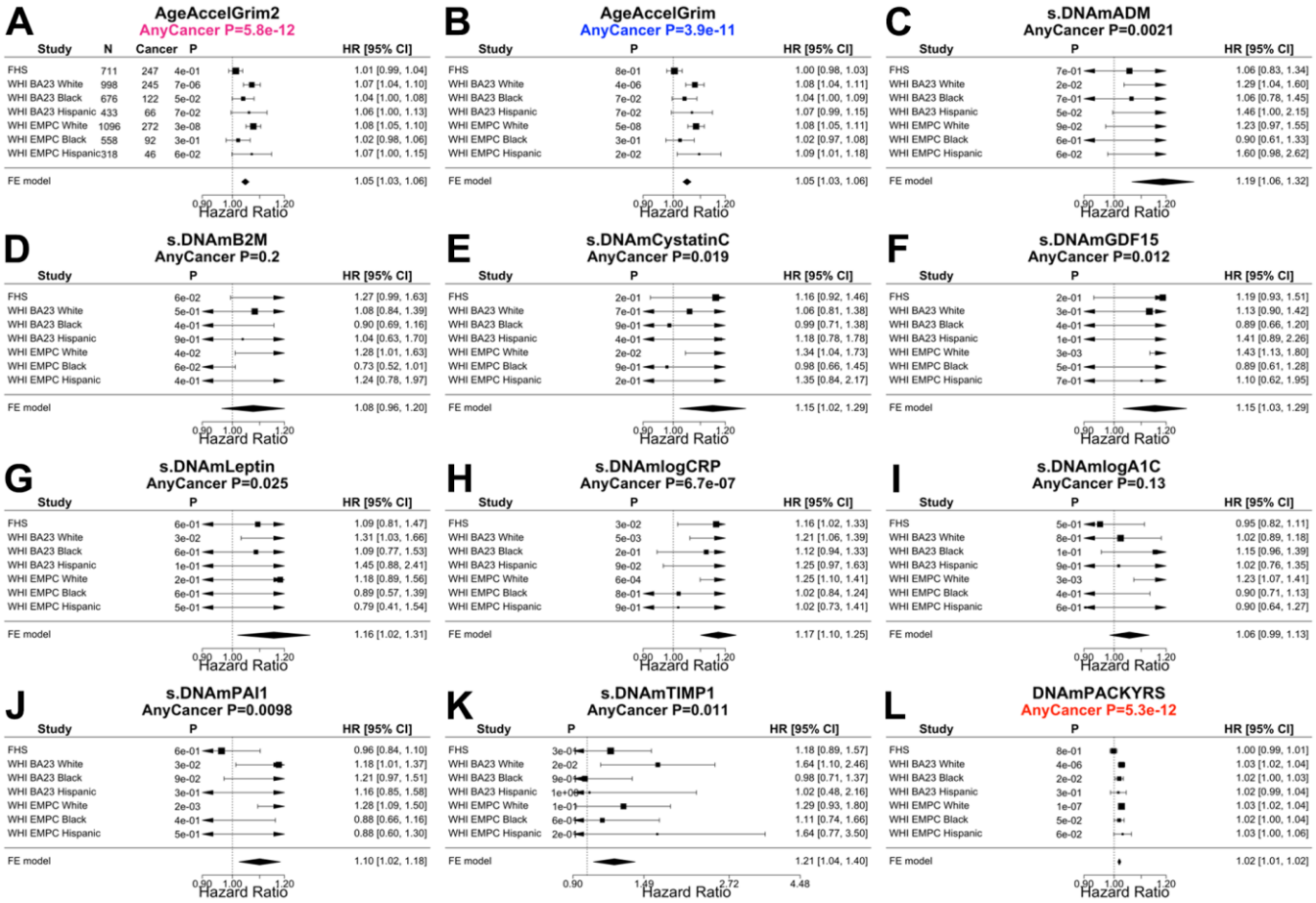

Supplementary Figure 7. Meta analysis forest plots for predicting time-to-any cancer. Fixed effect models meta analysis was performed to combine Cox regression analysis of any cancer across 7 strata from 3 study cohorts. Each panel reports a meta analysis forest plot for combining hazard ratios predicting time-to-any cancer based on a DNAm based biomarker (reported in the figure heading) across different strata formed by racial group within cohort. (**A**, **B**) display the results for AgeAccelGrim2 and AgeAccelGrim. Each row reports a hazard ratio (for time-to-any cancer) and a 95% confidence interval resulting from a Cox regression model in each strata (defined by cohort racial group). (**C**–**L**) display the results for (age-adjusted) DNAm based surrogate markers of (**C**) adrenomedullin (ADM), (**D**) beta-2 microglobulin (B2M), (**E**) cystatin C (Cystatin C), (**F**) growth differentiation factor 15 (GDF-15), (**G**) leptin, (**H**) log scale of C reactive protein (CRP), (**I**) log scale of hemoglobin A1C, (**J**) plasminogen activation inhibitor 1 (PAI-1), (**K**) tissue inhibitor metalloproteinase 1 (TIMP-1) and (**L**) smoking pack-years (PACKYRS). The sub-title of each panel reports the meta analysis p-value. (**A**, **B**) Each hazard ratio (HR) corresponds to a one-year increase in AgeAccelGrim. (**C**–**K**) Each hazard ratio corresponds to an increase in one-standard deviation. (**L**) Hazard ratios correspond to a 1 year increase in pack-years. A *non*-significant Cochran Q test p-value is desirable because it indicates that the hazard ratios don't differ significantly across the strata. The most significant meta analysis P value is marked in red (DNAm PACKYRS), followed by hot pink (AgeAccelGrim2) and blue (AgeAccelGrim), respectively.

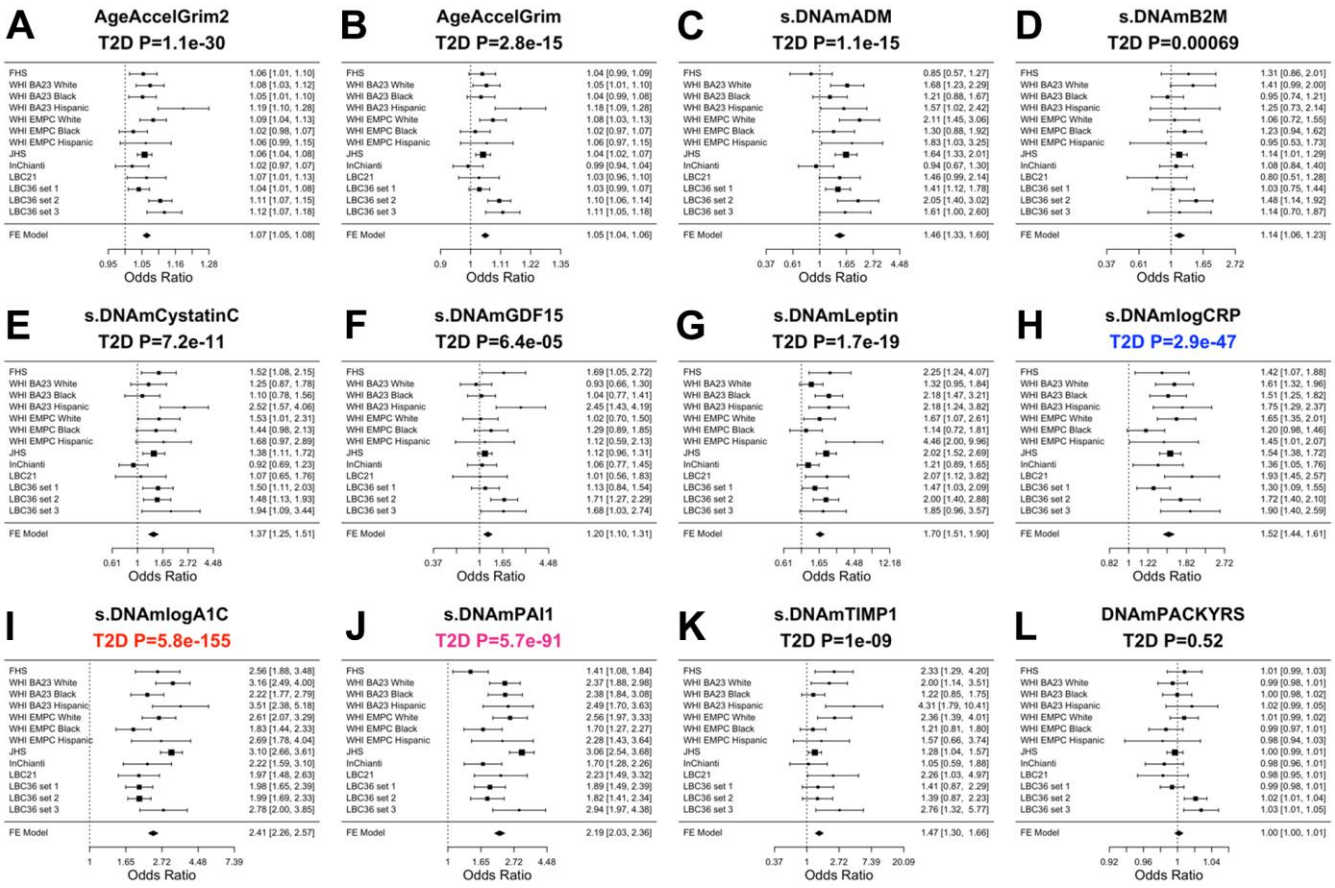

Supplementary Figure 8. Meta analysis for associations with Type 2 diabetes. Each panel reports a meta analysis forest plot based on Stouffer's method to combine association results between disease free status and the DNAm-based biomarker (reported in the figure heading) across different strata, which are formed by racial group within cohort. (**A**, **B**) displays the results for AgeAccelGrim2 and AgeAccelGrim. (**C**–**L**) display the results for scaled DNAm based surrogate markers of (**C**) adrenomedullin (ADM), (**D**) beta-2 microglobulin (B2M), (**E**) cystatin C (Cystatin C), (**F**) growth differentiation factor 15 (GDF-15), (**G**) leptin, (**H**) log scale of C reactive protein (CRP), (**I**) log scale of hemoglobin A1C, (**J**) plasminogen activation inhibitor 1 (PAI-1), (**K**) tissue inhibitor metalloproteinase 1 (TIMP-1) and (**L**) smoking pack-years (PACKYRS). The sub-title of each panel reports the meta analysis p-value. Each row reports an odds ratio (OR) and a 95% confidence interval resulting from a (GEE) logistic regression in each strata (defined by cohort racial or set group). (**A**, **B**) Each OR corresponds to a one-year increase in AgeAccel. (**C**–**K**) Each OR corresponds to an increase in one-standard deviation. (**L**) OR corresponds to a one-year increase in pack-years. The most significant meta analysis P-value is marked in red (DNAm logA1C), followed by hot pink (DNAm PAI1) and blue (DNAm logCRP), respectively.

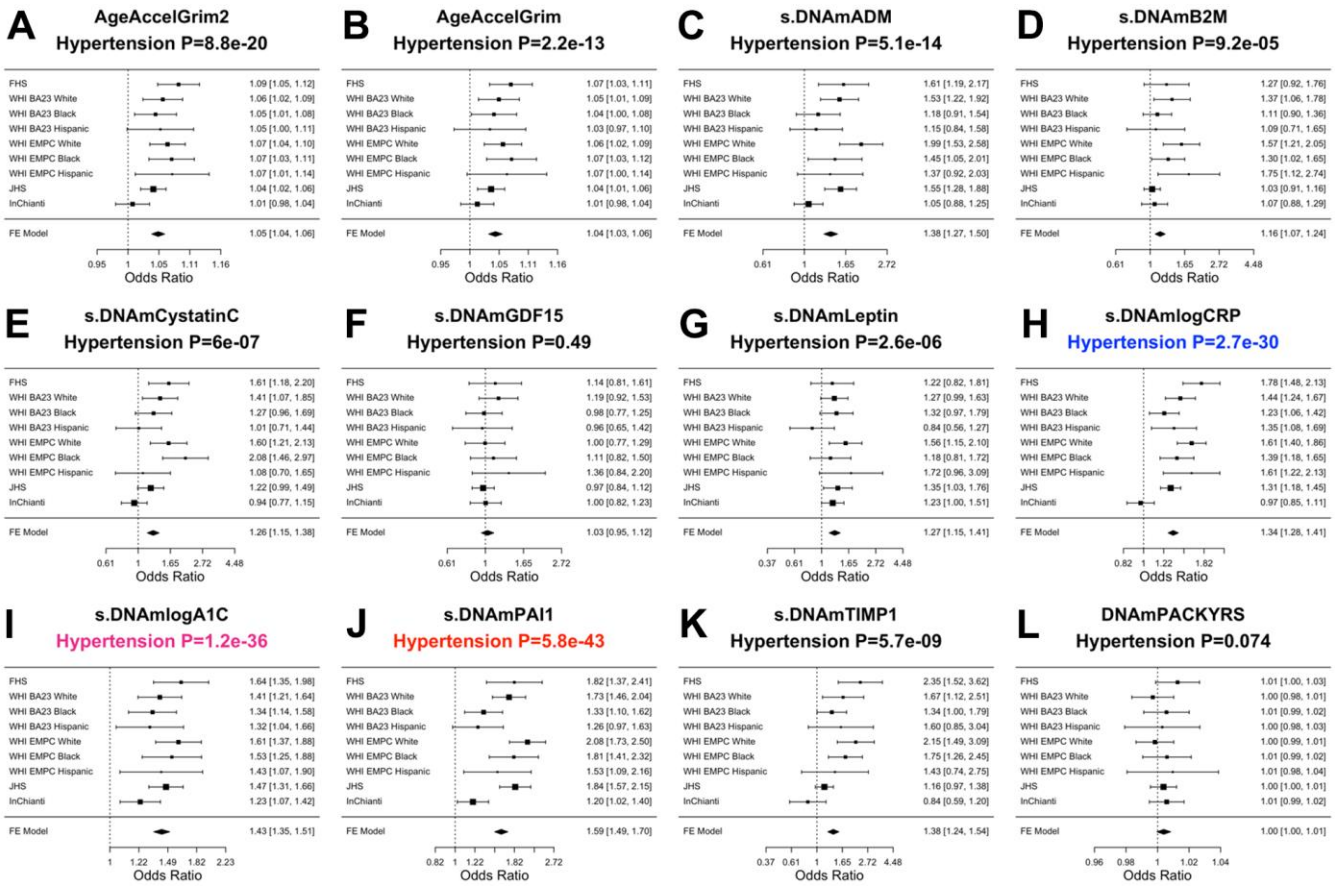

Supplementary Figure 9. Meta analysis for associations with hypertension. Each panel reports a meta analysis forest plot based on Stouffer's method to combine association results between disease free status and the DNAm-based biomarker (reported in the figure heading) across different strata, which are formed by racial group within cohort. (**A**, **B**) display the results for AgeAccelGrim2 and AgeAccelGrim. (**C**–**L**) display the results for scaled DNAm based surrogate markers of (**C**) adrenomedullin (ADM), (**D**) beta-2 microglobulin (B2M), (**E**) cystatin C (Cystatin C), (**F**) growth differentiation factor 15 (GDF-15), (**G**) leptin, (**H**) log scale of C reactive protein (CRP), (**I**) log scale of hemoglobin A1C, (**J**) plasminogen activation inhibitor 1 (PAI-1), (**K**) tissue inhibitor metalloproteinase 1 (TIMP-1) and (**L**) smoking pack-years (PACKYRS). The sub-title of each panel reports the meta analysis p-value. Each row reports an odds ratio (OR) and a 95% confidence interval resulting from a (GEE) logistic regression in each stratum (defined by cohort racial group). (**A**, **B**) Each OR corresponds to a one-year increase in AgeAccel. (**C**–**K**) Each OR corresponds to an increase in one-standard deviation. (**L**) OR corresponds to a one-year increase in pack-years. The most significant meta analysis P-value is marked in red (DNAm PAI-1), followed by hot pink (DNAm logA1C) and blue (DNAm logCRP), respectively.

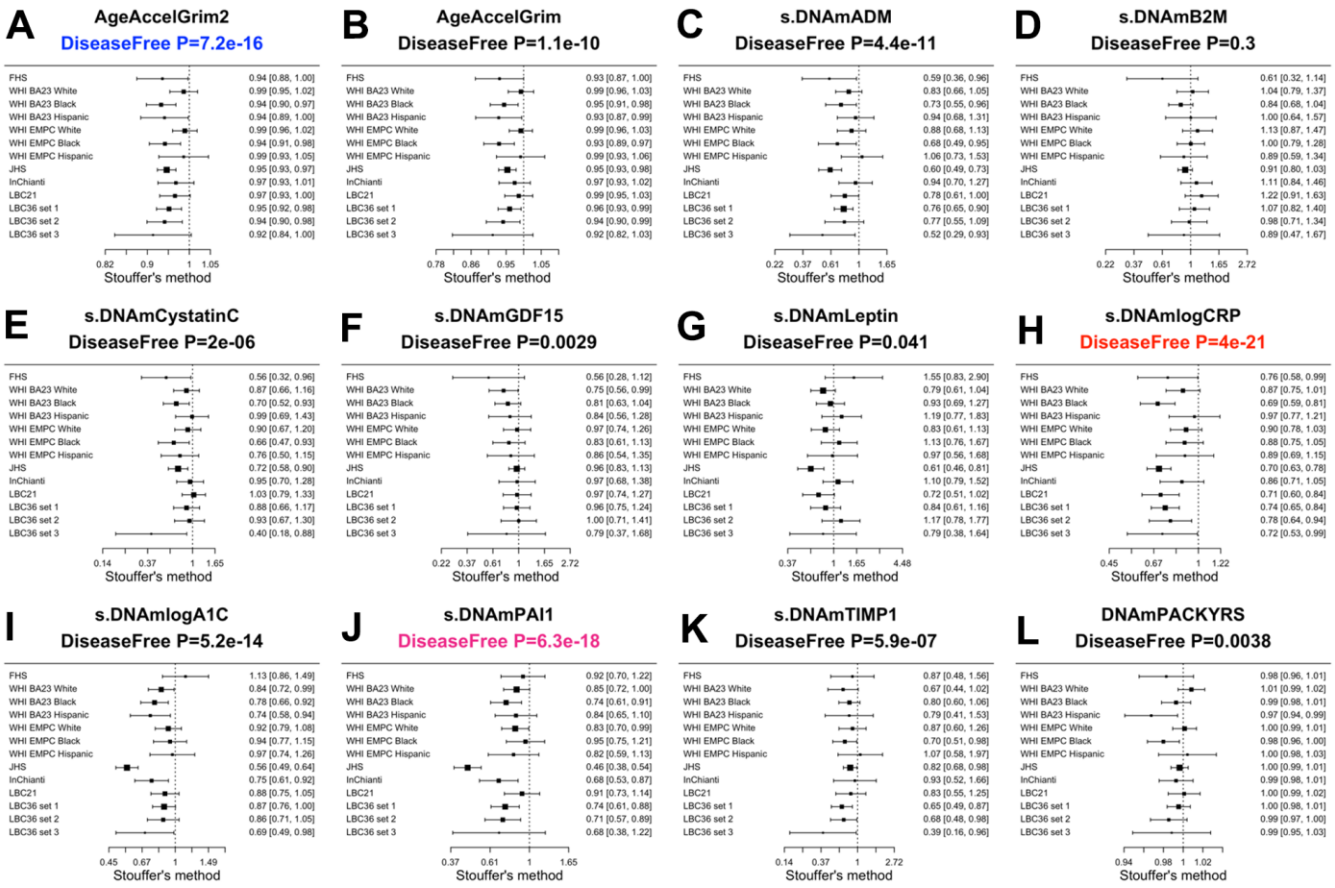

Supplementary Figure 10. Meta analysis for associations with disease free status. Each panel reports a meta analysis forest plot based on Stouffer's method to combine association results between disease free status and the DNAm-based biomarker (reported in the figure heading) across different strata, which are formed by racial group within cohort. (**A**, **B**) display the results for AgeAccelGrim2 and AgeAccelGrim. (**C**–**L**) display the results for scaled DNAm based surrogate markers of (**C**) adrenomedullin (ADM), (**D**) beta-2 microglobulin (B2M), (**E**) cystatin C (Cystatin C), (**F**) growth differentiation factor 15 (GDF-15), (**G**) leptin, (**H**) log scale of C reactive protein (CRP), (**I**) log scale of hemoglobin A1C, (**J**) plasminogen activation inhibitor 1 (PAI-1), (**K**) tissue inhibitor metalloproteinase 1 (TIMP-1) and (**L**) smoking pack-years (PACKYRS). The sub-title of each panel reports the meta analysis p-value. Each row reports an odds ratio (OR) and a 95% confidence interval resulting from a (GEE) logistic regression in each strata (defined by cohort racial/set group). (**A**, **B**) Each OR corresponds to a one-year increase in AgeAccel. (**C**–**K**) Each OR corresponds to an increase in one-standard deviation. (**L**) OR corresponds to a one-year increase in pack-years. The most significant meta analysis P-value is marked in red (DNAm logCRP), followed by hot pink (DNAm PAI1) and blue (AgeAccelGrim2), respectively.

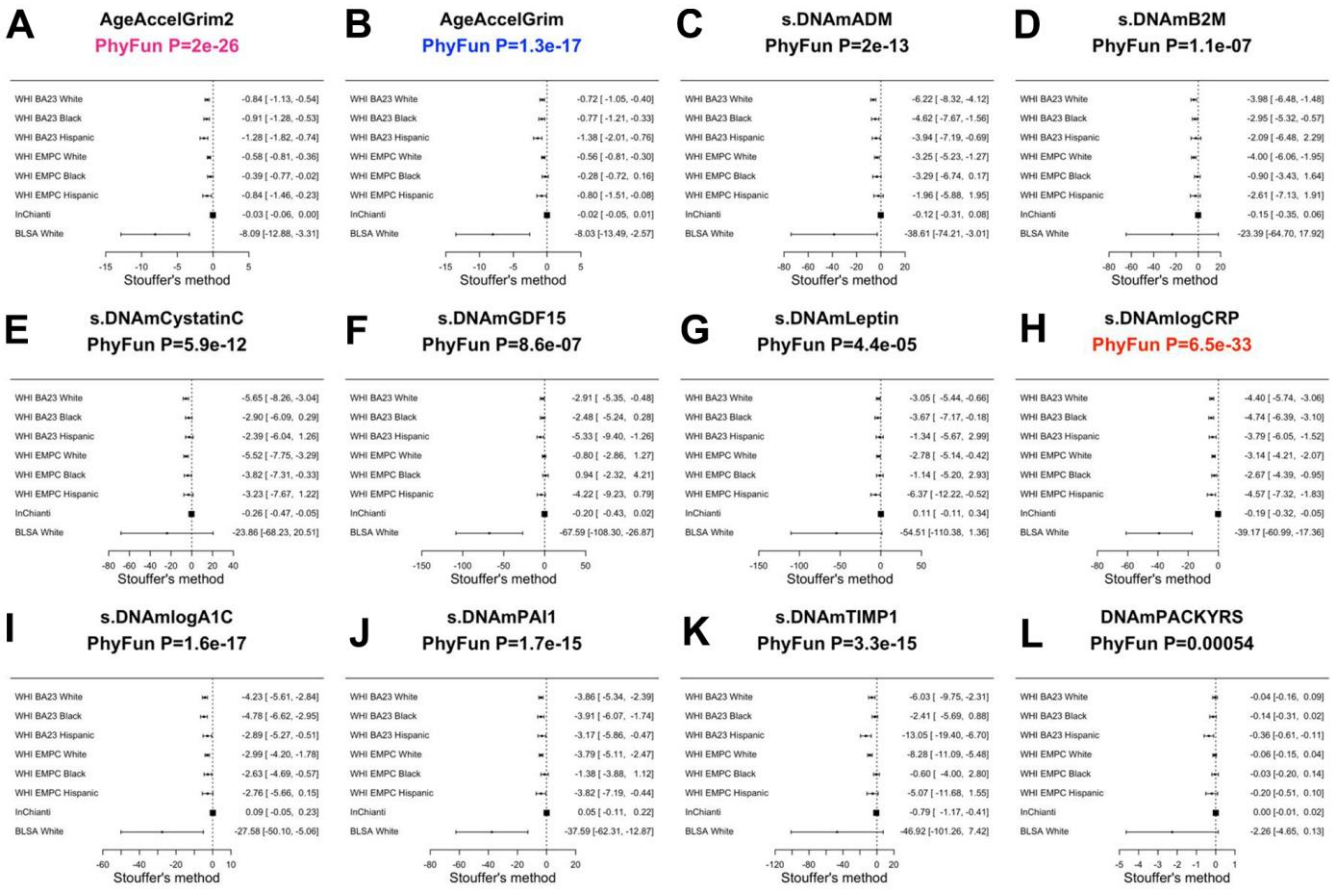

Supplementary Figure 11. Meta analysis for associations with physical functioning level. Each panel reports a meta analysis forest plot based on Stouffer's method to combine association results between physical functioning levels (dependent variable) and the DNAm-based biomarker (independent variable, reported in the figure heading) across different strata, which are formed by racial group within cohort. (**A**, **B**) display the results for AgeAccelGrim2 and AgeAccelGrim. (**C**–**L**) display the results for scaled DNAm based surrogate markers of (**C**) adrenomedullin (ADM), (**D**) beta-2 microglobulin (B2M), (**E**) cystatin C (Cystatin C), (**F**) growth differentiation factor 15 (GDF-15), (**G**) leptin, (**H**) log scale of C reactive protein (CRP), (**I**) log scale of hemoglobin A1C, (**J**) plasminogen activation inhibitor 1 (PAI-1), (**K**) tissue inhibitor metalloproteinase 1 (TIMP-1) and (**L**) smoking pack-years (PACKYRS). The sub-title of each panel reports the meta analysis p-value. Each row reports a beta coefficient β and a 95% confidence interval resulting from a (linear-mixed) regression model in each stratum (defined by cohort racial group). (**A**, **B**) Each β corresponds to a one-year increase in AgeAccel. (**C**–**K**) Each β corresponds to an increase in one-standard deviation. (**L**) β corresponds to a one-year increase in pack-years. The most significant meta analysis P-value is marked in red (DNAm logCRP), followed by hot pink (AgeAccelGrim2) and blue (AgeAccelGrim), respectively.

Supplementary Figure 12. Meta analysis of age-at-menopause. Each panel reports a meta analysis forest plot for combining regression coefficients (slopes) between age-at-menopause in women and the DNAm based biomarker (reported in the figure heading) across different strata, which are formed by racial group within cohort. Age at menopause was treated as independent variable as a causal effect on DNAm variables except for the association with DNAm PACKYRS, in which the pack year variable (independent variable) was used to predict age at menopause (dependent variable). (**A**, **B**) display the results for AgeAccelGrim2 and AgeAccelGrim. (**C**–**L**) display the results for scaled DNAm based surrogate markers of (**C**) adrenomedullin (ADM), (**D**) beta-2 microglobulin (B2M), (**E**) cystatin C (Cystatin C), (**F**) growth differentiation factor 15 (GDF-15), (**G**) leptin, (**H**) log scale of C reactive protein (CRP), (**I**) log scale of hemoglobin A1C, (**J**) plasminogen activation inhibitor 1 (PAI-1), (**K**) tissue inhibitor metalloproteinase 1 (TIMP-1) and (**L**) smoking pack-years (PACKYRS). The sub-title of each panel reports the meta analysis P-value. Each row reports a beta coefficient β and a 95% confidence interval resulting from a (linear-mixed) regression model in each stratum (defined by cohort racial group). Each β corresponds to a one-year late of age at menopause except for the regression analysis with respect to DNAm PACKYRS, in which β corresponds to a one-year increase in pack years. The most significant meta analysis P-value is marked in red (AgeaccelGrim2), followed by hot pink (AgeAccelGrim) and blue (DNAm PACKYRS), respectively.

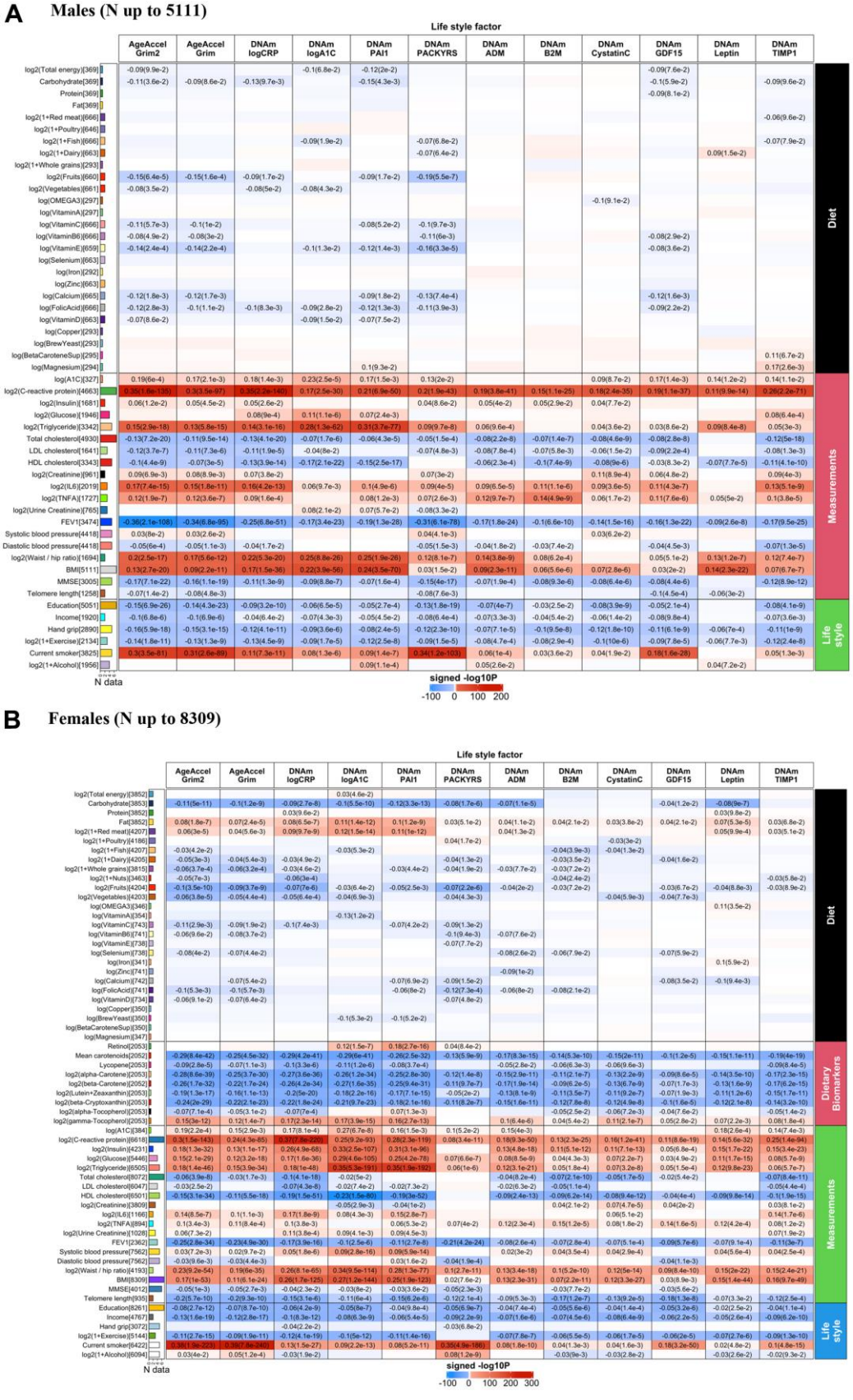

Supplementary Figure 13. Meta cross sectional correlations between DNAm biomarkers and lifestyle factors. Robust correlation coefficients (biweight midcorrelation [44]) between 1) AgeAccelGrim2, AgeAccelGrim, and ten age-adjusted underlying DNAm-

based surrogate biomarkers underlying DNAmGrimAge2, and 2) up to 61variables including 27 self-reported diet, 9 dietary biomarkers, 19 clinically relevant measurements related to vital signs, metabolic traits, inflammatory markers, cognitive function, lung function, central adiposity and leukocyte telomere length, and 6 life style factors including hand grip. Analysis was stratified by (**A**) Males and (**B**) Females, respectively. The y-axis lists lifestyle factor in the format of name (sample size), followed by a bar plot denoting number of studies. Variables are arranged by category displayed on the right annotation. The x-axis lists AgeAccelGrim2, AgeAccelGrim, followed by DNAm variables. The first few DNAm variables (log CRP, log A1C, PAI-1, smoking pack years) show strong correlation with the lifestyle factors in overall. Each cell presents meta bicor estimates and P-value, provided P<0.1. The color gradient is based on -log10 P-values times sign of bicor. P-values are unadjusted.

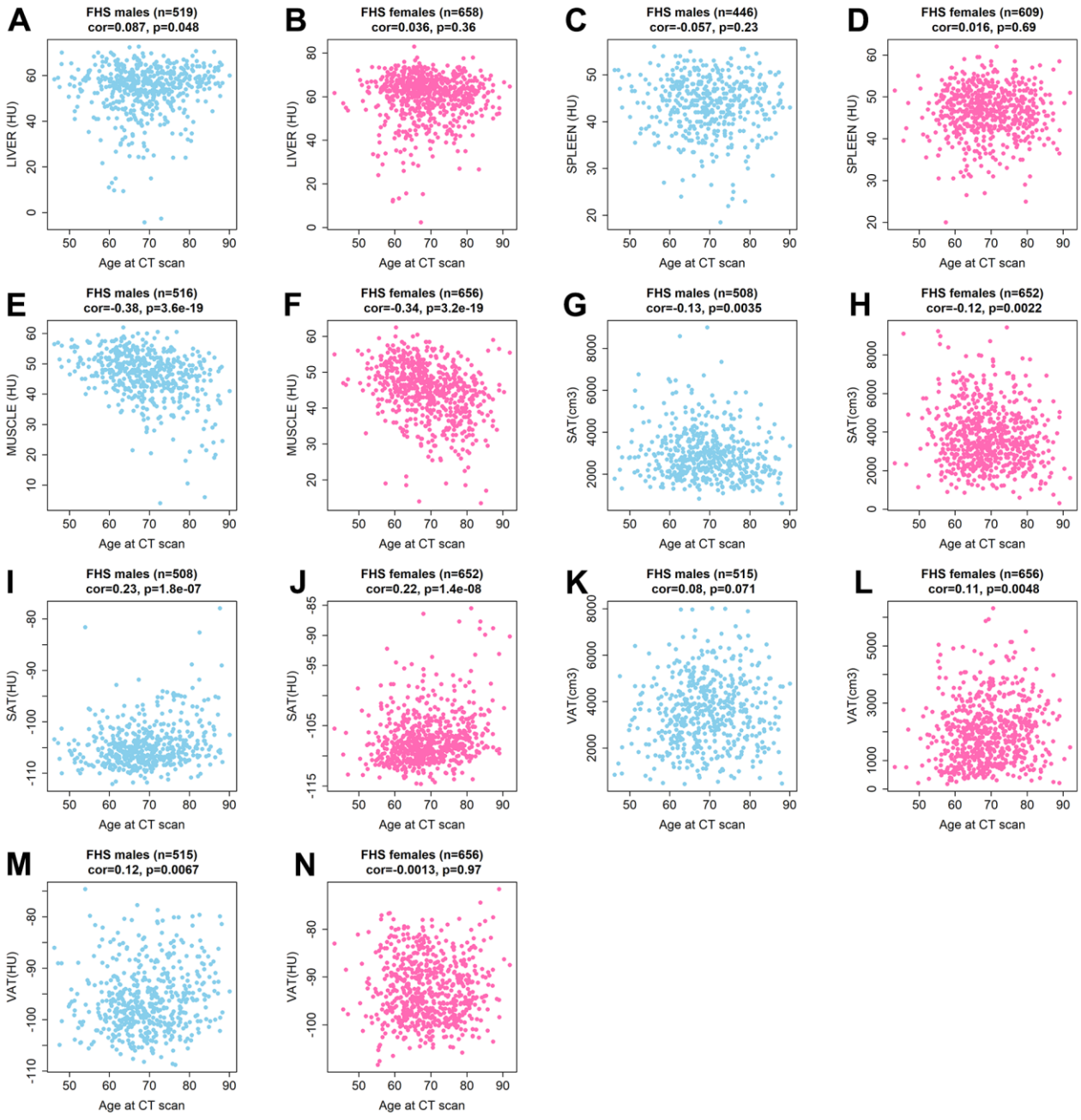

Supplementary Figure 14. Correlation analysis of chronological age versus CT-scan fatty liver and adipose tissue density in the FHS. We present the scatter plots of chronological age at computed tomography (CT) scan (x-axis) versus CT-scan derived measures in the FHS. The CT-scan measures included attenuation in (**A**, **B**) liver, (**C**, **D**) spleen, (**E**, **F**) paraspinal muscle, (**G**–**J**) subcutaneous adipose tissue (SAT) and (**K**–**N**) visceral adipose tissue (VAT). (**A**–**F**, **I**, **J**, **M**, **N**) are in Hounsfield (HU) unit, obtained from a linear transformation of attenuation coefficients. (**G**, **H**, **K**, **L**) are measures of volume in units of cm^3.

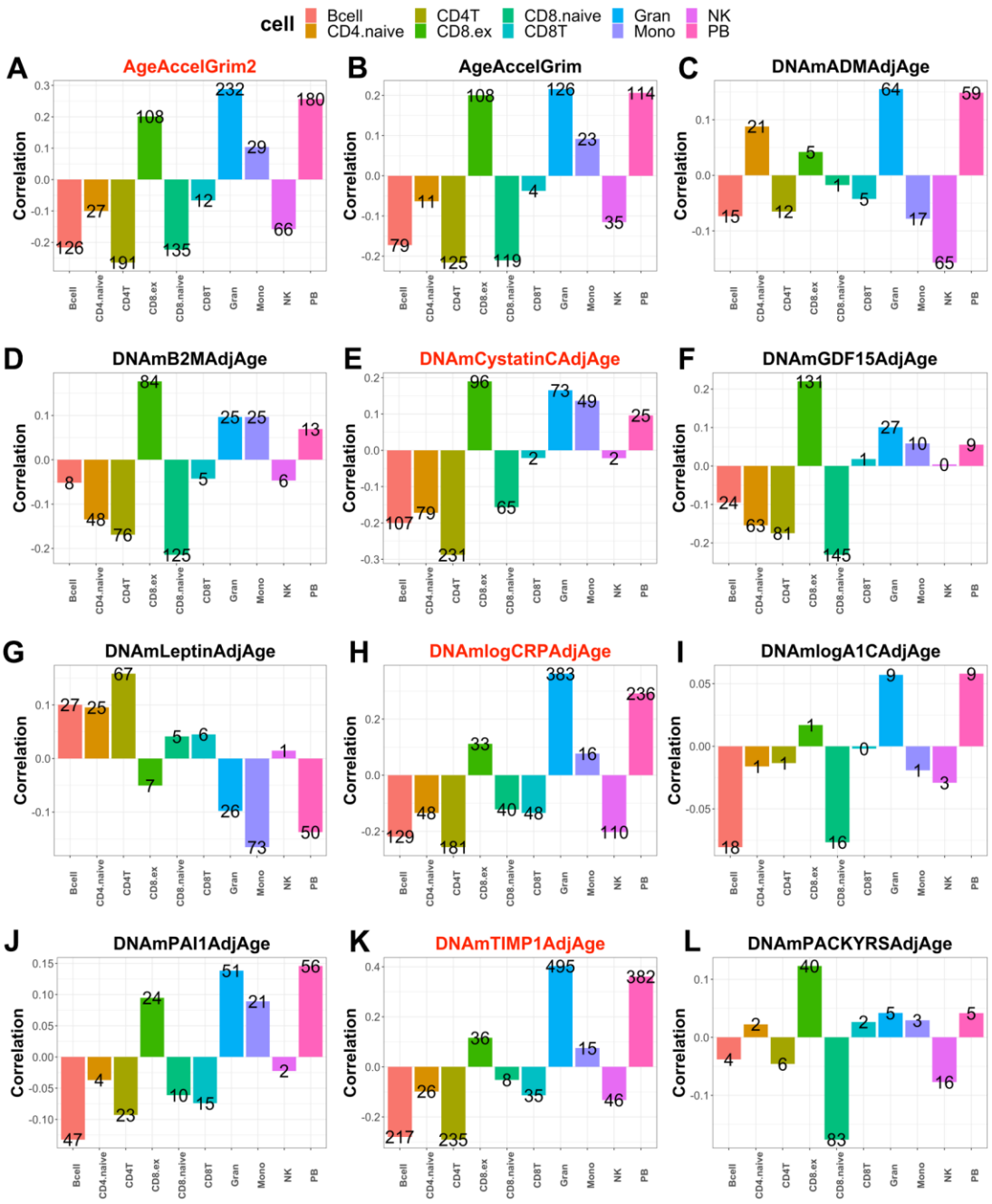

Supplementary Figure 15. Measures of blood cell composition versus DNAm based biomarkers. Each panel reports how the respective DNAm based biomarker (heading) relates to 10 imputed measures of blood cell counts. (**A**, **B**) display the results for AgeAccelGrim2 and AgeAccelGrim. (**C**–**L**) display the results for (age-adjusted) DNAm based surrogate markers of (**C**) adrenomedullin (ADM), (**D**) beta-2 microglobulin (B2M), (**E**) cystatin C (Cystatin C), (**F**) growth differentiation factor 15 (GDF-15), (**G**) leptin, (**H**) log scale of C reactive protein (CRP), (**I**) log scale of hemoglobin A1C, (**J**) plasminogen activation inhibitor 1 (PAI-1), (**K**) tissue inhibitor metalloproteinase 1 (TIMP-1) and (**L**) smoking pack-years (PACKYRS). The height of each bar corresponding to the statistical significance level (meta analysis p-value) of an association test between the blood cell measure and the age-adjusted DNAm biomarker. More precisely, the y-axis presents the meta analysis estimates of the Pearson correlation coefficients. The numbers displayed on top of each bar are minus logarithm (base 10) transformed meta P values. The title is marked by red if any absolute correlation >0.25. The association analysis is *not* confounded by chronological age because we used age adjusted DNAm based biomarkers. The fixed effects meta analysis was performed across the validation study sets (N=11672): FHS test, WHI BA23, JHS, InCHIANTI, BLSA, LBC21, LBC36 and NAS. Abbreviations for cell counts are listed in the following: nature killer (NK), monocyte (MONO) and granulocyte (Gran), CD8pCD28nCD45Ran (CD8.ex for exhausted cytotoxic T cells), and plasma blast (PB). The blood cell counts were imputed based on DNA methylation levels as described in [40, 42] and the Supplementary Methods section (above).

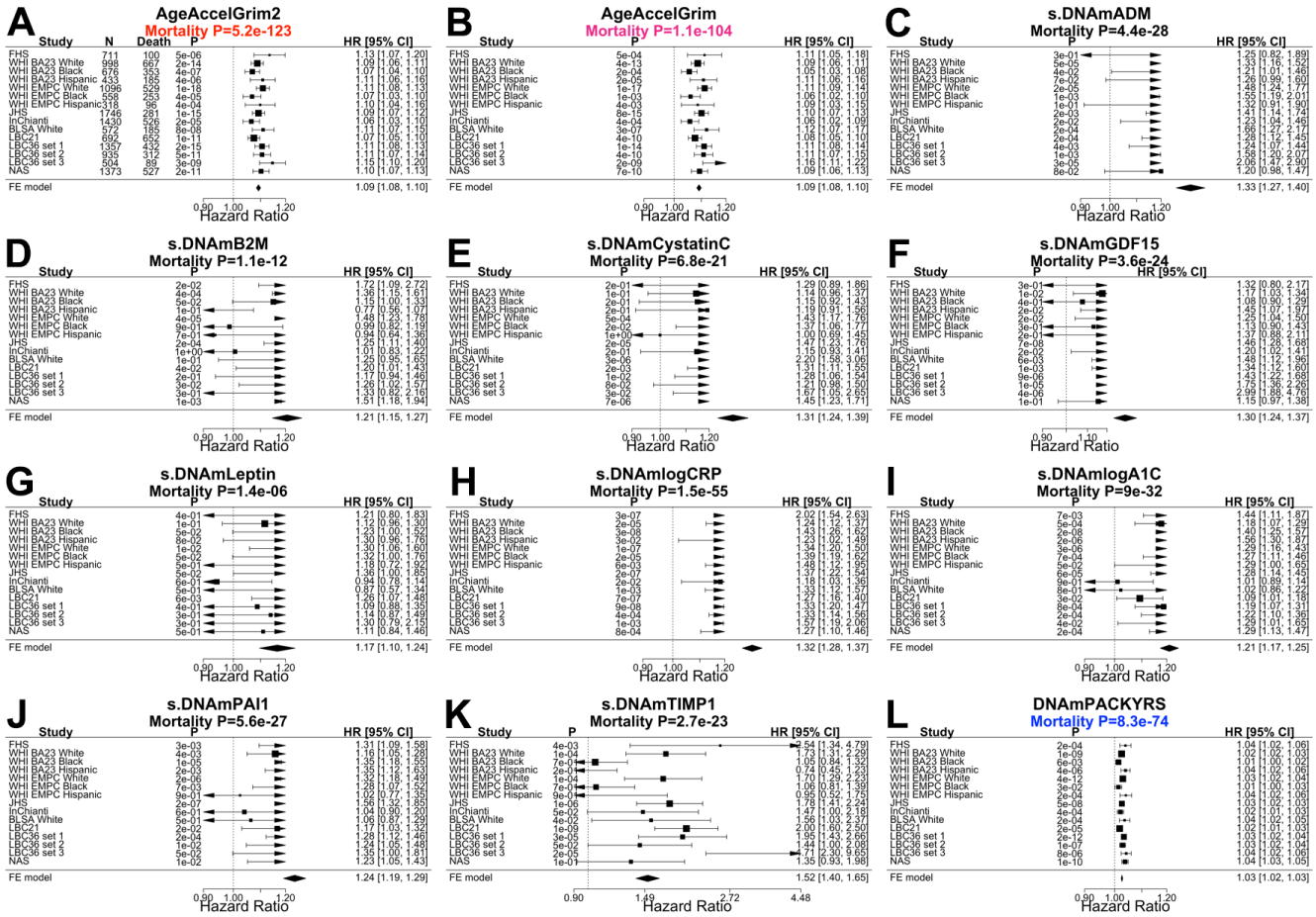

Supplementary Figure 16. Meta analysis forest plots for predicting time-to-death adjusted for blood cell composition. Each panel reports a meta analysis forest plot for combining hazard ratios predicting time-to-death based on a DNAm based biomarker (reported in the figure heading) across different strata formed by racial group within cohort and set within LBC36. Here we re-conducted the survival analysis as listed in Figure 2 and adjusted additional 7 imputed blood cell counts: CD8 naïve, CD8pCD28nCD45Ran, plasma blasts, CD4+ T, nature killer cells, monocytes and granulocytes. (**A**, **B**) display the results for AgeAccelGrim2 and AgeAccelGrim. Each row reports a hazard ratio (for time-to-death) and a 95% confidence interval resulting from a Cox regression model in each of 15 strata. (**C**–**L**) display the results for (age-adjusted) DNAm based surrogate markers of (**C**) adrenomedullin (ADM), (**D**) beta-2 microglobulin (B2M), (**E**) cystatin C (Cystatin C), (**F**) growth differentiation factor 15 (GDF-15), (**G**) leptin, (**H**) log scale of C reactive protein (CRP), (**I**) log scale of hemoglobin A1C, (**J**) plasminogen activation inhibitor 1 (PAI-1), (**K**) tissue inhibitor metalloproteinase 1 (TIMP-1) and (**L**) smoking pack-years (PACKYRS). The sub-title of each panel reports the meta analysis P-value. (**A**, **B**) Each hazard ratio (HR) corresponds to a one-year increase in AgeAccel. (**C**–**K**) Each hazard ratio corresponds to an increase in one-standard deviation. (**L**) Hazard ratios correspond to a one-year increase in pack-years. The most significant meta analysis P-value is marked in red (AgeAccelGrim2), followed by hot pink (AgeAccelGrim) and blue (DNAm PACKYRS), respectively.

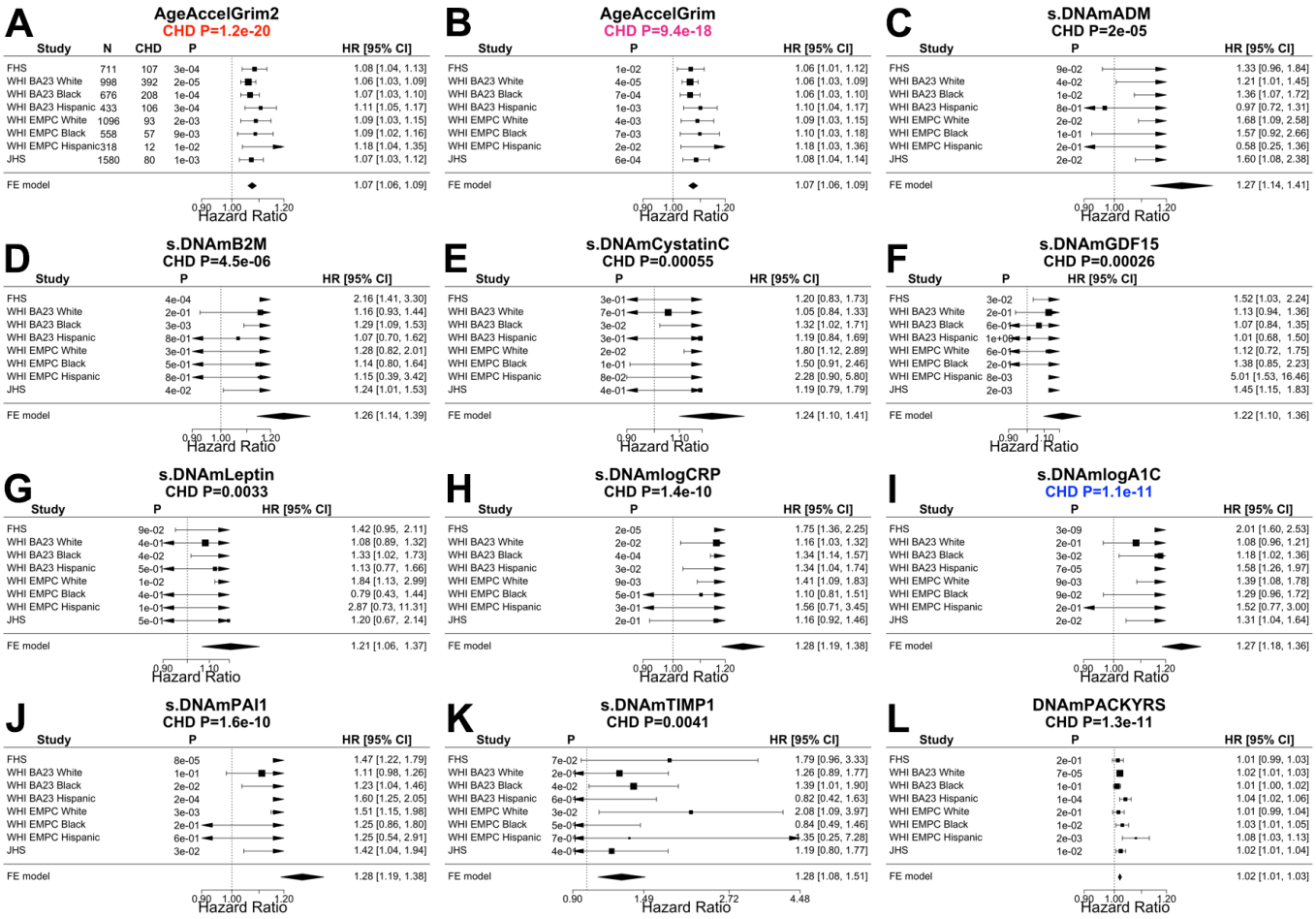

Supplementary Figure 17. Meta analysis forest plots for predicting time-to- coronary heart disease adjusted for blood cell composition. Each panel reports a meta analysis forest plot for combining hazard ratios predicting time-to-coronary heart disease (CHR) based on a DNAm based biomarker (reported in the figure heading) across different strata formed by racial group within cohort and set within LBC36. Here we re-conducted the survival analysis as listed in Figure 4 and adjusted additional 7 imputed blood cell counts: CD8 naïve, CD8pCD28nCD45Ran, plasma blasts, CD4+ T, natural killer cells, monocytes and granulocytes. (**A**, **B**) Results for AgeAccelGrim2 and AgeAccelGrim. Each row reports a hazard ratio (for time-to-CHD) and a 95% confidence interval resulting from a Cox regression model in each strata. (**C**–**L**) display the results for (age-adjusted) DNAm based surrogate markers of (**C**) adrenomedullin (ADM), (**D**) beta-2 microglobulin (B2M), (**E**) cystatin C (Cystatin C), (**F**) growth differentiation factor 15 (GDF-15), (**G**) leptin, (**H**) log scale of C reactive protein (CRP), (**I**) log scale of hemoglobin A1C, (**J**) plasminogen activation inhibitor 1 (PAI-1), (**K**) tissue inhibitor metalloproteinase 1 (TIMP-1) and (**L**) smoking pack-years (PACKYRS). The sub-title of each panel reports the meta analysis P-value. (**A**, **B**) Each hazard ratio (HR) corresponds to a one-year increase in AgeAccel. (**C**–**K**) Each hazard ratio corresponds to an increase in one-standard deviation. (**L**) Hazard ratios correspond to a one-year increase in pack-years. The most significant meta analysis P-value is marked in red (AgeAccelGrim2), followed by hot pink (AgeAccelGrim) and blue (DNAm logA1C), respectively.

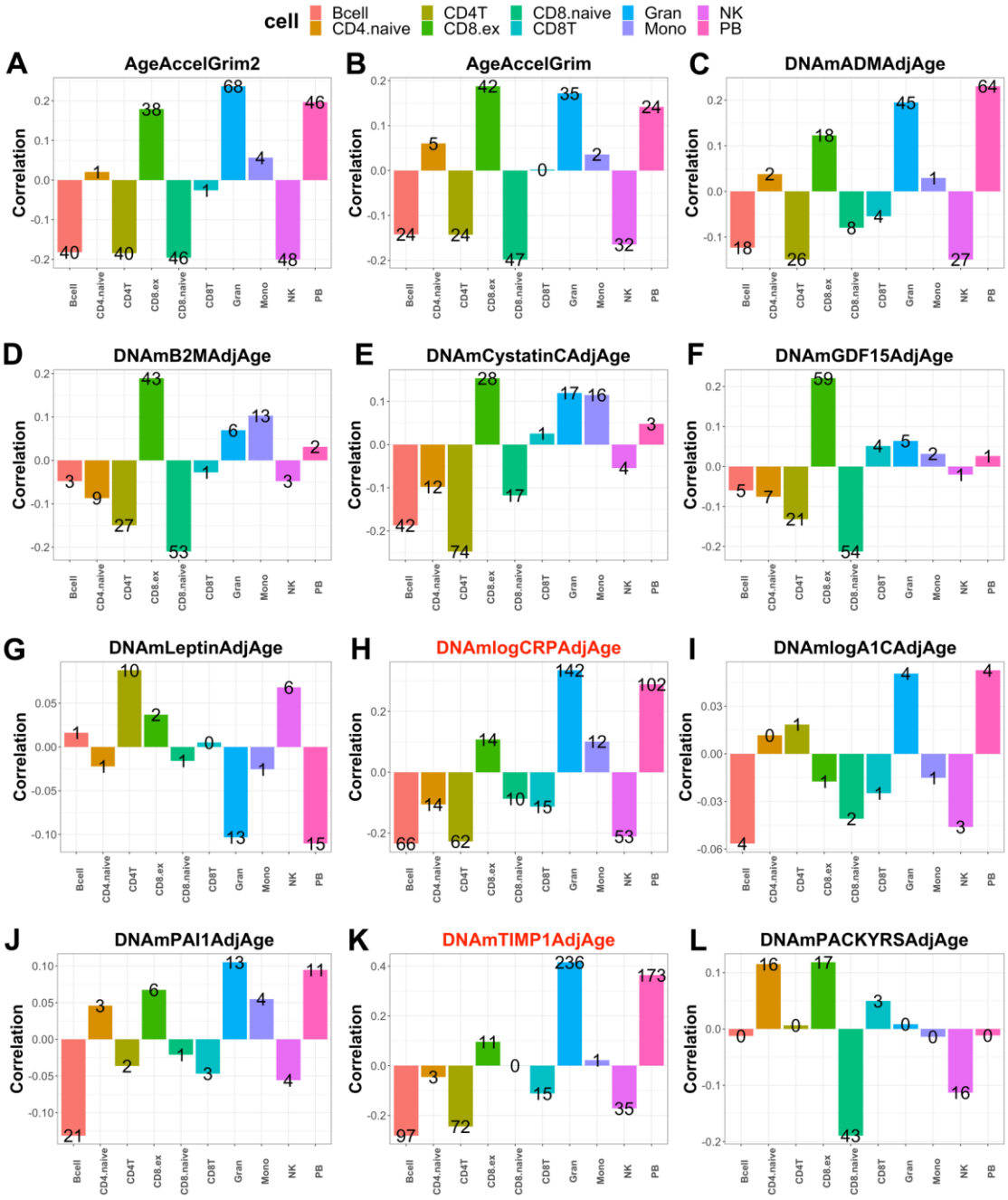

Supplementary Figure 18. Measures of blood cell composition versus DNAm based biomarkers in males. Each panel reports how the respective DNAm based biomarker (heading) relates to 10 imputed measures of blood cell counts. (**A**, **B**) display the results for AgeAccelGrim2 and AgeAccelGrim. (**C–L**) display the results for (age-adjusted) DNAm based surrogate markers of (**C**) adrenomedullin (ADM), (**D**) beta-2 microglobulin (B2M), (**E**) cystatin C (Cystatin C), (**F**) growth differentiation factor 15 (GDF-15), (**G**) leptin, (**H**) log scale of C reactive protein (CRP), (**I**) log scale of hemoglobin A1C, (**J**) plasminogen activation inhibitor 1 (PAI-1), (**K**) tissue inhibitor metalloproteinase 1 (TIMP-1) and (**L**) smoking pack-years (PACKYRS). The height of each bar corresponding to the statistical significance level (meta analysis p-value) of an association test between the blood cell measure and the age-adjusted DNAm biomarker. More precisely, the y-axis presents the meta analysis estimates of the Pearson correlation coefficients. The numbers displayed on top of each bar are minus logarithm (base 10) transformed meta P values. The title is marked by red if any absolute correlation >0.25. The association analysis is *not* confounded by chronological age because we used age adjusted DNAm based biomarkers. The fixed effects meta analysis was performed on males only across the validation study sets (N=5153): FHS test, JHS, InCHIANTI, BLSA, LBC21, LBC36 and NAS. Abbreviations for cell counts are listed in the following: nature killer (NK), monocyte (MONO) and granulocyte (Gran), CD8pCD28nCD45Ran (CD8.ex for exhausted cytotoxic T cells), and plasma blast (PB). The blood cell counts were imputed based on DNA methylation levels as described in [40, 42] and the Supplementary Methods section.

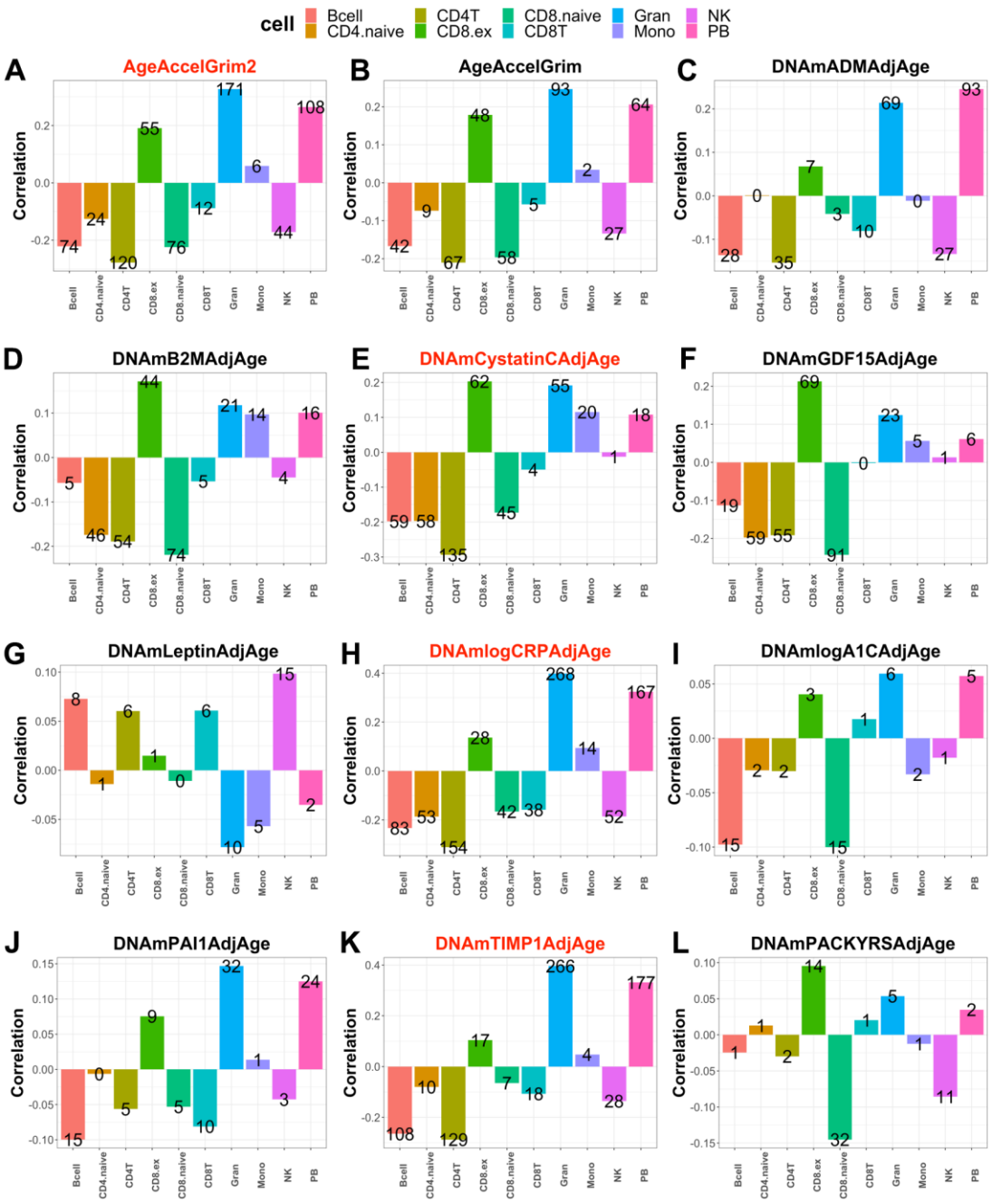

Supplementary Figure 19. Measures of blood cell composition versus DNAm based biomarkers in females. Each panel reports how the respective DNAm based biomarker (heading) relates to 10 imputed measures of blood cell counts. (**A**, **B**) display the results for AgeAccelGrim2 and AgeAccelGrim. (**C–L**) display the results for (age-adjusted) DNAm based surrogate markers of (**C**) adrenomedullin (ADM), (**D**) beta-2 microglobulin (B2M), (**E**) cystatin C (Cystatin C), (**F**) growth differentiation factor 15 (GDF-15), (**G**) leptin, (**H**) log scale of C reactive protein (CRP), (**I**) log scale of hemoglobin A1C, (**J**) plasminogen activation inhibitor 1 (PAI-1), (**K**) tissue inhibitor metalloproteinase 1 (TIMP-1) and (**L**) smoking pack-years (PACKYRS). The height of each bar corresponding to the statistical significance level (meta analysis p-value) of an association test between the blood cell measure and the age-adjusted DNAm biomarker. More precisely, the y-axis presents the meta analysis estimates of the Pearson correlation coefficients. The numbers displayed on top of each bar are minus logarithm (base 10) transformed meta P values. The title is marked by red if any absolute correlation >0.25. The association analysis is *not* confounded by chronological age because we used age adjusted DNAm based biomarkers. The fixed effects meta analysis was performed on females only across the validation study sets (N=6519): FHS test, WHI BA23, JHS, InCHIANTI, BLSA, LBC21, and LBC36. Abbreviations for cell counts are listed in the following: nature killer (NK), monocyte (MONO) and granulocyte (Gran), CD8pCD28nCD45Ran (CD8.ex for exhausted cytotoxic T cells), and plasma blast (PB). The blood cell counts were imputed based on DNA methylation levels as described in [40, 42] and the Supplementary Methods section.

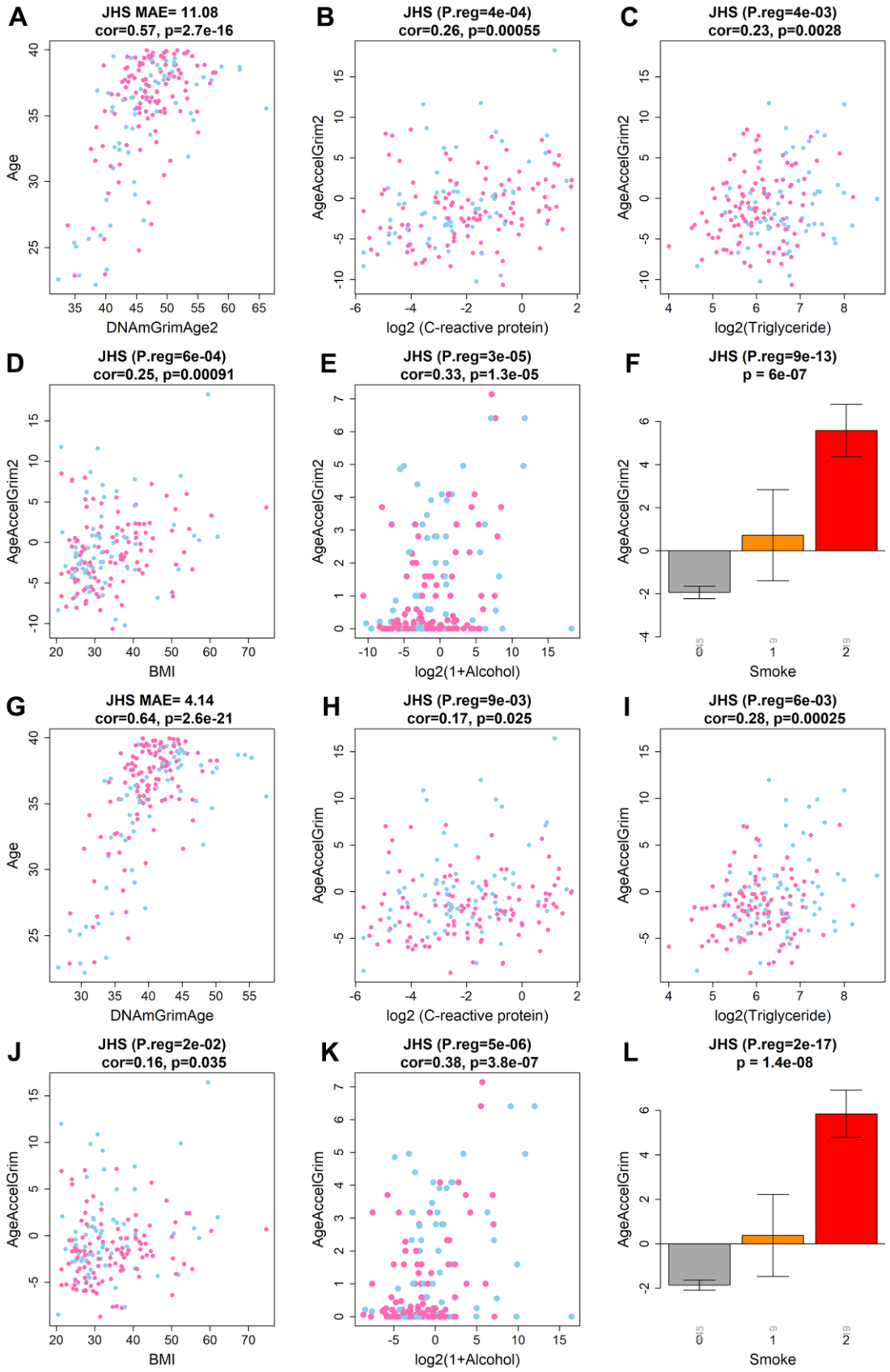

Supplementary Figure 20. Applying GrimAge clocks on young people in Jackson Heart Study. We evaluated our GrimAge clocks on the young population (age <40, n=173 with 62% females) in Jackson Heart Study (JHS) cohort. (**A**–**F**) present the assessments for (**A**)

correlation between chronological age and DNAmGrimAge2 and (**B**–**F**) associations between AgeAccelGrim2 with log2 C-reactive protein, log2 triglyceride, body mass index (BMI), log2 (alcohol assumption +1), and smoking status (0=never, 1=past, and 2=current). For (**B**–**E**) we report the P value (P.reg) from linear regression analysis, Pearson correlation estimate and P value. (**F**) reports the P value (P.reg) from linear regression analysis and the p-value of a non-parametric group comparison test (Kruskal-Wallis). The y-axis of the bar plot depicts the mean and one standard error. For (**B**–**D**) linear regression analysis was performed for outcome measures (as dependent variable) on AgeAccelGrim2 (as independent variable), adjusted for chronological age and gender. For (**E**, **F**) linear regression analysis was performed for AgeAccelGrim2 (as dependent variable) on life style variable (as independent variable), adjusted for chronological age and gender. The number under each bar presents number of individuals at each racial group. The lower (**G**–**L**) present the same assessments for DNAmGrimAge and AgeAccelGrim.

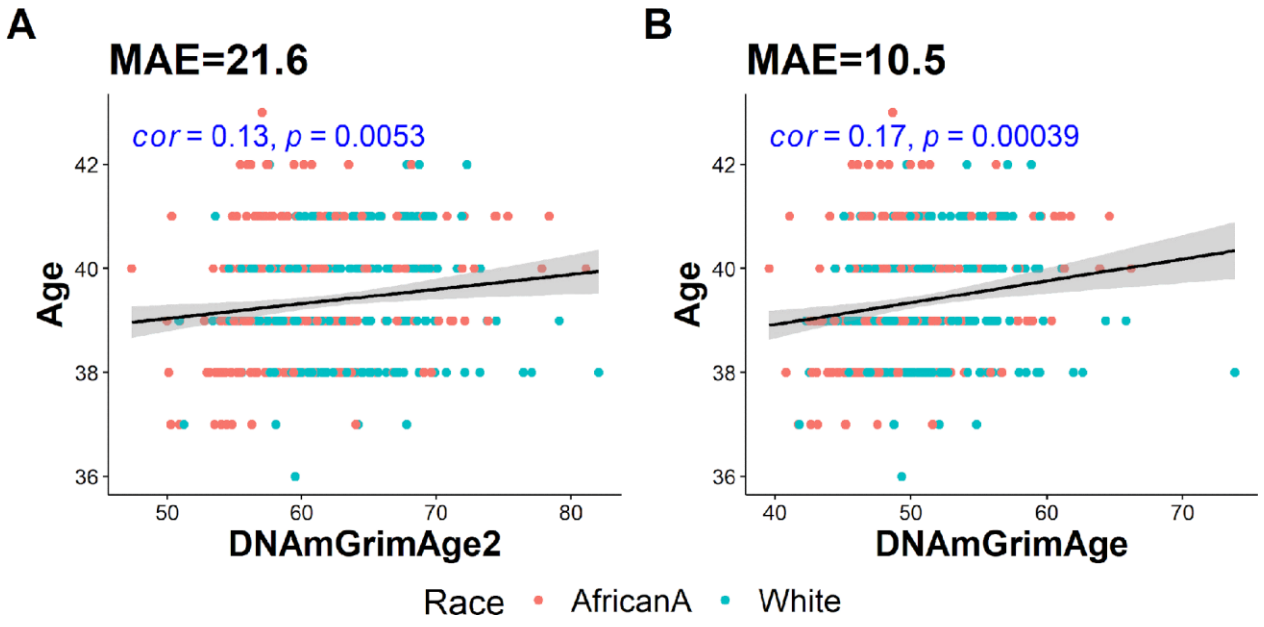

Supplementary Figure 21. Correlation analysis of DNAmGrimAge(2) versus chronological age in NGHS mothers . We present the scatter plots of chronological age versus (**A**) DNAmGrimAge2, and (**B**) DNAmGrimAge estimated in methylation array profiled in saliva samples from 432 mothers in NGHS. Each dot represents an individual sample colored based on ethnic/racial groups: White (n=218) and African American (n=214). The title of each panel repot the median of absolute error in units of years. The Pearson correlation coefficient (cor) and a corresponding correlation test p-value are reported at each panel.

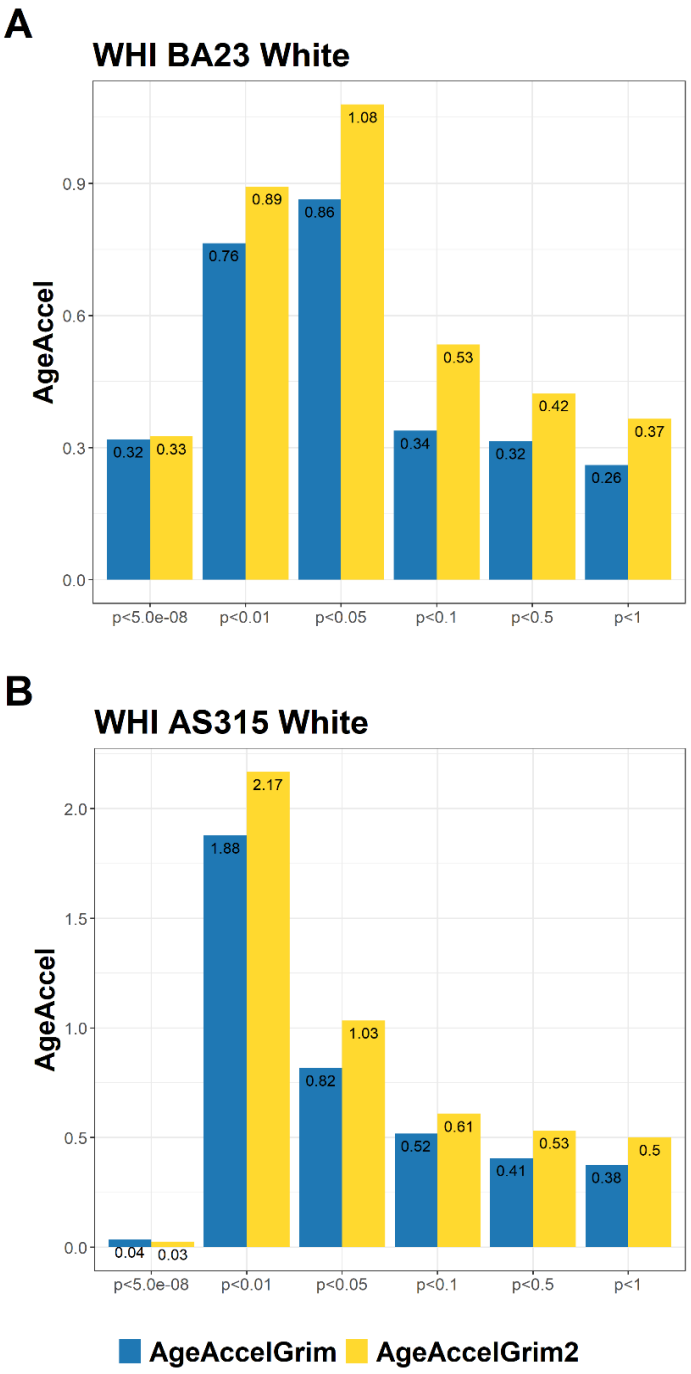

Supplementary Figure 22. Polygenic risk score analysis using WHI cohort. Polygenic risk score analysis (PRS) was applied to the women with European ancestry from (**A**) WHI BA23 and (**B**) EMPC cohorts, respectively. We calculate the proportion of the variation in AgeAccelGrim/AgeAccelGrim2 that can be explained by PRS at SNP P values thresholds set at <5.0e-08,0.01,0.05,0.1,0.5, and 1. The y-axis displays the proportion in percentage (%) and the x-axis displays different thresholds of P values. The proportions (in percentage %) are listed on the top of each bar.

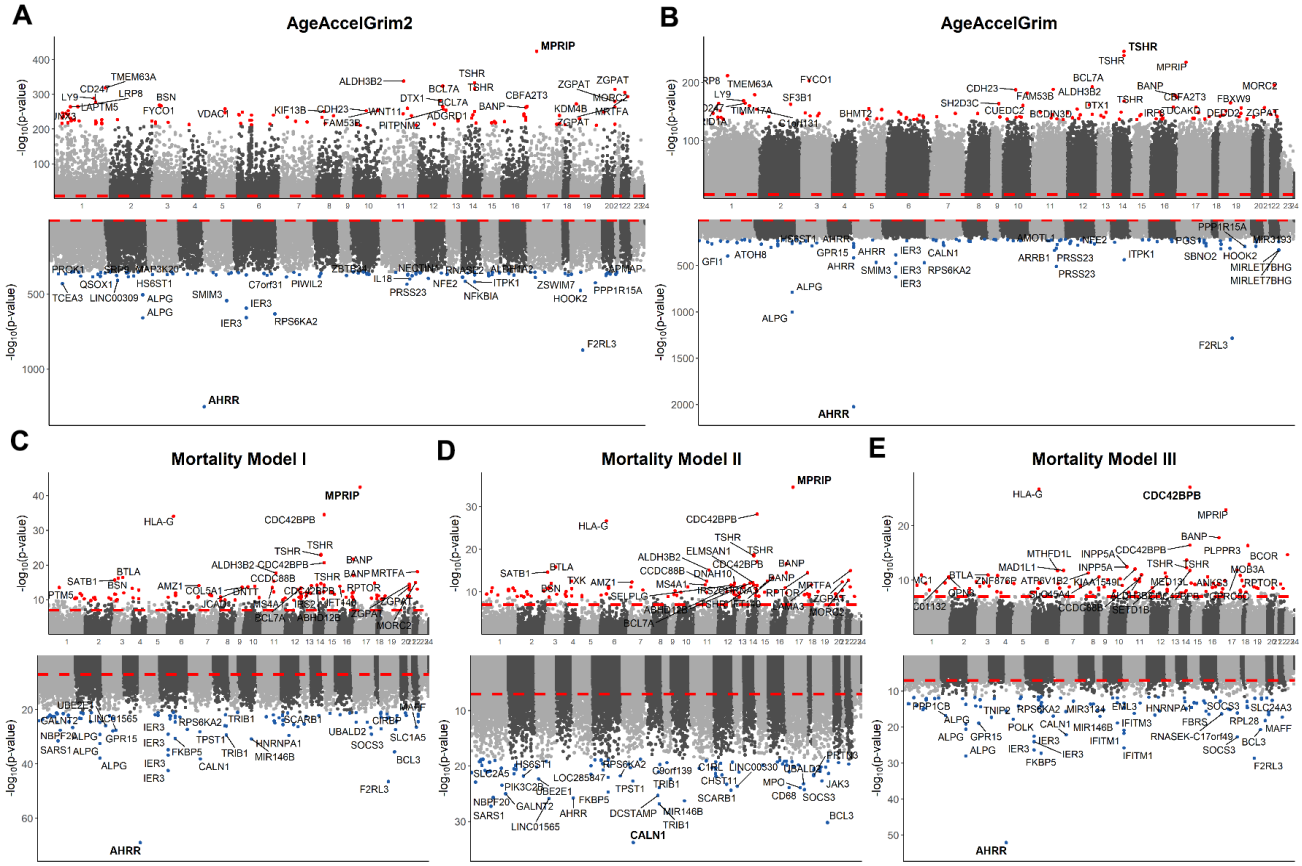

Supplementary Figure 23. Epigenome-wide association study (EWAS) for mortality related traits. Meta-analysis p-value (-log base 10 transformed) versus chromosomal location (x-axis) according to human genome assembly 19 (hg19) in (**A**), linear regression of AgeAccelGrim2, (**B**) linear regression of AgeAccelGrim, (**C**) Model I: Cox regression of time-to-death adjusted for age, gender, and batch effect (**D**) Model II: Cox regression of time-to-death adjusted for age, gender, batch effect, and smoking pack-years (or smoking status) and (**E**) Model III : Cox regression of time-to-death adjusted for age, gender, batch effect, and 7 imputed blood cell counts: CD8 naïve, CD8pCD28nCD45Ran, plasma blasts, CD4+ T, nature killer cells, monocytes and granulocytes. In (**A**, **B**) age acceleration of GrimAge clocks are increasing/decreasing with the methylation levels of the CpGs in the top/bottom panes. In (**C**, **D**) the hazard ratios of time-to-death are increasing/decreasing with the methylation levels of the CpGs in the top/bottom panes. Red dashed horizontal lines denote P at 1.0E-07. Gene names are annotated for the top 30 CpGs with positive and negative associations, respectively. CpGs are labeled by adjacent genes with the most significant one marked in bold in both top and bottom panes.

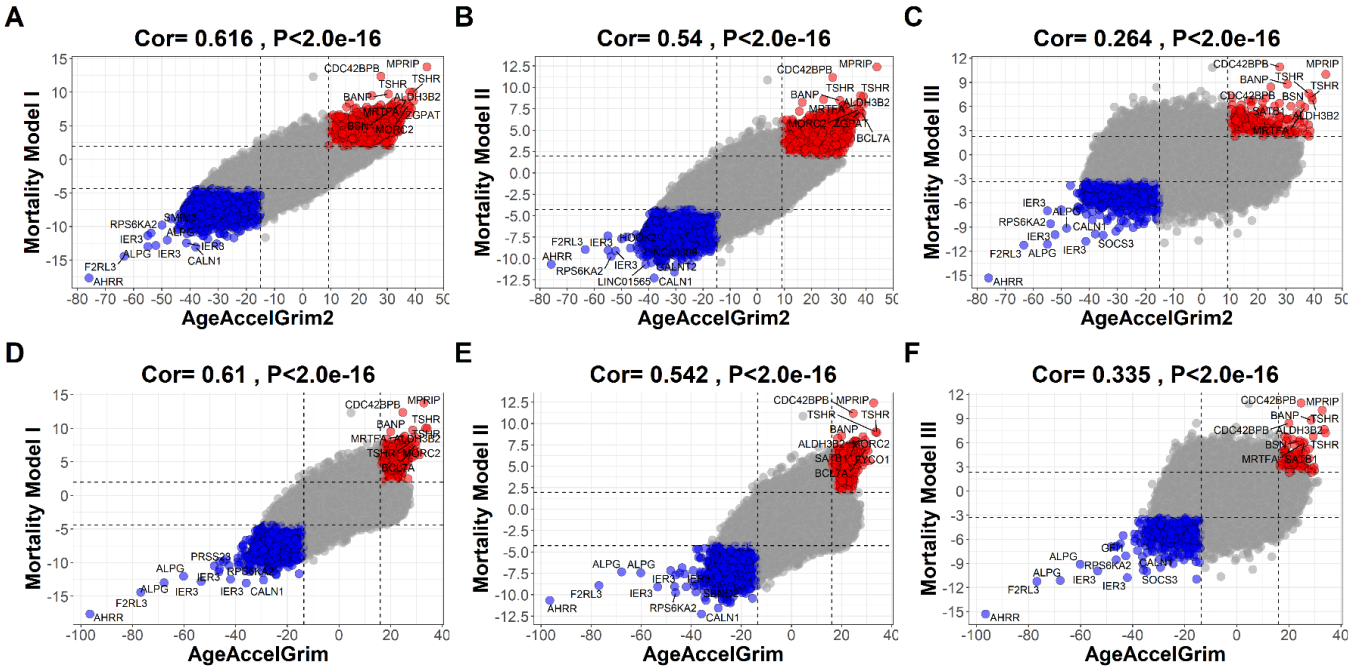

Supplementary Figure 24. Correlation between EWAS of age acceleration of GrimAge clocks and EWAS of time-to-death. Following the meta-analysis displayed in Supplementary Figure 23, the top panels display the meta Z scores from the EWAS of AgeAccelGrim2 on x-axis versus the meta Z scores from the EWAS of time-to-death based on Model I (**A**), Model II (**B**) and Model III (**C**) on y-axis. The bottom panels display the meta Z scores from the EWAS of AgeAccelGrim on x-axis versus the meta Z scores from the EWAS of time-to-death based on Model I (**D**), Model II (**E**) and Model III (**F**) on y-axis. Each dot corresponds to a CpG. Labels are provided for the top 10 CpGs in quadrant I and III, respectively, according to the product of Z scores in x and y axis. The title lists the Pearson correlation coefficient and corresponding nominal (unadjusted) two-sided correlation test P-value.

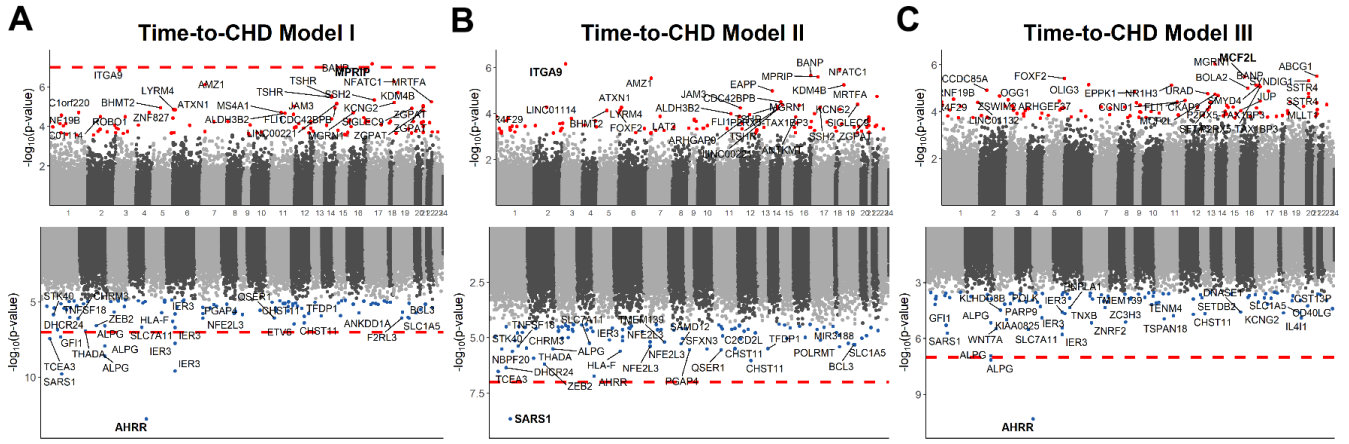

Supplementary Figure 25. Epigenome-wide association study (EWAS) for time-to-coronary heart disease. Meta-analysis p-value (-log base 10 transformed) versus chromosomal location (x-axis) according to human genome assembly 19 (hg19). (**A**) Model I: Cox regression of time-to-coronary heart disease (CHD) adjusted for age, gender, and batch effect (**B**) Model II: Cox regression of time-to-CHD adjusted for age, gender, batch effect, and smoking pack-years (or smoking status) and (**C**) Model III : Cox regression of time-to-CHD adjusted for age, gender, batch effect, and 7 imputed blood cell counts: CD8 naïve, CD8pCD28nCD45Ran, plasma blasts, CD4+ T, nature killer cells, monocytes and granulocytes. At each panel, the hazard ratios of time-to-CHD are increasing/decreasing with the methylation levels of the CpGs in the top/bottom panes. Red dashed horizontal lines denote P at 1.0E-07. Gene names are annotated for the top 30 CpGs with positive and negative associations, respectively. CpGs are labeled by adjacent genes with the most significant one marked in bold in both top and bottom.

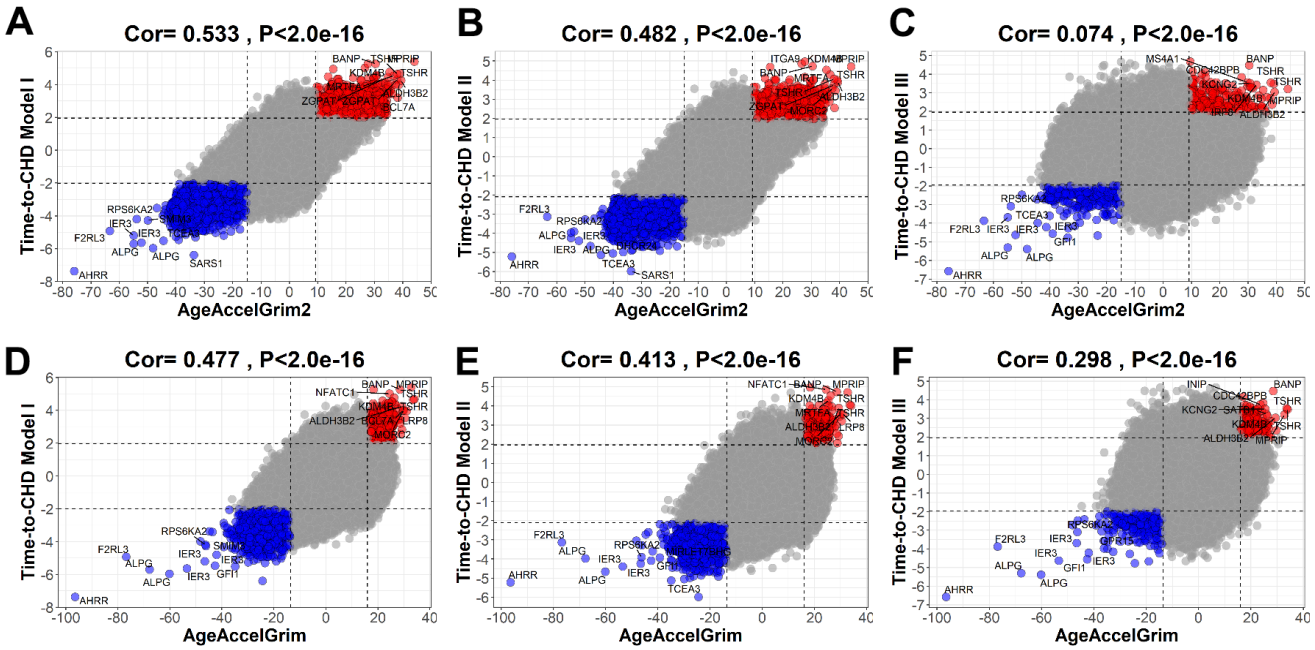

Supplementary Figure 26. Correlation between EWAS of age acceleration of GrimAge clocks and EWAS of time-to-coronary heart disease. Following the meta-analysis displayed in Supplementary Figures 23, 25, the top panels display the meta Z scores from the EWAS of AgeAccelGrim2 on x-axis versus the meta Z scores from the EWAS of time-to-coronary heart disease (CHD) based on Model I (**A**), Model II (**B**) and Model III (**C**) on y-axis. The bottom panels display the meta Z scores from the EWAS of AgeAccelGrim on x-axis versus the meta Z scores from the EWAS of time-to-CHD based on Model I (**D**), Model II (**E**) and Model III (**F**) on y-axis. Each dot corresponds to a CpG. Labels are provided for the top 10 CpGs in quadrant I and III, respectively, according to the product of Z scores in x and y axis. The title lists the Pearson correlation coefficient and corresponding nominal (unadjusted) two-sided correlation test P-value.

Supplementary Tables

Please browse Full Text version to see the data of Supplementary Tables 2.2–2.13, 4.1–4.3.

Supplementary Table 1.1. GrimAge2 stage 1: DNAm-based surrogate biomarkers of plasma proteins and smoking pack-years.

Variable	Num CpGs	correlation with biomarker in training data	correlation with age in training data	correlation with biomarker in test data	correlation with age in test data	Exam
adm	186	0.653693573174295	0.625525905864977	0.381687444097942	0.639017395854806	exam 7
B2M	91	0.617158399278239	0.825073799472286	0.426041190563136	0.848465319002703	exam 7
cd56	607	0.86375831161774	0.172605242662232	0.361637489604755	0.170522481815106	exam 7
Cystatin_C	87	0.580806669506421	0.812098347065102	0.392285471797308	0.827175556961344	exam 7
EFEMP1	57	0.589686685159107	0.719151039155843	0.412150311207909	0.872303871874163	exam 7
GDF_15	137	0.737468260449462	0.71492538275353	0.534804728797616	0.806519824631994	exam 7
leptin	187	0.681181180674115	0.0581128431496463	0.352344410014838	0.0514309778202585	exam 7
log.A1C	86	0.525131694119941	0.31582295531732	0.339957448360379	0.26677461707641	exam 8
log.CRP	132	0.569330798879011	0.272903575140915	0.476839364307574	0.261805340722653	exam 8
PACKYRS	172	0.785	0.17	0.66	0.13	exam 8
pai_1	211	0.691865627259714	0.190154508514923	0.362625398311644	0.16187195108164	exam 7
TIMP_1	42	0.431107933469501	0.917716575776463	0.350384409802195	0.898106800656296	exam 7

Supplementary Table 1.2. GrimAge2: Distribution of DNAm proteins based on FHS training dataset.

Variable	mean	sd
DNAmADM	337.443763330646	26.8386567435564
DNAmB2M	1633051.85941816	166877.416872265
DNAmCystatinC	591129.33954085	41113.1707392004
DNAmGDF15	678.704154283819	175.497882136521
DNAmLeptin	8360.49439150999	4368.05918344219
DNAmlogA1C	1.73769184385078	0.03209281978435
DNAmlogCRP	0.447021928835783	0.439141130146429
DNAmPAI1	19804.6891037806	3325.68848188053
DNAmTIMP1	34348.2946807127	1548.59018754715

Supplementary Table 2.1. Description of variable availability for Diet, clinically relevant measurements, and life style factors.

Order	Category	Var	NumData	n	FHS	WHI	JHS	InCHIANTI	BLSA	LBC21	LBC36	NAS
1	Diet	log2(Total energy)	2	4221		x					x	
2	Diet	Carbohydrate	2	4222		x					x	
3	Diet	Protein	2	4221		x					x	
4	Diet	Fat	2	4221		x					x	
5	Diet	log2(1+Red meat)	3	4873	x	x					x	
6	Diet	log2(1+Poultry)	3	4832	x	x					x	
7	Diet	log2(1+Fish)	3	4873	x	x					x	
8	Diet	log2(1+Dairy)	3	4868	x	x					x	
9	Diet	log2(1+Whole grains)	2	4108	x	x						
10	Diet	log2(1+Nuts)	1	3463		x						
11	Diet	log2(Fruits)	3	4864	x	x					x	
12	Diet	log2(Vegetables)	3	4864	x	x					x	
14	Diet	log(OMEGA3)	1	643	x							
15	Diet	log(VitaminA)	1	651	x							
16	Diet	log(VitaminC)	2	1409	x						x	
17	Diet	log(VitaminB6)	2	1407	x						x	
18	Diet	log(VitaminE)	2	1397	x						x	
19	Diet	log(Selenium)	2	1401	x						x	
20	Diet	log(Iron)	1	633	x							
21	Diet	log(Zinc)	2	1404	x						x	
22	Diet	log(Calcium)	2	1407	x						x	
23	Diet	log(FolicAcid)	2	1407	x						x	
24	Diet	log(VitaminD)	2	1397	x						x	
25	Diet	log(Copper)	1	643	x							
26	Diet	log(BrewYeast)	1	643	x							
27	Diet	log(BetaCaroteneSup)	1	645	x							
28	Diet	log(Magnesium)	1	641	x							
29	Dietary Biomarkers	Retinol	1	2053		x						
30	Dietary Biomarkers	Mean carotenoids	1	2052		x						
31	Dietary Biomarkers	Lycopene	1	2053		x						
32	Dietary Biomarkers	log2(alpha-Carotene)	1	2053		x						
33	Dietary Biomarkers	log2(beta-Carotene)	1	2052		x						
34	Dietary Biomarkers	log2(Lutein+Zeaxanthin)	1	2053		x						
35	Dietary Biomarkers	log2(beta-Cryptoxanthin)	1	2053		x						
36	Dietary Biomarkers	log2(alpha-Tocopherol)	1	2053		x						
37	Dietary Biomarkers	log2(gamma-Tocopherol)	1	2053		x						
38	Measurements	log(A1C)	1	711	x							
39	Measurements	log2(C-reactive protein)	8	11281	x	x	x	x	x	x	x	x
40	Measurements	log2(Insulin)	3	5912		x		x				x
41	Measurements	log2(Glucose)	5	7392	x	x		x	x			x
42	Measurements	log2(Triglyceride)	6	9847	x	x	x	x	x			x
43	Measurements	Total cholesterol	8	13002	x	x	x	x	x	x	x	x
44	Measurements	LDL cholesterol	4	7688		x	x	x	x			
45	Measurements	HDL cholesterol	6	9844	x	x	x	x	x			x
46	Measurements	log2(Creatinine)	3	4770	x	x		x				

47	Measurements	log2(IL6)	3	3185				x	x			x
48	Measurements	log2(TNFA)	3	2621				x	x			x
49	Measurements	log2(Urine Creatinine)	3	1793	x		x	x				
50	Measurements	FEV1	5	5836	x				x	x	x	x
52	Measurements	Systolic blood pressure	6	11980	x	x	x	x			x	x
53	Measurements	Diastolic blood pressure	6	11980	x	x	x	x			x	x
54	Measurements	log2(Waist / hip ratio)	3	5887	x	x						x
55	Measurements	BMI	8	13420	x	x	x	x	x	x	x	x
56	Measurements	MMSE	6	7017	x	x		x	x	x	x	
57	Measurements	Telomere length	3	2193	x	x						x
58	Life style	Education	8	13312	x	x	x	x	x	x	x	x
59	Life style	Income	3	6687		x	x					x
60	Life style	Hand grip	5	5962	x			x	x	x	x	
61	Life style	log2(1+Exercise)	4	7278		x	x		x			x
62	Life style	Current smoker	6	10247	x	x			x	x	x	x
63	Life style	log2(1+Alcohol)	5	8050	x	x	x	x			x	

Supplementary Table 2.2. AgeAccelGrim:Diet, clinically relevant measurements, and life style factors.

Supplementary Table 2.3. AgeAccelGrim2:Diet, clinically relevant measurements, and life style factors.

Supplementary Table 2.4. DNAmADMAdjAge:Diet, clinically relevant measurements, and life style factors.

Supplementary Table 2.5. DNAmB2MAdjAge:Diet, clinically relevant measurements, and life style factors.

Supplementary Table 2.6. DNAmCystatinCAdjAge:Diet, clinically relevant measurements, and life style factors.

Supplementary Table 2.7. DNAmGDF15AdjAge:Diet, clinically relevant measurements, and life style factors.

Supplementary Table 2.8. DNAmLeptinAdjAge:Diet, clinically relevant measurements, and life style factors.

Supplementary Table 2.9. DNAmlogA1CAdjAge:Diet, clinically relevant measurements, and life style factors.

Supplementary Table 2.10. DNAmlogCRPAdjAge:Diet, clinically relevant measurements, and life style factors.

Supplementary Table 2.11. DNAmPACKYRSAdjAge:Diet, clinically relevant measurements, and life style factors.

Supplementary Table 2.12. DNAmPAI1AdjAge:Diet, clinically relevant measurements, and life style factors.

Supplementary Table 2.13. DNAmTIMP1AdjAge:Diet, clinically relevant measurements, and life style factors.

Supplementary Table 3.1. Multivariate regression analysis of AgeAccelGrim2 on CT-scan derived fatty liver and adipose tissue density in FHS.

Model	Y	X	Beta	SE	P
I	AgeAccelGrim2	LIVER	-0.0725552450066406	0.0157640950628678	0.000052462134978876
		SPLEEN	-0.0641606466770295	0.0314759794731426	0.0420133477051177
		MUSCLE	-0.0299140728046785	0.0217670903459476	0.1699445683868
		Female	-2.05039351096843	0.291933038291549	6.7760496877205E-12
		BMI	0.0318418769471347	0.0376401403591607	0.39796528544538
		Age at CT scan	-0.00992439979265223	0.0185602226136875	0.593075731831915
		SAT_CM3	0.0001175063321704	0.000168522663672719	0.485902386408158
		VAT_CM3	0.000648438884697252	0.000143475978795086	0.0000074714159508801
II	AgeAccelGrim2	Female	-1.79179445483356	0.377885807483643	2.65222492382836E-06
		BMI	0.0423208062396213	0.0516700617304267	0.413078749384451
		Age at CT scan	-0.0137130451222446	0.0166979368071955	0.411835229253499
		SAT_CM3	0.000213266609903971	0.000185658369273936	0.251137868322493
		SAT_HU	0.0518858581680036	0.0496768333623689	0.296691687990567
		VAT_CM3	0.000696277354148539	0.000225770022520319	0.00213665798620851
III	AgeAccelGrim2	VAT_HU	-0.00215892686800074	0.0479969355962227	0.964137881257326
		Female	-1.66540746493659	0.393922098195233	0.000027303482094446
		BMI	0.026757674678966	0.053215234920054	0.615276396289478
		Age at CT scan	-0.0180851191986976	0.0171297109908854	0.291498115855943
		LIVER	-0.0626818541708387	0.0170574563176948	0.00026328300052734
		SPLEEN	-0.054951643047811	0.0333075558382417	0.0995944208257338
		MUSCLE	-0.0326249567509138	0.022474793765515	0.147220950242196
		SAT_CM3	-0.0000979759784997684	0.000188785005675917	0.60399856899
IV	AgeAccelGrim2	VAT_CM3	0.000374339356189572	0.00016747464759595	0.0258363385051958
		Female	-1.46955858341664	0.423578131683179	0.000565817215577898
		BMI	0.0104187753954827	0.0559296045453909	0.852296337315191
		Age at CT scan	-0.0232044991761183	0.0190935020988578	0.224810675512135

Supplementary Table 3.2. Multivariate regression analysis of AgeAccelGrim on CT-scan derived fatty liver and adipose tissue density in FHS.

Model	Y	X	Beta	SE	P
I	AgeAccelGrim	LIVER	-0.0546693939781844	0.0142894416560176	0.000146089526183766
		SPLEEN	-0.0730238668554368	0.0285204177186902	0.0107352358788065
		MUSCLE	-0.0254844566773724	0.0197229816192019	0.196887362219345
		Female	-2.68970443896693	0.26432393954252	2.61572412382749E-22
		BMI	0.0105132397941722	0.0341221556735657	0.758124605518281
		Age at CT scan	-0.00651440056132528	0.0168534212592124	0.699259606048942
		SAT_CM3	0.000157670637968458	0.000153593630455081	0.305049536220618
		VAT_CM3	0.000498830492411192	0.000130756509830738	0.00015034122401784
II	AgeAccelGrim	Female	-2.58845270816718	0.344355524447278	2.0572998267966E-13
		BMI	0.0229333865618026	0.0470891168061544	0.626421646578195
		Age at CT scan	-0.00818237393770103	0.0152280190294081	0.591243652428715
		SAT_CM3	0.000220531127826131	0.00016921748252493	0.192994953803833
		SAT_HU	0.021640035705448	0.0452770463366346	0.632862767943247
		VAT_CM3	0.000635656503675089	0.000205758533910126	0.00209935350529376
III	AgeAccelGrim	VAT_HU	0.0272304577727766	0.0437427061130195	0.533841472589256
		Female	-2.471149627248	0.358947669020785	1.47274397318319E-11
		BMI	0.0128250099228703	0.0484980890476067	0.791529375255242
		Age at CT scan	-0.0120919656881404	0.0156250044919964	0.439304797792829
		LIVER	-0.0475308664009919	0.0154590687712233	0.00222060338431433
		SPLEEN	-0.0655966151283918	0.0301814115886675	0.0302088092527874
		MUSCLE	-0.0288585724605927	0.0203601148345682	0.156974546502247
IV	AgeAccelGrim	SAT_CM3	-0.000645277569592293	0.000171118131252568	0.706260014989643
		VAT_CM3	0.000267511621204019	0.000151750496110608	0.0785266023805075
		Female	-2.27613778068489	0.383729334000118	5.53838746676851E-09
		BMI	-0.00329955058654534	0.0506937234630215	0.948129478492866
		Age at CT scan	-0.0180955318334558	0.0173395230458529	0.297164756461088

Supplementary Table 3.3. Multivariate regression analysis of DNAmPAI1AdjAge on CT-scan derived fatty liver and adipose tissue density in FHS.

Model	Y	X	Beta	SE	P
I	DNAmPAI1AdjAge	LIVER	-93.1160498683119	11.1566433936582	6.34802166163233E-16
		SPLEEN	-9.46221758578595	22.3749459732659	0.672547175092448
		MUSCLE	1.50197350069059	15.4690268717859	0.922687791190797
		Female	-1548.14293098737	209.468920594888	5.83551954372997E-13
		BMI9	58.241260706491	26.6190276309504	0.0291154380846502
		Age at CT scan	5.85774251435321	12.8861722223888	0.649603394362432
		SAT_CM3	0.278474449545414	0.11761948706386	0.0182212234117412
		VAT_CM3	0.764719539974853	0.100362509401461	9.99534455778813E-14
II	DNAmPAI1AdjAge	Female	-1185.68188545405	265.106918280431	9.25250195939522E-06
		BMI9	-18.1112674638562	36.1673090704662	0.616721540615711
		Age at CT scan	-12.6372328432492	11.4360903315457	0.269589868759395
		SAT_CM3	0.348479480147811	0.129430579607252	0.00729296406555991
		SAT_HU	65.0792546734262	34.6363839191448	0.0607413584402037
		VAT_CM3	0.569510500269957	0.157782337342776	0.000332578216044617
III	DNAmPAI1AdjAge	VAT_HU	-64.1739654035311	33.535306514281	0.0561461426188171
		Female	-1171.47467020196	276.165889678789	0.0000256828920671473
		BMI9	-29.7270181063069	37.1901222248041	0.424419520489371
		Age at CT scan	-13.6131465698224	11.7440482420606	0.246857321082752
		LIVER	-73.0814526252046	11.8486649492233	1.40977703397388E-09
		SPLEEN	13.2395901044582	23.1746825945454	0.568051069566604
		MUSCLE	-1.16768020363668	15.668413693673	0.940622293606083
IV	DNAmPAI1AdjAge	SAT_CM3	0.305262987704478	0.130871772484245	0.0200606974925636
		VAT_CM3	0.631192083678622	0.116514425102993	9.34151169101383E-08
		Female	-1063.2913100898	295.19219180069	0.000346655934718117
		BMI9	-59.0176129450417	38.8452015553271	0.129306031677585
		Age at CT scan	-7.74139415834141	13.0351867068401	0.55285274549796

Supplementary Table 3.4. Multivariate regression analysis of DNAmlogCRPAdjAge on CT-scan derived fatty liver and adipose tissue density in FHS.

Model	Y	X	Beta	SE	P
I	DNAmlogCRPAdjAge	LIVER	-0.00780143813357888	0.00135865529996456	1.58923063186677E-08
		SPLEEN	0.00184718877057261	0.00272140514411132	0.497588935065418
		MUSCLE	-0.00110300818926791	0.00188190714149873	0.558053651258652
		Female	0.203304682834499	0.0254062027717669	7.96441025158663E-15
		BMI	0.0134030663180608	0.00324206486118264	0.0000415110836793144
		Age at CT scan	-0.000982251385415205	0.00157747554513246	0.533771363011607
		SAT_CM3	0.0000200597481523092	0.0000145217529854608	0.167683781857688
		VAT_CM3	0.0000549319489027089	0.000012382355443839	0.0000108915405143277
II	DNAmlogCRPAdjAge	Female	0.21061338971306	0.0326729016255463	2.3624915827945E-10
		BMI	0.00711705268065337	0.00446049554545465	0.111111269960812
		Age at CT scan	-0.00174607502539682	0.00142077528165995	0.219569630405629
		SAT_CM3	0.0000320524594988421	0.0000159819165804588	0.0453555604941175
		SAT_HU	0.00851327102506476	0.00427687493696753	0.0469874908294514
		VAT_CM3	0.0000437656295960282	0.0000194657512869669	0.024918505461753
III	DNAmlogCRPAdjAge	VAT_HU	-0.00494246127130323	0.00413771126527481	0.232760084235606
		Female	0.220732514611499	0.0340409966410324	1.87007287920982E-10
		BMI	0.00514539586289426	0.00458830461081485	0.262561906328698
		Age at CT scan	-0.00213946455128356	0.00145732380758355	0.14260977827154
		LIVER	-0.00652565473064705	0.00146822997100933	0.0000108119617565713
		SPLEEN	0.00354378934615982	0.00287020416541773	0.217517443301476
		MUSCLE	-0.000904409619672705	0.00193971730671087	0.641229585826029
IV	DNAmlogCRPAdjAge	SAT_CM3	0.0000201274044847075	0.0000162298017621343	0.215489821931786
		VAT_CM3	0.0000364285045369923	0.0000144333453528689	0.0119082147047212
		Female	0.224349787525412	0.0365489444612348	1.67705762083865E-09
		BMI	0.00540326213183127	0.00481296824459281	0.26211587010049
		Age at CT scan	-0.00145663212648968	0.00162319617077255	0.369936859405074

Supplementary Table 3.5. Multivariate regression analysis of DNAmlogA1CAdjAge on CT-scan derived fatty liver and adipose tissue density in FHS.

Model	Y	X	Beta	SE	P
I	DNAmlogA1CAdjAge	LIVER	-0.000886026145980581	0.000104515193453869	2.36931537104274E-16
		SPLEEN	0.0000539545090005328	0.000208681172918216	0.79608440974091
		MUSCLE	-0.0000863308257918765	0.000144312594205194	0.549951938534319
		Female	0.00405851826142004	0.00193541896672057	0.0364766380341877
		BMI	0.000397450587047914	0.000249553164556365	0.111844292206913
		Age at CT scan	0.0000479742781959997	0.000123061465613299	0.696813893289029
		SAT_CM3	-6.95761606082695E-07	1.10853729924978E-06	0.530479425152961
		VAT_CM3	7.58779757829765E-06	9.44120867660531E-07	4.92559999606763E-15
II	DNAmlogA1CAdjAge	Female	0.0126329755006024	0.00248770020810905	5.09585747438412E-07
		BMI	0.000287382014295494	0.000340019110863444	0.398340159071714
		Age at CT scan	-0.000136011233502378	0.000109502327109008	0.214691163753782
		SAT_CM3	8.48946007625696E-07	1.21022613490267E-06	0.483278625204431
		SAT_HU	0.00136184271902832	0.000323838785763361	0.0000300728268376565
		VAT_CM3	3.91453755062786E-06	1.47226301375199E-06	0.00805090738099513
III	DNAmlogA1CAdjAge	VAT_HU	-0.00124305231457744	0.000312986705597368	0.000080110639284532
		Female	0.0131916675535521	0.0025704731474462	0.0000003883233966291
		BMI	0.0000308550730229477	0.000347028177090041	0.929181427163583
		Age at CT scan	-0.000161614306873522	0.000111303689050094	0.147023550524075
		LIVER	-0.000706010410787347	0.000111258710493928	4.89407595344815E-10
		SPLEEN	0.000130584499919972	0.000217298775464703	0.548143946031757
		MUSCLE	-0.000100052075614054	0.000146674601482737	0.495462423372083
		SAT_CM3	-1.18094156504028E-06	1.23112588499746E-06	0.337893861513122
IV	DNAmlogA1CAdjAge	VAT_CM3	6.02335217277869E-06	1.09265587636537E-06	5.62401973827812E-08
		Female	0.013255014929255	0.00276426806108236	2.13670536595381E-06
		BMI	0.0000148746940111846	0.000364766907404142	0.967488336247237
		Age at CT scan	-0.000105767228089239	0.00012421602671623	0.394903441179087

Supplementary Table 4.1. Association with blood cell composition.

Supplementary Table 4.2. Association with blood cell composition in males.

Supplementary Table 4.3. Association with blood cell composition in females.